Author's Response

Article: Evaluation of Monte Carlo tools for high energy atmospheric physics II : relativistic runaway electron avalanches
by D. Sarria, C. Rutjes, et al.

Journal: Geoscientific model development (GMD)
Manuscript reference: gmd-2018-119

Contents

1 Response to Referee # 1 (with relevant changes listed with italic font)

We thank the Referee for his careful reading, and the valuable comments. We considered each of the comments and questions and provided an adequate answer. The comments of Referee #1 are written in bold and the answers in plain text. Sentences indicating a modification to the manuscript are written using italic font.

The latex diff of the revised manuscript, accounting for comments of referees #1 and #2 is provided as an attached file.

General comment

The authors compare simulations made by several M-C codes and come with useful recommendations on simulation procedures (energy cuts, etc..). The analysis is detailed and there are no doubts that all codes in own limits produce rather coherent results. The code verification and comparisons of different code options, as well as different codes, are necessary first step of simulation experiments and constructing of models to be compared with experiment.

We would like to clarify that we do not intend to validate/verify any code in this article. The general purpose code Geant4 has already undergone multiple verification and validation studies in several physical contexts, but nothing guarantees it can be straightforwardly applied to HEAP (also referred as HEPA by the referee) phenomena, in particular concerning the capacity of simulating Relativistic Runaway Electron Avalanches (RREA) that we are extensively testing here. This issue was first raised by (*Skeltved et al.*, 2014). Therefore, we think it is important to provide the researchers of the community with clear tests frameworks, together with reference data, to make it possible for them to benchmark their custom made codes. On our side, with this series of two GMD papers (*Rutjes et al.* (2016) and this one), we are settling the first foundations of a larger, long-term work.

However, we have to understand, that M-C simulations for such a complicated domain as High-energy Physics in Atmosphere (HEPA) is not a precise tool! We don't know the distribution of the electric charges in the cloud and, therefore, strength and elongation of the emerging electric fields. Therefore, very time-consuming and detailed verification of different M-C programs, for opinion of this referee is not too important on the present stage of HEPA progress. As I mention in my review to the first paper of this series in 2016, the validation of the available experimental observations is vital for the progress of HEPA. There are published numerous gamma ray energy spectra observed on the mountain altitudes and few electron energy spectra; why not to try to compare simulations with observations? Continuous simulations with different codes and arbitrary parameters (sometimes nonrealistic, see my comment below to 4.3.1) can make illusion of intense scientific research; however only comparisons with observations and physical inference on the observed phenomena really values. Sure, authors will argue that model validation is out of scope of their paper. And they will be right. However, I can ask, when they will use their verified models for coming with comprehensive model of HEPA? When they will develop models with realistic parameters and compare it with data (energy spectra measured on Earth's surface and in the space)?

Comparison with experimental data is not the goal of this work. However, we think it is worth mentioning here that we are working on other projects in parallel, for which having tested the coherence between these three different codes beforehand is important. Also, we would like to point out that the REAM model, tested in this study, was used to analyze experimental data detected from space and from the atmosphere in many occasions (see *Dwyer et al.* (2012)). Furthermore, compared to our status in 2016, a part of the team involved in the present study (including the first author) is now conducting, in parallel, Geant4 simulations attempts in comparison with experimental data, through two separate studies. They both concern aircraft-based measurements, one from 12 km altitude (ILDAS campaign) and the other from 20 km altitude (ALOFT/FEGS campaign); and there also having first found that

there is a form of consensus between the different available RREA models is important to interpret the results. Some of these results have been very recently published *Kochkin et al.* (2018).

[...] Continuous simulations with different codes and arbitrary parameters (sometimes non-realistic, see my comment below to 4.3.1) [...]

See answer below.

To be not too didactic, I'll cite our old paper, where we try for the first time to compare simulated energy spectra with measured ones and establish a TGE model (see Figs 8-12 of Chilingarian, Mailyan and Vanyan, 2012). "With newly estimated thundercloud height, we re-estimate several phenomenological parameters of the RREA process as the following: the most probable height of thundercloud (and electrical field therein) is ˜50 m. The number of electrons with energies ˚ above 1 MeV at the exit from the cloud is 1.97107 electrons/m2/min; if we assume that the radiation region in the thundercloud has a radius of 1 km the total number of ˚ electrons crossing this region in a minute is ˜61013.

Sure, we use not optimized M-C; and, maybe we make some mistakes in our inference. We discuss possible sources of the systematic errors:

"We do not measure the electric field within the thundercloud; near surface electric field is not a good proxy of the intracloud fields accelerating electrons downward. We also do not measure vertical extension of the field and only estimate the height of the cloud. Therefore, simulations of the RREA process in the atmosphere with chosen parameters, although are in an agreement with the available measurements of electric fields in the thunderclouds, cannot be used for direct comparisons with TGE measurements. However, these simulations give us understanding of the RREA scale and MOS processes and expected behavior of the energy spectra."

However, it was the first time we present gamma ray and electron energy spectra along with simulations and achieve overall agreement. Now we develop a new method of cloud height estimation and can approach observations with more realistic simulations with more reliable better parameters. What I want to demonstrate is that simulation should be paired with experimentation; and each should profit from other.

We thank the referee for pointing out and explaining some of the very interesting projects his team has been working on. Fortunately, his review will stay available for future use on the GMD webpage of our article.

After our recently observation of Long Lasting Low energy TGEs (LLL TGEs) – a hours extending flux of gamma rays of 0.3 − 3 MeV energies, we started a cycle of simulations to get answer if remote Extensive Cloud Showers (ECSs) can contribute to this flux, or we should consider stochastic electron acceleration by a "sea" of randomly distributed charges in the thundercloud. Thus, simulations are pairing with observations and with hypothesis testing.

We thank the referee for pointing out this very interesting work in progress.

Specific questions :

5 The emerging field of High Energy Atmospheric Physics studies events producing high energy particles and associated with thunderstorms, such as terrestrial gamma-ray flashes and gamma-ray glows. Without mentioning Thunderstorm Ground Enhancements (TGEs) this statement is biased. The difference in duration between TGF and gamma-ray glows can be explained by two possible different scenario to create runaway electrons. Largest TGE detection prove that long duration can be explained by the continuous acceleration and multiplication of seed electrons entering strong prolonged electric field. Such a condition can sustain for minutes and, so called, extensive cloud showers (ECSs) will produce fluxes of electrons, gamma rays and neutrons on the earth's surface, i.e. TGEs (see Chilingarian et al., 2017).

In the first version of the manuscript, the expression "Thunderstorm Ground Enhancements (TGEs)" is mentioned in the introduction (page 2, line 16 of the non-revised manuscript) but not in the abstract. We first decided not to

use it in the abstract for simplification for the reader, as we think they are not an intrinsically different phenomenon from gamma-ray glows. That is also the opinion expressed in the review paper *Dwyer et al.* (2012). However, it is not a problem to present the expression "thunderstorm ground enhancements" in the abstract too.

page 1, line 3 of the revised manuscript : The expression "thunderstorm ground enhancements" was added in the abstract.

In general, this issue touches on present discussions in the HEAP community, but giving a judgment of who is "right" about it, is far from the scope of our article.

1.3 5 "The physics behind TGF, TGF afterglows and gamma ray glows are studied with the help of computer simulations, which necessarily involves model reduction and assumptions."

Hopefully physics is experimental science and most of results are obtained by experimentation, not simulation.

We think that a lot of important results in the HEAP community were obtained by comparing experimental results with simulations, together with analytical calculations. The sentence has been reworded to be more adequate.

page 7, line 4-6 of the revised manuscript : "The physics behind TGF, TGF afterglows and gamma- ray glows are studied with the help of computer simulations, which necessarily involves model reduction and assumptions."
→ "Apart from analytical calculations, the physics behind TGFs, TGF afterglows and gamma-ray glows are also studied with the help of experimental data, computer simulations, and often a combination of both."

4.3.1 5 Figure 7 compares the electron spectra recorded at 128 meters, for an electric field E = 0.80 MV/m, for a RREA generated from 200 seed electrons with ε = 100 keV. Do you especially choose the field never measured in the atmosphere (0.8 MV/m) ?

First of all, we found in the literature one reported measurement from balloon soundings, that shows an electric field of about 200 kV/m at 12 km altitude (see *Stolzenburg and Marshall* (2009), figure 3.2 on page 65). As a reminder this is equivalent to about 0.86 MV/m at sea level, as it scales with density. In this article, such a field is associated with the balloon being close to a lightning leader. All the results are presented at STP for reference, but can be scaled to higher altitude (-> lower densities), the scaling of the different parameters being function of air density.

Furthermore, it is important keep in mind that the codes we are testing here are used by researchers that try to explore extreme hypothetical cases, because it is what may be needed to explain some gamma ray glows, and TGFs. Monte Carlo codes are routinely used by some researcher in the HEAP community in such regimes. The TGF production mechanism in particular is poorly understood, but it may require extreme potentials (>200 MV), leading to electric fields of $E = 0.80$ MV/m or more; maybe only possible for extreme thunderstorms, where measurement are not easy to get (because of rarity, and extreme conditions); maybe only possible from some extreme lightning leaders or thunderstorm configurations.

In addition, an electric field of $E = 0.80$ MV/m is about three time less the classical breakdown field ≈ 3 MV/m at sea level, and we cannot exclude that such fields can exist, at least on a small scale and/or at high altitude (with the proper scaling factor), at which it is rather complicated to obtain in-situ measurements. In particular, simulations investigating the cold runway mechanism can require to simulate localized electric fields of 4 MV/m or more, as presented, e.g., in the recent theoretical work of *Lehtinen and Østgaard* (2018). This last article also points out that 1 MV/m is the typical field in the electrode gap used in laboratory spark experiments (typically 1 meter distance), that is also a possible application of the models used in this study; even if when simulated, these high electric fields usually extend only in a very short range (centimeter or less) and time ($\sim$ micro-second scale).

Page 3, lines 8-13 of the revised manuscript: For completeness, a sentence was added in the introduction about x-ray emissions observed in laboratory spark experiments with a series of interesting references.

Or it is not in atmosphere?

All the electric fields of this study are applied in the earth's atmosphere at sea level, Standard Temperature and Pressure (STP).

Why 128 m? Where do you inject 200 electrons?

For the results presented in this figure, 200 electrons are generated at the origin $(x = 0, y = 0, z = 0)$, the record is made at 128 m $(x = 0, y = 0, z = 128)$, z being the direction of the electric field, and electrons are accelerated towards positive z.

This was clarified throughout the text, also responding to a comment of referee #2. See page 24, figure 7; page 25 figure 8; page 22, line 19 and page 23, line 21.

This distance of 128 m is chosen because it corresponds to a large enough number of avalanches lengths (about 8.5 avalanche lengths in this case), that corresponds to a maximum multiplication factor of about 5000, where we are sure that RREA is fully developed and has reached the self-similar state. Such multiplication factor were also necessary to be able to produce a database with enough statistic to build, with low noise, the avalanche length and avalanche times curves (figure 3 and 4).

page 22, line 20-21 of the revised manuscript : a sentence was added to justify the record at z=128 meters.

Spectra where the particles are recorded at sorter distances are also presented in the supplementary material, and correspond to snapshots of the RREA evolution with lower multiplication factors.

Furthermore, a multiplication factor of 1000 or more can be obtained by some groups when they attempt to model possible TGF production mechanisms (see, e.g., (*Dwyer*, 2008; *Carlson et al.*, 2010)), and may also be necessary to explain the most extreme gamma-ray glow observations, where increases of the background intensity of this order of magnitude were detected (see, e.g., (*Eack et al.*, 1996; *Eack et al.*, 2000), and some up-coming glow studies).

One way of deciding which model is the most accurate might be to compare these results with experimental measurements. but in the context of TGF and Gamma-ray glows it is complicated to get a proper measurement of electron spectra produced by RREA. Finally, yes, only way to decide which model is true is the comparison with experiment that is missing in this paper.

See response to the general comment above.

Others changes (not directly suggested by referees)

During the revision process, several extra improvements to the paper were suggested by the authors:

- *Page 16, line 26 of the revised manuscript: A citation to the article "Fundamental parameters of the relativistic runaway electrons avalanche in air" by Babich et al. (2004) was added; as it is an important study to mention in the context of this work.*

- *Page 2, line 21 of the revised manuscript: For completeness, we added two citations to the recent gamma-ray glow observations of (Kochkin et al., 2018; Dwyer et al., 2015) in the introduction.*

- *abstract (page 1-2): Improvements in the English, added more details on the Electric field range.*

- *conclusions (page 26-27): Improvements in the English, added more details on the Electric field range, and more details.*

- *The second paragraph of the introduction (page2, line 11-13) was updated to give two more interesting citations about TGF satellite observations (one for RHESSI, one for AGILE and a more recent one for Fermi).*

- *Figure 2: The 10%, 50% and 90% probability contours for the REAM model (red curves) were added, together with a paragraph discussing how it compares with Geant4 (Page 13-14, lines 34-35 and 1-9).*

- *Page 3, lines 29-32 of the revised manuscript: We added a small paragraph clarifying the differences between the different values (between 2.36 and 3.2 MV/m) of the classical breakdown field, that can been seen in the literature.*

- *Page 13, lines 4-5 of the revised manuscript: a sentence was added to justify the use of this particular $\{E,\epsilon\}$ set.*

- *Page 23, lines 1-4 of the revised manuscript:* a sentence indicating why an electric field of $E = 0.80$ MV/m is used for the comparison case was added.

- *Page 13, lines 15-16 of the revised manuscript:* an indication that we provide Geant4 examples source codes with tweakale α_R and $\delta\ell_{max}$ parameters was added.

- Page 12, lines 23-25 of the revised manuscript: We added a sentence about the chosen direction of the initial electrons in the RREA probability simulation and its impact on the probability.

References

Babich, L. P., E. N. Donskoy, R. I. Il'kaev, I. M. Kutsyk, and R. A. Roussel-Dupre (2004), Fundamental parameters of a relativistic runaway electron avalanche in air, *Plasma Physics Reports*, *30*(7), 616–624, doi:10.1134/1.1778437.

Carlson, B. E., N. G. Lehtinen, and U. S. Inan (2010), Terrestrial gamma ray flash production by active lightning leader channels, *Journal of Geophysical Research: Space Physics*, *115*(A10), doi:10.1029/2010JA015647.

Dwyer, J. R. (2008), Source mechanisms of terrestrial gamma-ray flashes, *Journal of Geophysical Research: Atmospheres*, *113*(D10), n/a–n/a, doi:10.1029/2007JD009248, d10103.

Dwyer, J. R., D. M. Smith, and S. A. Cummer (2012), High-Energy Atmospheric Physics: Terrestrial Gamma-Ray Flashes and Related Phenomena, *Space Science Review*, *173*, 133–196, doi:10.1007/s11214-012-9894-0.

Dwyer, J. R., D. M. Smith, B. J. Hazelton, B. W. Grefenstette, N. A. Kelley, A. W. Lowell, M. M. Schaal, and H. K. Rassoul (2015), Positron clouds within thunderstorms, *Journal of Plasma Physics*, *81*(4), 475810405, doi:10.1017/S0022377815000549.

Eack, K. B., W. H. Beasley, W. D. Rust, T. C. Marshall, and M. Stolzenburg (1996), Initial results from simultaneous observation of x-rays and electric fields in a thunderstorm, *Journal of Geophysical Research: Atmospheres*, *101*(D23), 29,637–29,640, doi:10.1029/96JD01705.

Eack, K. B., D. M. Suszcynsky, W. H. Beasley, R. Roussel-Dupre, and E. Symbalisty (2000), Gamma-ray emissions observed in a thunderstorm anvil, *Geophysical Research Letters*, *27*(2), 185–188, doi:10.1029/1999GL010849.

Kochkin, P., D. Sarria, C. Skeie, A. P. J. Deursen, A. I. Boer, M. Bardet, C. Allasia, F. Flourens, and N. Østgaard (2018), In-flight observation of positron annihilation by ildas, *Journal of Geophysical Research: Atmospheres*, *0*(0), doi:10.1029/2018JD028337.

Lehtinen, N. G., and N. Østgaard (2018), X-ray emissions in a multiscale fluid model of a streamer discharge, *Journal of Geophysical Research: Atmospheres*, *123*(13), 6935–6953, doi:10.1029/2018JD028646.

Rutjes, C., D. Sarria, A. B. Skeltved, A. Luque, G. Diniz, N. Østgaard, and U. Ebert (2016), Evaluation of monte carlo tools for high energy atmospheric physics, *Geoscientific Model Development*, *9*(11), 3961, doi:10.5194/gmd-9-3961-2016.

Skeltved, A. B., N. Østgaard, B. Carlson, T. Gjesteland, and S. Celestin (2014), Modeling the relativistic runaway electron avalanche and the feedback mechanism with geant4, *Journal of Geophysical Research: Space Physics*, *119*(11), 9174–9191, doi:10.1002/2014ja020504.

Stolzenburg, M., and T. C. Marshall (2009), *Electric field and charge structure in lightning-producing clouds*, Springer.

2 Response to Referee # 2 (with relevant changes listed with italic font)

Response to referee #2

We thank the Referee for his careful reading, and the valuable comments and suggestions he made that helped to improve the quality of the manuscript. We considered each of the comments and questions and provided an adequate answer. The comments of Referee #2 are written in bold and the answers in plain text. Sentences indicating a modification to the manuscript are written using italic font.

The latex diff of the revised manuscript, accounting for comments of referees #1 and #2 is provided as an attached file.

Response to the general comment

Specific questions :

Abstract:

The authors mention the "effects of electric fields" (l. 5). I assume, this study is only about ambient fields and does not include self-consistent electric fields by solving the Poisson equation.

Indeed, the study does not include self-consistent electric fields.

The abstract has been updated to indicate the range of electric field we used to avoid the necessity to have self consistent models.

Also, in line 10, it would already good to mention what kind of "stepping methodology" (line 10) is meant, i.e. of particles.

page 1, line 10 of the revised manuscript: The sentence has been updated to indicate "[...] stepping methodology of particles [...]".

The authors mention that they only tested electric fields until 3 MV/m; however, the electric field for thermal runaway, i.e. for all electrons to run away irrespective of their initial energy, is approx. 26 MV/m, why not consider fields between 3 MV/m and 26 MV/m?

We did do a range of electric fields when investigating the runaway threshold, but we were limited to classical breakdown threshold for the chosen set-up / approximations. To go above classical breakdown, lower energy physics and self consistent electric fields must be considered. And the latter is not possible for Geant4 because of the space oriented, non-synchronous particle trajectories.

The reason why we chose not use E-fields above 3 MV/m has been has been added or clarified in three parts of paper: page 3, line 27-28; page 4, line 7-8; page 8, line 13-16

1. Introduction:

1.1: line 4: If it is about observations of high-energy phenomena, I would suggest to cite Fishman et al., 1994 in addition to Williams, 2010.

We agree that citing (*Fishman et al.*, 1994) is relevant here.
page 2, line 9 of the revised manuscript: the suggested citation was added.

1.2: In line 14, the authors talk about the energy regime of HEAP. However, they do not define this energy regime. Please be more precise in defining the energy range.

The energy regime we are considering here is up to about 100 MeV. However we think now that it was over-stating to qualify it "the energy regime of HEAP", since, some researchers in the community may encounter higher energies, e.g. when working on cosmic rays and lightning.

page 4, line 2 of the revised manuscript: "In the energy regime of HEAP, ..." → "In the energy regime of a kilo-electronvolt to a hundred of mega-electronvolts, ...".

Futhermore, the authors write that some individual electrons do not survive. Especially, for high-energy electron beam, it would be good to name the reason for this.

Any electron has a chance to undergo "hard" collisions where a large amount of energy is transferred to the photon in a bremsstrahlung or ionisation interaction. In such interaction, if the energy drops below the runaway threshold (or the energy threshold, as both should ideally bet set to similar values), it is a process that removes a high energy electron from the considered population. We agree with the referee that it can be indicative to give this reason in the article.

page 4 line 16-17 of the revised manuscript: the reason just described here was added.

Also, please specify what values you consider "much larger than the ionisation threshold" (page 3, lines 23-24).

Such a value can be set to above a few keV.

page 4, line 19-20 of the revised manuscript: an indicative value of "a few kilo-electronvolts" is now specified.

On page 4, lines 14-15, the authors write "The minimum energy $\epsilon_2^{\min}$ that can runaway is given by the requirement $F(\epsilon_2^{\min}) > E$ [...]." But should the friction force not be smaller for runaway? Please clarify this.

The friction force is split into two parts. One part is below the electron low energy cutoff and used as a friction. The other part is considered by explicit discrete collisions. This first friction part for electrons above 10 keV is indeed a function of energy and decreases for increasing electron energy, but converges to a constant for electron energies above 1 MeV. So the lower the energy, the higher the friction and the threshold $F(\text{electron energy}) = qE$, lies orders of magnitude higher than ionization energy (i.e. ≈ 10 eV comparing to ≈ 10 keV).

Also, to be more correct, it is $q \times E$ that has the unit of the friction force F.

page 5, line 13 of the revised manuscript: "$F(\epsilon_2^{\min}) > E$" was changed to "$F(\epsilon_2^{\min}) \approx q\,E$"

On page 5, the authors discuss the angular dependency (between the electron motion and electric field direction) on the run-away process. This has already been discussed very extensively by [O. Chanrion et al., 2016. Influence of the angular scattering of electrons on the runaway threshold in air. Plasma Phys. Contr. Fus., vol. 58, 044001]. Please cite this article.

This article was already cited in another section of the non-revised manuscript (p.2, line 28). But we agree that citing it again inside this section discussing the angular effects is a good idea.

page 6, line 22 of the revised manuscript: A second citation to the article (Chanrion et al., 2016) was added.

2. Model descriptions:

2.1: The authors say that different sets of electro-magnetic cross sections are used. However, the authors do not state (neither in the main text nor in the supplementary material) which processes are actually taken into account. This is clearly missing, but crucial since simulation results strongly depend on the chosen processes and cross sections. The authors state where the cross sections come from and they make some comparison plots in section 8 of the supplementary material, but only for a few processes. Say, in the future, other researchers want to compare their results. Then, the knowledge of the used cross section data is crucial to interpret results. I would thus suggest to elaborate more on the processes and cross sections.

We agree with this point: it would be more practical for future researchers that would like to use this work to have an easy-to-read summary of the process and which cross section sets are used by the models we tested.

We added a table providing all this information (i.e. processes cross sections and/or models used by each code) as part of the supplementary material .pdf file (section 13). We also added a reference to this table in the revised manuscript (page 8, lines 4-5).

2.2: On page 8/line 29, the authors say that GRRR uses the "energy at that instant" to calculate the collision rate ν_k . However, it is not clear which energy: the energy of each individual particle, the maximum energy of all particles or the mean energy of all particles. Please clarify.

Thanks for pointing out this ambiguity. Now we state clearly that it is the energy of each particle that is used to calculate collision rates.

page 10, line 9 of the revised manuscript: "the rate ν_k is calculated using the energy at that instant" $\rightarrow$ "the rate ν_k for each particle is calculated using that particle's energy at that instant".

2.4.1: For space-oriented codes, "a single particle is simulated over its entire life-time" (page 9/line 21). However, what is the reason to lose an electron (especially in the regime above several keV). The only reason to lose an electron would be attachment to air molecules. However, for this process to occur the electron normally needs to lose more energy than down to 10 keV. Please be more precise here.

Our wording "a single particle is simulated over its entire life-time" was not accurate, since the particles are usually simulated until they go below the energy threshold, for most of the codes. Note that Geant4, by default, does simulate all primary particles down to zero energy (the "energy threshold", in Geant4, is a minimum energy for the secondary produced particles to be tracked or not). As shown in the section 3 (RREA probability study), the probability for an initial electron to produce a RREA is negligible below 10 keV. In this energy range, the electrons will slow down in a small length and time scale; and indeed it is only when they go down to energy in the eV scale that they will attach to air molecules and that we can consider that it is "really lost"; and this will happen a little bit later in their lifetime.

Page 1, line 4 of the revised manuscript : "a single particle is simulated over its entire life-time" $\rightarrow$ "is simulated until it goes below the low energy threshold ϵ_c, chosen by the user". We also repeated the precison that Geant4 follows all primary particles until zero energy (that was also indicated before in the Geant4 description section 2.1).

2.4.2:Why would "acceptable values of $\delta\ell_{max}$ depend on the electric field" (page 10/line 28)? It is very clear that it should be smaller than the electron's mean free path. But the mean free path depends on the electron energy rather than on the electric field. Please clarify the dependence on the electric field.

The gain or loss in energy by a particle due to the E-field depends on the distance it propagated along its direction, and its magnitude. The electron may move from point A to point B, and could do a collision or a null-collision at point B. The result of the collision at point B depends on the (differential) cross sections at this point, that depends on the energy, that depends on the energy it gained (or lost) when traveling from A to B, that depends on the electric field and the distance between the two points , that will be affected by $\delta\ell_{max}$ in some case. For the tracking to be accurate, the cross sections should remain approximately constant between point A and B, that is

3

only acceptable if the A-B distance is not too high. The mean free path is important, but so is also the distance at which the gain in energy due to the electric field is small enough so that the change in the cross sections between point A and B is small enough. Depending on the context, it could be greater or smaller than the mean free path, and one should always use a step length that is small enough compared to both quantities. In Geant4, that can be achieved by forcing the maximum acceptable step $\delta\ell_{max}$ to be small enough, or, more cleverly, by reducing the α_R parameter. However, an exact quantification of the dependence of the good values of $\delta\ell_{max}$ (or α_R) for different electric fields is not easy to perform, and would require extra simulations, that we did not have time to run.

However we think this explanation should not be included in the main text, since is bit too long and we could not precisely quantify the dependency of $\delta\ell_{max}$ with E. Thankfully, this response to the reviewer will be available in the GMD web-page of this paper.

3. Probability of generating RREA:

In Figure 1, the authors present the probability that a single electron with an initial energy of 75 keV in an ambient field of 0.8 MV/m creates an RREA. As a criterion, they use that at least 20 electrons with an energy of 1 MeV are created. Please specify which value for $\delta\ell_{max}$ is used in panel a) and which value for α_R is used in panel b).

The values are the default ones. That is $\delta\ell_{max} = 1$ km and $\alpha_R = 0.2$ for O4 and $\alpha_R = 0.8$ for O1.

page 14 of the revised manuscript: The caption of figure 1 has been updated to indicate this.

However, I am confused, though. The friction force based on [A.V. Gurevich, 1961. On the theory of runaway electrons. Sov. Phys. JETP-USSR, vol. 12, pp. 904–912] is supposed to be 0.65 MeV/m for a 75 keV electron, thus the ambient field is definitely sufficient to accelerate the electron into the run-away regime. Of course, this does not mean that 20 electrons with energies are above 1 MeV, but 12% seems low.

The RREA probability value for this case is around 10 to 12% and is given by two independent codes (GRRR and Geant4). We think that going from the (average) friction force to this probability is by no means straightforward, as it is a stochastic process, and it requires computer simulations to be evaluated (as far as we known). We encourage other researchers to evaluate this probability independently, and maybe by different methods from Monte-Carlo if possible.

But this might depend on the simulation time. How long has the shower been simulated?

The simulation is running for as much time as needed for one of the two possibilities to happen for each single electron seed:

- [i]: it is absorbed

- [ii]: there is at least 20 electrons of more than 1 MeV in the system.

The simulation space is large enough so that the particles will never encounter the border. In pratice, for this configuration ($\epsilon = 75$ keV and $E = 0.80$ MV/m), the electron time is ≈ 2 ns (times are given from the global / laboratory fame) if [i] is reached and ≈ 230 ns on average if [ii] is reached. For information, it takes ≈ 190 ns on average if 10 electrons of more than 1 MeV are required, ≈ 130 ns for 5, and ≈ 17 ns for 1.

It would also be good to see the RREA percentage for different criteria (20 electrons above 1 MeV, 10 electrons above 1 MeV, 5 electrons and finally 1 electron above 1 MeV which should give almost 100%).

The RREA percentages as function of the number of 1 MeV electrons requested are presented here for two cases: ($\epsilon = 75$ keV, $E = 0.8$ MV/m) and ($\epsilon = 800$ keV, $E = 0.35$ MV/m). It was obtained using the Geant4 O4 model with $\alpha_R = 0.001$.
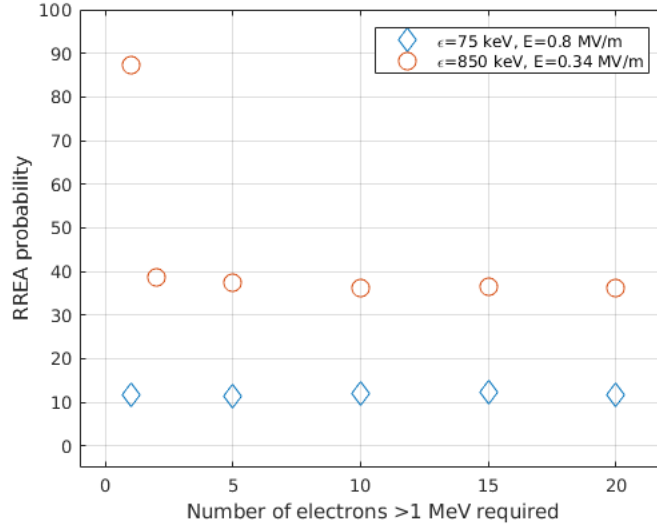
For the ($\epsilon = 75\,\text{keV}$, $E = 0.8\,\text{MV/m}$) case, the probability does not significantly changes if 20, 10, 5 or 1 electron of more than 1 MeV are required. This result is actually consistent with the RREA probabilities we found for higher energy electron seed with the 0.8 MV/m field (see supplementary material section 5.2, or the figure just below here). Once the seed electron has reached 1 MeV, then its probability to generate the 20 MeV electrons in the 0.8 MV/m field is 100 %. Actually, for this values of (ϵ, E), what mainly affects the final probability is what happens at the start of the simulation. i.e. if the single initial electron is able to gain enough energy, or goes below the energy threshold before (that is here set to 990 eV). However, for ($\epsilon = 75\,\text{keV}$, $E = 0.8\,\text{MV/m}$), the "required number of 1 MeV electrons" does play a significant role in the probability. It is coherent with what is indicated in the manuscript: "The difference [between requiring 1 or 20 MeV electrons] is mainly noticeable for low electric field (< 0.4 MV/m) and high seed energies (> 700 keV)." (page X, lines XX)

Supplementary material, section 5.3: the previous plot was added as the reader may be interested to know this information.

page 12, line 32-33 of the revised manuscript: a reference to this plot in the supplementary material was added.

In Figure 2, the authors show the avalanche probabilities (10%, 50% and 90%) as a function of initial electron energy and ambient electric field. What about the right top (high energy, high field) and bottom left (low energy, low field) part? What are the probabilities there?

Plots indicating the values for the other probabilities for the four models are presented in the supplementary material (section 5). For high field or high energy, the probability is 100%, For low field and low energy, the probability is 0%.

However, the primary objective of figure 2 was not to present the full probability domain, but to compare the codes for three probabilities in-between the 0% and the 100% case, where we expected to see most of the differences. Furthermore the 0% and 100% contour lines tend to be more noisy than the three other ones, making it more difficult to compare the models. However for the Geant4 O4 model (supposingly the most accurate model), we could build a distribution with very large statistics ($>$50,000 seeds per parameter set), and we could produce a noiseless plot with the 0%, 10%, 50%, 90% and 100% probabilities contour lines :

(b)
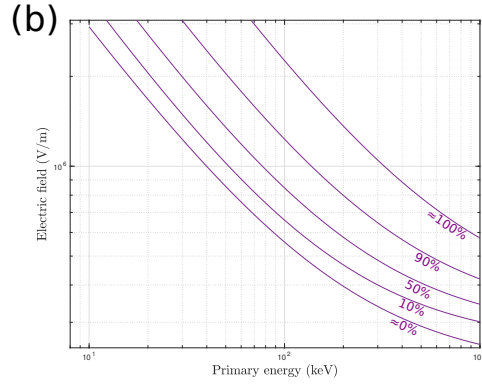
There is so much space in this figure. Why not add some curves or values for these two regimes.

As suggested by thre referee, we think it will be helpful for the reader to see the level curves corresponding these two regimes, i.e. the 0% and the 100 % levels. So we integrated this last plot in the manuscript in addition to Figure 2 (→"Figure 2.b."). And the former "Figure 2" is now "Figure 2.a."

However we don't want to add more level curves (e.g. from other codes) to Figure 2.a. because it will make it hard to read.

4. Characterisation of RREA showers:

When discussing the evolution of the self-similar state , the authors say that they used a different number of seed electrons for Geant4, REAM and GRRR (page 16, lines 12–13). For consistency, I suggest to add one more case where the same number of seed electrons is used.

For very large electric field (> 2 MV/m), Geant4 used 200 seed electrons, but GRRR only used 20 and REAM used 16, due to limitations in our computation resources. In addition for low E-fields, only a few of the 200 sampled electrons did trigger a RREA for O1 and REAM (as the RREA probability is low for $\epsilon = 100$ keV, $E = 0.8$ MV/m), meaning also larger error bars for the two models. As we do not have the capability to run GRRR or REAM with larger statistics, the cases with the same number of seed electrons would mean showing Geant4 results with lower statistics. But we think this is not really necessary: it will make the figure less readable, without providing extra information. Actually, the uncertainty intervals for Geant4 simulations with reduced statistics can be easily guessed: they would expand by about a factor of 3.2 ($\approx \sqrt{\frac{200}{20}}$) for 20 seeds and 3.5 ($\approx \sqrt{\frac{200}{16}}$) for 16 seeds.

Figure 5 shows the time to reach the self-similar state. Comparing all the different models, it seems that the time to reach that is consistent within one order of magnitude. I propose to add this to line 14 on page 16.

Indicating that the models are consistent within one order of magnitude is largely over-evaluating the difference, since:

- Without considering the error bars, the relative difference between the models is never more than 200%

- for most of the electric fields, the models are consistent within the statistical error bars; that are a bit large for REAM and GRRR due to the limited amount of seed electrons we could simulate

We think the way it is is already discussed in the non-revised manuscript is good and should not be changed.

4.3.1: In Figure 6, the authors present the mean energy (of the self-similar state) as a function of the ambient field. It might be good to remind the reader in the figure caption which value for α_R was used here for O1 and O4.

The value of α_R is set to the default for O1 and O4, that is 0.8 and 0.2 respectively. In this case the maximum acceptable step of 1 millimeter ensures that we have accurate simulations.

Page 21: the caption of figure 6 has been updated to give the suggested information.

6

I am wondering how the plots for O1 and O4 would look for α_R. It would be good to plot one case for a different α_R to show the dependence of the mean electron energy as a function of α_R.

The main point of this section (4.3) of the paper is to compare the models in the case were we think they are set-up optimally, so we do not think that adding this α_R comparison in this section is a good idea. In the original (and revised) manuscript, we just show one case where the maximum acceptable step is too large to give the reader an idea of how bad it can be, without discussing it further.

However it is informative to see if reducing α_R makes the mean energies converge towards similar values compared to reducing $\delta\ell_{max}$ to 1 mm. *We added plots of mean energy as function of α_R for O1 ($\delta\ell_{max}$ is set to 1 cm to have a common reference with figure 6), in the supplementary material (section 7), for several electric fields.* Unfortunately, we could not cover the same number of electric fields, and could not simulate the same number of seed (i.e. the new data is more noisy).

Page 21, line 12-13 of the revised manuscript: A reference to the supplementary material pointing to this curve was added. Here is a reproduction of this curve:
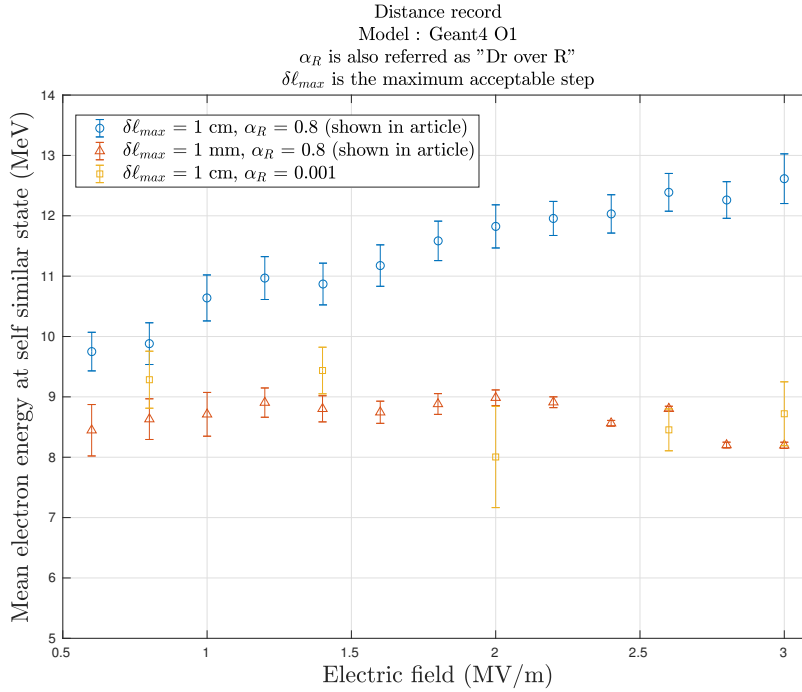
As expected, $\delta\ell_{max} = 1$ mm is close to $\delta\ell_{max} = 1$ cm with $\alpha_R = 0.001$

In Table 2, the authors present the fit parameters a_1, a_2 and a_2 of Eq. (20) for different models. Please add the error bars in order to judge the quality of these fits.

Table 2 (page 22) has been updated to give confidence intervals on the fitted parameters a_1, a_2 and a_2, and the text was also updated accordingly (page XX, line XX-XX). The best fit values have also been re-evaluated compared to the previous version of the manuscript.

We want to make clear that the confidence intervals given are not error bars. They indicate what is the range of values of the three parameter that are able to give good quality fits, assuming a 95% confidence threshold. The quality of the fits can be evaluated using the r-squared coefficient, and it is larger than 0.90 for all the fits of table 2, meaning that the model (equation 20) fits very well the data, as can be qualitatively observed in Figure 6.

In Figure 7, the authors present the electron spectra at 128 m. But does 128 m refer to the z-coordinate or to the travelled distance $r = (x^2 + y^2 + z^2)^{1/2}$. Please clarify this in the figure caption and in line 5 (page 19), line 2 (page 20) and in the caption of Figure 8.

The distance of 128 meters refers to the Z coordinates (-Z being the direction of the E-field so that electrons are accelerated towards positive Z).

page 24, figure 7, page 25 figure 8, page 22, line 19 and page 23, line 21: the manuscript were updated as requested.

4.3.2: In section 4.3.2, the authors state that a comparison with photon measurements is difficult because of the attenuation of photons in air. Whereas I agree in general, there are some issues I would like to address. The authors say that a 100 keV photon at 12 km altitude travels 1540 m in average, a 50 keV photon 671 m and a 20 keV photon 63 m. Where do these values come from? Is this a result of their simulations (if so, how did you obtain these); if not, please cite your source. I made a brief comparison with NIST data (http://physics.nist.gov/PhysRefData/Xcom/Text/XCOM.html) and obtained attenuation lengths of approx. 2000 m for 100 keV, 1600 m for 50 keV and 500 m for 20 keV. This needs to be clarified.

The given average path lengths come from Geant4 simulations. It is a simple set up where M >10,000 mono-energetic photons are sampled (in air at 12 km density) and their total path length before absorption is recorded, and then the M length values are averaged. The standard deviations around the averages are also calculated and given in the article. If requested, we would be glad share the Geant4 source code.

We agree with the attenuation lengths given by the referee. However, the attenuation length and the average path length are different quantities: the average path length is lower because a photon will not keep the same attenuation length over his full track (it will be reduced at each step) since it is losing energy along its path. These mean path lengths values also have large variations from event to event (stochastic process) that are evaluated with the standard deviations indicated in the manuscript.

Page 24, line 2-4 of the revised manuscript : to clarify this point, a sentence was added.

Additionally, the authors say that the "photons have no chance to escape the atmosphere and to be detected by a satellite" (pages 20/21). I would like to remind the authors that the "average path travelled" (page 20/line 14) or the attenuation length is only an average. Hence, there can always be photons which escape the atmosphere and may be detected at satellite altitudes even though the probability is low. Actually, Fermi has measured photons with energies between 10 and 500 keV (see https://gammaray.nsstc.nasa.gov/gbm/science/terr_grf.html). Please be more precise here.

It is close to impossible for a photon of less than 500 keV to reach space, if it is emitted from 12 km altitude (and even more impossible for 100 keV photons). The vast majority of photons (if not all of them) observed below 500 keV by the Fermi space telescope (and also RHESSI) are actually photons that, at emission, had larger energies (likely more than 1 MeV) and lost some part of it by collisions with air, and eventually reached the satellite.

Page 24, line 6-11 of the revised manuscript : to clarify this point in the paper, three sentences was added.

For information, here is a plot giving the probability of photons to escape the atmosphere as function of energy, assuming a source at 12 km altitude:
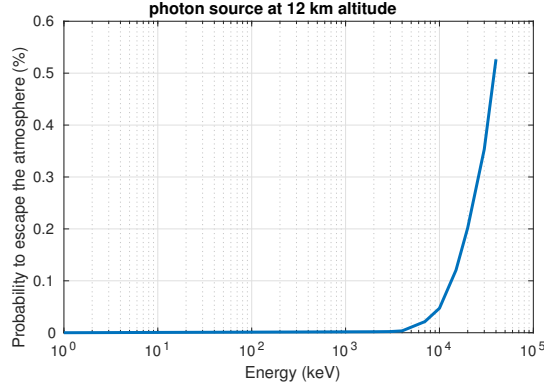
Note that, even for 40 MeV photons, the probability to escape is less than 1%, indicating that if a TGF is produced from this altitude, it must be very strong to be detected in space. The curve was obtained from Geant4 simulations and, if requested, we would be happy to share the source code.

Supplementary material, section 14 : the previous curve was added, as it may be helpful for other researchers.

4.4: In the supplementary material, section 9.2., I cannot find any plot showing the parallel velocity $\beta_\parallel$ (only the mean Z speed; or is the mean Z speed meant to be $\beta_\parallel$). Maybe, it is there, but at least not apparent. Could the authors please point me to the correct plot?

The mean $\beta_\parallel$ and the mean Z speed are indeed the same, since the the electric field is on the Z direction. We only compare mean $\beta_\parallel$ values and do not show the full distributions of $\beta_\parallel$.

Page 25, line 4 of the revised manuscript : the sentence has been updated to clarify this.

page 24, lines 24/25: The authors say that single Coulomb scattering would "increase the necessary computation time". Should using a single scattering (instead of multiple scattering) not decrease the computation time?

The number of interactions experienced by an electron (or positron) before being stopped increases with its kinetic energy and so a detailed simulation becomes very demanding in computation time at high energies: that's why multiple scattering method were developed. The idea behind the multiple scattering algorithms is to avoid to explicitly simulate every "hard" collision of every single electron (i.e. avoid doing single scatterings), but to do multiple scatterings inside one step length (or one collision). It permits to use step lengths substantially larger (usually >10 times) compared to a pure single scattering strategy, and so reduces the necessary computation time to simulate the propagation of a given electron (or positron), but can be less accurate. Such algorithms usually rely on several tweakable parameters that should be optimized to shorten necessary computation time while keeping an acceptable physical accuracy. Remark also that what is maybe the biggest difference between {REAM-GRRR} and {Geant4 O1-O4} (in the set-ups used in this paper), is that the former use single (Coulomb) scattering algorithms and the later uses multiple scattering.

Page 28, lines 4-7 of the revised manuscript : the point about single scattering has been updated to clarify this.

Technical corrections:

All the suggested technical correction have been applied. We thank the referee for his very careful reading.

Others changes (not suggested by referees)

During the revision process, several extra improvements to the paper were suggested by the authors:

- *Page 16, line 26 of the revised manuscript: A citation to the article "Fundamental parameters of the relativistic runaway electrons avalanche in air" by Babich et al. (2004) was added; as it is an important study to mention in the context of this work.*

- *Page 3, lines 8-13 of the revised manuscript: A sentence was added in the introduction about x-ray emissions observed in laboratory spark experiments, that is also a potential case where the models we are comparing can be applied.*

- *Page 2, line 21 of the revised manuscript: For completeness, we added two citations to the recent gamma-ray glow observations of (Kochkin et al., 2018; Dwyer et al., 2015) in the introduction.*

- *abstract (page 1-2): Improvements in the English, added more details on the Electric field range.*

- *conclusions (page 26-27): Improvements in the English, added more details on the Electric field range, and more details.*

- *The second paragraph of the introduction (page2, line 11-13) was updated to give two more interesting citations about TGF satellite observations (one for RHESSI, one for AGILE and a more recent one for Fermi).*

- *Figure 2: The 10%, 50% and 90% probability contours for the REAM model (red curves) were added, together with a paragraph discussing how it compares with Geant4 (Page 13-14, lines 34-35 and 1-9).*

- *Page 3, lines 29-32 of the revised manuscript: We added a small paragraph clarifying the differences between the different values (between 2.36 and 3.2 MV/m) of the classical breakdown field, that can been seen in the literature.*

- *Page 13, lines 4-5 of the revised manuscript: a sentence was added to justify the use of this particular $\{E,\epsilon\}$ set.*

- *Page 23, lines 1-4 of the revised manuscript: a sentence indicating why an electric field of $E = 0.80$ MV/m is used for the comparison case was added.*

- *Page 13, lines 15-16 of the revised manuscript: an indication that we provide Geant4 examples source codes with tweakale α_R and $\delta\ell_{max}$ parameters was added.*

- Page 12, lines 23-25 of the revised manuscript: We added a sentence about the chosen direction of the initial electrons in the RREA probability simulation and its impact on the probability.

References

Babich, L. P., E. N. Donskoy, R. I. Il'kaev, I. M. Kutsyk, and R. A. Roussel-Dupre (2004), Fundamental parameters of a relativistic runaway electron avalanche in air, *Plasma Physics Reports*, *30*(7), 616–624, doi:10.1134/1.1778437.

Chanrion, O., Z. Bonaventura, A. Bourdon, and T. Neubert (2016), Influence of the angular scattering of electrons on the runaway threshold in air, *Plasma Physics and Controlled Fusion*, *58*(4), 044001, doi:10.1088/0741-3335/58/4/044001.

Dwyer, J. R., D. M. Smith, B. J. Hazelton, B. W. Grefenstette, N. A. Kelley, A. W. Lowell, M. M. Schaal, and H. K. Rassoul (2015), Positron clouds within thunderstorms, *Journal of Plasma Physics*, *81*(4), 475810405, doi:10.1017/S0022377815000549.

Fishman, G. J., P. N. Bhat, R. Mallozzi, J. M. Horack, T. Koshut, C. Kouveliotou, G. N. Pendleton, C. A. Meegan, R. B. Wilson, W. S. Paciesas, S. J. Goodman, and H. J. Christian (1994), Discovery of Intense Gamma-Ray Flashes of Atmospheric Origin, *Science*, *264*, 1313–1316, doi:10.1126/science.264.5163.1313.

Kochkin, P., D. Sarria, C. Skeie, A. P. J. Deursen, A. I. Boer, M. Bardet, C. Allasia, F. Flourens, and N. Østgaard (2018), In-flight observation of positron annihilation by ildas, *Journal of Geophysical Research: Atmospheres*, *0*(0), doi:10.1029/2018JD028337.

3 Manuscript with highlighted changes (marked-up manuscript version)

Evaluation of Monte Carlo tools for high energy atmospheric physics II : relativistic runaway electron avalanches

David Sarria[1], Casper Rutjes[2], Gabriel Diniz[2,3], Alejandro Luque[4], Kevin M. A. Ihaddadene[5], Joseph R. Dwyer[5], Nikolai Østgaard[1], Alexander B. Skeltved[1], Ivan S. Ferreira[3], and Ute Ebert[2,6]

[1]Birkeland Centre for Space Science, Department of Physics and Technology, University of Bergen, Bergen, Norway
[2]Centrum Wiskunde & Informatica (CWI), Amsterdam, The Netherlands
[3]Instituto de Física, Universidade de Brasília, Brazil
[4]Instituto de Astrofísica de Andalucía (IAA-CSIC), P.O. Box 3004, Granada, Spain
[5]University of New Hampshire Main Campus, Department of Physics, Durham, NH, United States
[6]Eindhoven University of Technology, Eindhoven, The Netherlands

Correspondence to: David Sarria (david.sarria@uib.no)

Abstract.

The emerging field of High Energy Atmospheric Physics studies ~~events producing~~ how high energy particles ~~and associated with thunderstorms, such as~~ are produced in thunderstorms, in the form of terrestrial gamma-ray flashes and gamma-ray glows (also referred as thunderstorm ground enhancements). Understanding these phenomena requires appropriate models of the interaction of electrons, positrons and photons with air molecules and electric fields. ~~This work is made as a continuation of Rutjes et al. (2016) , now including the effects of electric fields. We investigated~~ We investigated the results of three codes used in the community (Geant4, GRRR and REAM) ~~, for simulating the process of~~ to simulate Relativistic Runaway Electron Avalanches ~~. From analytical considerations, we show~~ (RREAs). This work continues the study of Rutjes et al. (2016) , now also including the effects of electric fields, up to the classical breakdown field, which is about 3.0 MV/m at standard temperature and pressure.

We first present our theoretical description of the RREA process, that is based and incremented over previous published works. This analysis confirmed that the avalanche is mainly driven by electric fields and the ionisation and scattering processes determining the minimum energy of electrons that can runaway, that was found to be above ≈ 10 keV for any fields up to the classical breakdown field.

To investigate this point further, we ~~used a first simulation set-up to estimate~~ then evaluated the probability to produce a RREA ~~from a relevant range of electron energies and electric field magnitudes~~ as a function of the initial electron energy and of the magnitude of the electric field. We found that the stepping methodology ~~is important, and the stepping parameters have~~ in the particle simulation has to be set up very carefully ~~for~~ in Geant4. For example, a too large step size can lead to an avalanche probability reduced by a factor of 10, or ~~to~~ a 40% over-estimation of the average electron energy. When properly set-up, both Geant4 models show an overall good agreement (within ≈ 10 %) with REAM and GRRR. Furthermore, the probability ~~for the~~ that particles below 10 keV ~~to~~ accelerate and participate in the ~~penetrating radiation is actually negligible for the full range of electric field we tested ($E < 3$ MV/m)~~ high energy radiation is found negligible for electric fields below the classical breakdown

1

~~value~~. The added value of ~~using models able to accurately track~~ accurately tracking low energy particles (~~< 10~~< 10 keV) is minor, and ~~is~~ mainly visible for ~~high E-fields (*E* > 2~~fields above 2 MV/m~~)~~.

In a second simulation set-up, we compared the physical characteristics of the avalanches produced by the four models: avalanche (time and length) scales, ~~time to~~ convergence time to a self-similar state and ~~photon/electron energy spectra~~ energy spectra of photons and electrons. The two Geant4 models and REAM showed a good agreement on all ~~the~~ parameters we tested. GRRR ~~also~~ was also found to be consistent with the other codes, except for the electron energy spectra. That is probably because GRRR does not include straggling for the radiative and ionisation energy losses, hence implementing these two processes is of primary importance to produce accurate RREA spectra. Including precise modelling of the interactions of particles below 10 keV (e.g. by taking into account molecular binding energy of secondary electrons for impact ionisation) also ~~provided~~ produced only small differences in the recorded spectra.

1 Introduction

1.1 Phenomena and observations in high energy atmospheric physics

~~Wilson (1925) had the conceptual awareness of the generation of high energy radiation from thunderclouds, already~~ In 1925, C.T.R. Wilson proposed that thunderstorms could emit a "measurable amount of extremely penetrating radiation of β or γ type" (Wilson, 1925) , about 60 years before ~~contemporary theoretical publications and observational results (Williams, 2010)~~ . ~~Traditionally, thunderclouds have been studied by classical electromagnetism, but understanding the production and propagation of high energy radiation from thunderstorms falls in the context~~ such radiation was observed from the atmosphere and from space (Parks et al., 1981; Fishman et al., 1994; Williams, 2010) . This, and subsequent observations and modeling are now being investigated withing the field of High Energy Atmospheric Physics (HEAP). A review is provided by Dwyer et al. (2012). ~~Two space missions specifically designed to study HEAP related phenomena will be available in the years 2018-2019 : ASIM (Atmosphere-Space Interaction Monitor) (Neubert et al., 2006) , successfully launched in April 2018; and TARANIS (Tool for the Analysis of Radiation from lightning and Sprites) (Lefeuvre et al., 2009; Sarria et al., 2017) .~~

Observationally different ~~penetrating radiation types~~ types of high energy emissions have been identified coming from thunderclouds, naturally categorized by duration. Microsecond-long burst of photons, which were first observed from space ~~(Fishman et al., 1994; Briggs et al., 2010)~~ (Fishman et al., 1994; Grefenstette et al., 2009; Marisaldi et al., 2014; Roberts et al., 2018) , are known as Terrestrial Gamma-ray Flashes (~~TGF). TGF produces~~ TGFs). TGFs also produce bursts of electron ~~positron pairs and positrons~~ (Dwyer et al., 2008; Briggs et al., 2011; Sarria et al., 2016) that follow the geomagnetic field lines into space ~~.~~ and show longer durations. Two space missions specifically designed to study TGFs and related phenomena will provide new observations in the near future : ASIM (Atmosphere-Space Interaction Monitor) (Neubert et al., 2006) , successfully launched in April 2018; and TARANIS (Tool for the Analysis of Radiation from lightning and Sprites) (Lefeuvre et al., 2009; Sarria et al., 2017) to be launched at the end of 2019.

Seconds to minutes or even hours long ~~of penetrating~~ X and gamma radiation have been observed on ground, from balloons and aircraft, by ~~McCarthy and Parks (1985); Eack et al. (1996); Torii et al. (2002); Tsuchiya et al. (2007); Adachi et al. (2008); Chilingaria~~

which are called gamma-ray glows or thunderstorm ground enhancements. ~~In between,~~ Some modeling attempts of both gamma ray and electron observations are also presented in Chilingarian et al. (2012).

TGFs were predicted to create a neutron emission on the millisecond duration, ~~a new radiation mechanism has been introduced as TGF afterglows by Rutjes et al. (2017) and measured by Bowers et al. (2017); Teruaki et al. (2017), based on the intermediate neutrons produced by a TGF, creating a prolonged and relocated signal~~ with associated isotope production (Babich, 2006). Such emission was observed from the ground (Bowers et al., 2017; Teruaki et al., 2017). A similar phenomenon was modeled at higher altitudes by Rutjes et al. (2017), that also proposed to call it "TGF afterglow".

Following the idea of Wilson (1925), ~~penetrating~~ high energy X and gamma radiation is created by runaway electrons, which may further grow by the effect of Møller scattering in the form of so called relativistic runaway electron avalanches (~~RREA~~ RREAs) (Gurevich et al., 1992). For the multiplication to occurre, a threshold electric field of $E_{\mathrm{th}} = 0.28$ MV/m (at STP) is required (Babich et al., 2004a; Dwyer, 2003).

The difference in duration between ~~TGF~~ TGFs and gamma-ray glows can be explained by two possible ~~different scenario~~ scenarios to create runaway electrons, which ~~traditionally is~~ is traditionally illustrated using the average energy-loss or friction curve (see, e.g., figure 1 of Dwyer et al. (2012)). In this curve, there is a maximum at around ~~$\varepsilon \approx 130$~~ $\varepsilon \approx 123$ eV, illustrating the scenario that for electric fields higher than ~~the~~ a critical electric field, of

~~maximally~~ $E_c \approx 26$ MV/m at standard temperature and pressure (STP), thermal electrons can be accelerated into runaway regime, described in the so-called Cold Runaway theory (Gurevich, 1961). The effective value of E_c may be significantly lower, as electrons could overcome the friction barrier due to their intrinsic random interactions (Lehtinen et al., 1999; Li et al., 2009; Liu et al., 2016; Chanrion et al., 2016). Cold Runaway could happen in the streamer phase

~~(Moss et al., 2006; Li et al., 2009; Chanrion and Neubert, 2010; Köhn and Ebert, 2015)~~
(Moss et al., 2006; Li et al., 2009; Chanrion and Neubert, 2010) or leader phase
~~(Celestin and Pasko, 2011; Celestin et al., 2012; Chanrion et al., 2014; Köhn et al., 2014, 2017)~~
(Celestin and Pasko, 2011; Celestin et al., 2012; Chanrion et al., 2014; Köhn et al., 2014; Köhn and Ebert, 2015; Köhn et al., 2017) of
a transient discharge, explaining the high energy electron seeding that will evolve to ~~RREA~~ RREAs and produce gamma-rays by bremsstrahlung emission from the accelerated electrons. The cold runaway mechanism may be further investigated with laboratory experiments, in high voltage and pulsed plasma technology, and may be linked to the not fully understood x-ray emissions that have been observed during nanosecond pulsed discharges and the formation of long sparks, (Rahman et al. (2008); Dwyer et al. (2008); Shao et al. (2011); Kochkin et al. (2016), and references therein), with different possible production mechanism that were proposed and tested using analytical modeling (Cooray et al., 2009) and computer simulations (Ihaddadene and Celestin, 2015; Luque, 2017; Lehtinen and Østgaard, 2018). Alternatively, the relativistic feedback discharge model is also proposed to explain TGF production using large scale and high potential electric fields (Dwyer, 2012), where the RREA initial seeding may be provided by cosmic-ray secondaries, background radiation, or cold runaway ~~(Dwyer, 2008; Celestin and Pasko, 2011)~~ (Dwyer, 2008).

For fields significantly below the thermal runaway critical electric field ~~E_c~~ $E_c \approx 26$ MV/m but above the RREA threshold electric field of ~~$E_{\mathrm{rb}} = 0.28$~~ $E_{\mathrm{th}} = 0.28$ MV/m (at STP), runaway behaviour is still observed in detailed Monte Carlo studies

~~(Dwyer et al., 2012)~~ (see Dwyer et al. (2012), and references therein). At thundercloud altitudes, cosmic particles create energetic electrons that could runaway in patches of the thundercloud where the electric field satisfies this criterion. ~~RREA~~ RREAs are then formed if space permits and could be sustained with feedback of photons and positrons creating new avalanches (Babich et al., 2005; Dwyer, 2007, 2012). Gamma-ray glows could be explained by this mechanism, as they are observed irrespectively of ~~lighting~~ lightning or observed to be terminated by lightning (McCarthy and Parks, 1985; Chilingarian et al., 2015; Kelley et al., 2015; Kochkin et al., 2017). The fact that gamma-ray glows are not (necessarily) accompanied by classical discharges, results in the conclusion that the electric fields causing ~~gamma-ray glows~~ them are usually also below ~~the~~ conventional breakdown. The ~~classical~~ conventional (or classical) breakdown field, of $E_k \approx 3.2$ $E_k \approx 3.0$ MV/m ~~at STP~~ (at STP), is where low energy electrons (~ 200 < 123 eV) exponentially grow in number, as ionisation overcomes attachment. ~~In this work we~~ This exponential growth of charged particles will affect the electric field, which requires a self-consistent simulation to be properly taken into account. That is not something we want to test in this study, since Geant4 is not capable of simulating it. Therefore we will focus on electric fields ~~above RREA threshold $E_{\mathrm{rb}} = 0.28$~~ below the breakdown field $E_k \approx 3.0$ MV/m, and above the RREA threshold $E_{\mathrm{th}} \approx 0.28$ MV/m.

As a note, one can find in the literature that E_k can be given between 2.36 MV/m and ~~below classical breakdown $E_k \approx 3.2$~~ 3.2 MV/m (Raizer, 1997), the theoretical lowest breakdown field being between 2.36 and 2.6 MV/m ~~to investigate RREA responsible for Terrestrial Gamma-Ray Flashes and gamma-ray glows~~ (see Raizer, 1997, page 338). The value of ≈ 3.2 MV/m is the measured breakdown field in centimeter gaps in laboratory spark experiments (see Raizer, 1997, page 135), that can be lower for longer gaps.

1.2 ~~Theoretical understanding of RREA~~

1.2 Theoretical understanding of RREAs

In the energy regime of ~~HEAP~~ a kilo-electronvolt (keV) to a hundred of mega-electronvolts (MeV), the evolution of electrons is ~~mostly~~ driven by electron impact ionisation ~~(Rutjes et al., 2016)~~ (Landau et al., 2013), as this energy loss channel is much larger than the radiative (bremsstrahlung) energy loss~~, by a few orders of magnitude~~. However, ~~this is only true for the average, and bremsstrahlung does have significant effect on the electron spectrum because of straggling Rutjes et al. (2016).~~ ~~For the electron impact ionisation, straggling only occurs for thin targets, as the energy is much more unequally separated (Rutjes et al., 2016). Almost~~ the bremsstrahlung process does impact the shape of the electron energy spectrum, that can be understood by the straggling effect, that is discussed in the next section. When the electric field is below the classical breakdown $E_k \approx 3.0$ MV/m (at STP), the system can be simplified, because the effect of the electrons below a certain energy can be neglected, in particular the population that would otherwise (if $E > E_k$) multiply exponentially and have an important effect on the electric field. The part of the electron population that decelerates, and eventually attaches, cannot contribute to the production of the high energy radiation. Let $\epsilon_2^{\mathrm{min}}$ be the minimum energy for a secondary electron to have a chance to runaway, thus participate to the production of high energy radiation. The subscript index $i = 2$ indicates a secondary electron. A precise value of $\epsilon_2^{\mathrm{min}}$ will be evaluated in section 3 with the help of simulations, but, by looking at the friction curve, one

can guess it is located in the keV to tens of keV energy regime (see Dwyer et al., 2012, Figure 1) . As almost all energy loss of ionisation is going into producing secondary electrons of lower energy (~~$\epsilon_2 \ll 200$~~$\epsilon_2 \lesssim 200$ eV)~~. For this reason~~, it is reasonable to approximate that channel as a continuous energy loss~~or friction because it does not alter the primary electron significantly,~~ or friction.

5 In the case of electric fields above the RREA threshold (~~$E_{\rm rb} = 0.28$~~$E_{\rm th} = 0.28$ MV/m at STP), ~~there is a possible mode where~~ the electrons, when considered as a population, ~~keeps on growing~~will undergo avalanche multiplication. Some individual electrons do not survive (because there can be hard bremsstrahlung or ionisation collisions that will remove enough energy to get below $\epsilon_2^{\min}$), but the ensemble grows exponentially as new electrons keep being generated from the ionisation collisions on air molecules, including a fraction with energy larger than $\epsilon_2^{\min}$. The production of secondaries ~~, above a value~~ with energies

10 much larger than the ionisation threshold (a few kilo-electronvolts being a reasonable value), can be ~~approximated by~~ described using the Møller cross section~~(~~, which is the exact solution for a free-free electron-electron interaction (see, e.g.~~see page 321 of Landau et al. (2013)) multiplied by~~, Landau et al. (2013, page 321)) :

$$
\frac{d\sigma_{\rm M}}{d\delta_2} \;\tilde{=}\; Z \frac{2\pi r_e^2}{\gamma_1^2 - 1} \left[\frac{(\gamma_1 - 1)^2 \gamma_1^2}{\delta_2^2 (\gamma_1 - 1 - \delta_2)^2} \right.
$$
$$
\left. \tilde{-}\; \frac{2\gamma_1^2 + 2\gamma_1 - 1}{\delta_2(\gamma_1 - 1 - \delta_2)} + 1 \right], \tag{1}
$$

15 where Z ~~,~~is the number of electrons in the molecule~~:~~

$$
\frac{d\sigma_{\rm M}}{d\delta_2} \;=\; Z \frac{2\pi r_e^2}{\gamma_1^2 - 1} \left[\frac{(\gamma_1 - 1)^2 \gamma_1^2}{\delta_2^2 (\gamma_1 - 1 - \delta_2)^2} \right.
$$
$$
\left. -\; \frac{2\gamma_1^2 + 2\gamma_1 - 1}{\delta_2(\gamma_1 - 1 - \delta_2)} + 1 \right],
$$

~~where~~, the index $i = 1$ indicates the primary electron, $i = 2$ the secondary, γ_i is the Lorentz factor, $\delta_i = \gamma_i - 1 = \epsilon_i/(m_e c^2)$ is the kinetic energy divided by the electron rest energy (with rest mass m_e) and $r_e = \frac{1}{4\pi\epsilon_0} \frac{e^2}{m_e c^2} \approx 2.8 \times 10^{-15}$ m is the classical

20 electron radius. In the case $\delta_2 \ll \gamma_1 - 1$ and $\delta_2 \ll 1$, we observe that the term $\propto 1/\delta_2^2$ is dominating. Thus, we can write equation 2 as:

$$
\frac{d\sigma_{\rm M}}{d\delta_2} \approx Z \frac{2\pi r_e^2}{\beta_1^2} \frac{1}{\delta_2^2}, \tag{2}
$$

with $\beta_1 = v_1/c$ the velocity of the primary particle. Integrating equation (2) from δ_2 to the maximum energy ($\epsilon_1/2$) yields a production rate

25 $$
\sigma_{\rm prod} \approx Z \frac{2\pi r_e^2}{\beta_1^2} \frac{1}{\delta_2} \propto \frac{1}{\epsilon_2}, \tag{3}
$$

using again $\epsilon_2 \ll \epsilon_1$. The remaining sensitivity of $\sigma_{\rm prod}$ in units of area to the primary particle is given by the the factor β_1^2 which converges strongly to 1 as the mean energy of the primary electrons exceeds 1 MeV. In other words, as the mean energy

of the electrons grows towards even more relativistic energies, the production rate σ_{prod} becomes independent of the energy spectrum.

For illustrative purposes, we now consider the one dimensional deterministic case, which results in an analytical solution of the electron energy spectrum. We make the system deterministic by assuming that the differential cross section is a delta-function at ϵ_2^{min} (the minimum energy at which a secondary electron can runaway) and use $\Lambda_{\text{prod}} = \frac{1}{N\sigma_{\text{prod}}}$ as the constant collision length, with N the air number density. In other words, every length Λ_{prod} a secondary electron of energy ϵ_2^{min} is produced. The derivation below is close to what was presented ~~in~~ by Celestin and Pasko (2010); Dwyer et al. (2012); Skeltved et al. (2014) and references therein.

Consider a population of electrons in ~~1-dimension~~ one dimension with space-coordinate z, a homogeneous and constant electric field E above the RREA threshold and a friction force $F(\epsilon)$. The minimum energy ϵ_2^{min} ~~that~~ at which an electron can runaway is given by the requirement ~~$F(\epsilon_2^{\text{min}}) > E$~~ $F(\epsilon_2^{\text{min}}) \approx qE$ (where q is the elementary charge), that is to say $\epsilon_2^{\text{min}} = \text{function}(F, E)$ is constant. Assuming that the mean energy of the ensemble is relativistic ~~,~~ results in a constant production rate $\Lambda_{\text{prod}} = \Lambda_{\text{prod}}(\epsilon_{\text{min}})$. Thus, in space, the distribution f_e grows exponentially as,

$$\frac{\partial f_e}{\partial z} = \frac{1}{\Lambda_{\text{prod}}} f_e. \tag{4}$$

While in energy, the differential equation is given by the net force,

$$\frac{\mathrm{d}\epsilon}{\mathrm{d}z} = qE - F(\epsilon). \tag{5}$$

Solving for steady state means,

$$\frac{\mathrm{d}f_e}{\mathrm{d}z} = \frac{\partial f_e}{\partial z} + \frac{\partial f_e}{\partial \epsilon}\frac{\mathrm{d}\epsilon}{\mathrm{d}z} = 0, \tag{6}$$

and using equation 4 and 5 results in,

$$\frac{\partial f_e}{\partial \epsilon} = -\frac{1}{\Lambda_{\text{prod}}(qE - F(\epsilon))} f_e. \tag{7}$$

For the largest part of the energy spectrum, specifically above 0.511 MeV and below 100 MeV, $F(\epsilon)$ is not sensitive to ϵ (e.g. see Rutjes et al. (2016)). Only at around $\epsilon \approx 100$ MeV electron energy $F(\epsilon)$ starts increasing again because of ~~bremsstrahlung~~ the bremsstrahlung process. Thus, one may assume $F(\epsilon) \approx F$ constant, which yields that the RREA energy spectrum $f(\epsilon)$ at steady state is given by,

$$f_e(\epsilon) = \frac{1}{\bar{\epsilon}} \exp\left(-\frac{\epsilon}{\bar{\epsilon}}\right), \tag{8}$$

with the exponential shape parameter and approximated average energy $\bar{\epsilon}(E)$ given by,

$$\bar{\epsilon}(E) = \Lambda_{\text{prod}}(qE - F). \tag{9}$$

Equivalently, in terms of collision frequency $\nu_{\text{prod}} = \frac{\beta c}{\Lambda_{\text{prod}}}$, equation 9 can be written as,

$$\bar{\epsilon}(E) = \frac{\beta c}{\nu_{\text{prod}}}(qE - F), \tag{10}$$

with β the velocity v/c of the RREA avalanche front. For the 1-d case there is no momentum-loss or diffusion, so $\beta \approx 1$. Note that Λ_{prod} depends on ~~$\epsilon_2^{\min} = \epsilon_2^{\min}(E)$, which in turn~~ $\epsilon_2^{\min}$ (the minimum energy at which a secondary electron can runaway), which depends on the electric field E as that determines the minimum electron energy that can go into runaway. ~~With this simple analysis~~In this analysis, we illustrate with ~~equation~~ equations 8 and 9, that the full RREA characteristics, such as the mean energy $\bar{\epsilon}$ or the collision length Λ_{prod} (directly related to the avalanche length scale λ discussed in section 4.1) are driven by processes determining $\epsilon_2^{\min}$.

In reality there are important differences compared to the one dimensional deterministic case described previously, which we propose to discuss qualitatively for understanding the Monte Carlo simulations evaluated in this study. During collisions, electrons deviate from the path parallel to E. Therefore in general, electrons experience a reduced net electric field as the cosine function of the opening angle θ, which reduces the net force to $qE\cos(\theta) - F$ and thereby the mean energy $\bar{\epsilon}$ of equation 9. In reality the 3D scattering (with angle parameter θ) changes of the path of the particle. Although the velocity remains still close to c (as the mean energy is still larger than several MeV), the RREA front velocity parallel to ~~E~~ the electric field ($\mathbf{E}$) is reduced again because of the opening angle as function of its cosine:

$$\beta_{\parallel} = \beta \cos(\theta), \tag{11}$$

which also reduces the mean energy $\bar{\epsilon}$. Note that θ is not a constant and may change with each collision. Equivalently the avalanche scale length Λ_{prod} in 3-D changes to $\approx \Lambda_{\mathrm{prod}} \times \cos(\theta)$. However, most importantly, the momentum-loss of the lower energetic electrons results in a significant increase of $\epsilon_2^{\min}$, as it is much harder for electrons to runaway. The increase of $\epsilon_2^{\min}$ significantly increases Λ_{prod} and thereby increases the characteristic mean energy $\bar{\epsilon}$. On the other hand, the stochasticity creates ~~a~~ an interval of possible energies $\epsilon_2^{\min}$ that can runaway with a certain probability and for thin targets a straggling effect (Rutjes et al., 2016). A recent article discussed the influence of the angular scattering of electrons on the runaway threshold in air (Chanrion et al., 2016).

The effects discussed above prevent a straight forward analytical derivation of the RREA characteristics in 3 dimensions, but what remains is the important notion that the physics is completely driven by the intermediate energy electron production. ~~Intermediate electrons in the sense~~ "Intermediate" means they are far above ionisation threshold ($\gg$ ~~200~~$\gg$ 123 eV) but much below relativistic energies ($\ll 1$ MeV). The ~~parametrization~~ parametrisation of the electron energy spectrum, given by equation 9 turns out to be an accurate empirical fit, as it was already shown in Celestin and Pasko (2010); Dwyer et al. (2012); Skeltved et al. (2014) and references therein. Nevertheless in these works $\lambda^{\min}(E)$, or equivalently the velocity over collision frequency $\beta c/\nu_{\mathrm{prod}}$, is fitted by numerical Monte Carlo studies and the final direct relation to $\epsilon_2^{\min}$ is not executed. Celestin and Pasko (2010) calculated that $\nu^{\mathrm{prod}}(E) \propto E$, thus explains why $\bar{\epsilon}(E)$ must saturate to constant value. Celestin and Pasko (2010) argue that $\epsilon_2^{\min}(E)$ is given by the deterministic friction curve F, for which they use the Bethe's formula and an integration of a more sophisticated electron impact ionisation cross section (RBEB) including molecular effects, but that is only true in ~~1-D~~ one dimension without stochastic fluctuations. Other attempts to simulate RREA by solving the kinetic equation instead of using Monte-Carlo methods are presented in Roussel-Dupre et al. (1994); Gurevich and Zybin (1998); Babich et al. (2001) and references therein. An analytical approach is provided by Cramer et al. (2014).

1.3 Model reductions and previous study

~~The physics behind TGF~~Apart from analytical calculations, the physics behind TGFs, TGF afterglows and gamma-ray glows are also studied with the help of experimental data, computer simulations, ~~which~~ and often a combination of both. Simulations necessarily involves model reduction and assumptions. ~~Fortunately~~As we argued in the previously, in scenarios where the electric field is below ~~classical breakdown the system can be simplified, because electrons that~~ the classical breakdown field ($E_k \approx 3.0$ MV/m at STP), electrons below a certain energy can be neglected, because they will decelerate and eventually attach~~will not contribute~~, thus not contributing to the production of the ~~penetrating~~ hard radiation. In Monte Carlo simulations it is therefore common to apply a so-called "low energy cutoff" ~~,~~ (or threshold), noted ε_c, that is a threshold where particles with lower energy can be discarded (or not produced), to improve code performance~~(i.e. computation time)~~. It is different from $\epsilon_2^{\min}$ (the minimum energy at which a secondary electron can runaway) as one is a simulation parameter and the other is a physical value. Ideally, ε_c should be set as close as possible to $\epsilon_2^{\min}$. A second simplification can be made for the energetic enough particles that stay in the ensemble, by treating collisions that would produce particles below the low energy cutoff as a friction.

Both simplifications can be implemented in different ways, leading to different efficiencies and accuracies. Rutjes et al. (2016) benchmarked the performance of the Monte Carlo codes Geant4 (Agostinelli et al., 2003), EGS5 (Hirayama et al., 2005), FLUKA (Ferrari et al., 2005) developed in other fields of physics, and of the custom-made codes GRRR (Luque, 2014) and MC-PEPTITA (Sarria et al., 2015) within the parameter regime relevant for HEAP, in the absence of electric and magnetic fields. In that study they focused on basic tests of electrons, positrons and photons with kinetic energies between 100 keV and 40 MeV through homogeneous air using a low energy cutoff of 50 keV and found several differences between the codes and invited other researchers to ~~also~~ test their codes on the provided test configurations. ~~Most of the differences revealed that using~~ We found that the usage of an average friction fails ~~also~~ in the high energy regime ($\gg$ ~~200 eV~~$\gtrsim$ 100 keV), as the energy loss is ~~averaged out too much~~ too much averaged, resulting in an incorrect energy distribution (Rutjes et al., 2016)~~, called the straggling effect~~.

~~Since including or not this straggling effect in the simulation is of primary importance for the present study as well, it is worth summarizing what it consists in. This~~ As we indicated in section 1.2, the ionisation energy loss channel is much larger than the radiative (bremsstrahlung) energy loss, by a few orders of magnitude. However, this is only true for the average, and bremsstrahlung does have a significant effect on the electron spectrum because of straggling (Rutjes et al., 2016). This straggling effect was first studied by Bethe and Heitler (1934). If it is not taken into account in the implementation of the low energy cut-off, the primary particle suffers a uniform (and deterministic) energy loss. This means that only the energy of the primary particle is altered, but not its direction. The accuracy of the assumed uniform energy loss is a matter of length scale : on a small length scale, the real energy loss distribution (if all interactions are considered explicitly) among the population would have a large spread. One way to obtain ~~the real~~ an accurate energy distribution is by implementing a stochastic friction mimicking the straggling effect.

Rutjes et al. (2016) also indicated that including electric fields in the simulations would potentially enhance the differences found by introducing new errors, the simulation results ~~begins~~ being supposingly sensitive to the low energy cutoff. This effect is believed to be responsible of the observed differences between the two Geant4 physics lists ~~test in the comparison study of~~ tested in Skeltved et al. (2014): for all fields between 0.4 and 2.5 MV/m (at STP), they found that ~~the~~ energy the spectrum and

5　the mean energy of runaway electrons depended on the low energy cutoff, even when it was chosen between 250 eV and 1 keV. In the ~~present article~~following, this interpretation is challenged.

1.4　Content and order of the present study

In the context of High Energy Atmospheric Physics, the computer codes that were used are either general purpose codes developed by large collaborations, or custom made codes programmed by smaller groups or individuals. Examples of general

10　purpose codes that were used are Geant4 (e.g., Østgaard et al., 2008; Carlson et al., 2010; Bowers et al., 2017; Sarria et al., 2015, 2017; Skeltved et al., 2014) and FLUKA (e.g., Dubinova et al., 2015; Rutjes et al., 2017). Custom made codes were used in

~~Lehtinen et al. (1999); Dwyer (2003); Østgaard et al. (2008); Celestin and Pasko (2011); Luque (2014); Köhn et al. (2014); Chanrion et~~
Roussel-Dupre et al. (1994); Lehtinen et al. (1999); Dwyer (2003); Babich et al. (2004b); Østgaard et al. (2008); Celestin and Pasko (20

15　among others. Rutjes et al. (2016) presented in their section 1.3 the reasons why different results between codes (or models) can be obtained and why defining a comparison standard (based on the physical outputs produced by the codes) is the easiest way (if not the only) to compare and ~~validate~~ verify the codes. Here we continue the work of Rutjes et al. (2016), now with electric fields up to the classical breakdown field ($E_k \approx 3.0$ MV/m). As mentioned previously, we chose not to use larger electric fields because that would produce an exponential growth of low energy electrons (< 123 eV) which would affect the electric field

20　and therefore require a self-consistent simulation, that Geant4 is not capable of. We aim to provide a comparison standard for the particle codes able to simulate Relativistic Runaway Electron Avalanches, as simple and informative as possible, by only considering their physical outputs. These comparison standards are ~~extensively~~ described in the Supplementary Material (Sections 1 and 2).

~~To prove our new insights~~In section 1.2, we illustrated that the full RREA characteristics, such as the mean energy $\bar{\epsilon}$ or

25　the collision length Λ_{prod} are driven by processes determining $\epsilon_2^{\min}$ (the minimum energy at which a secondary electron can runaway). To prove this insight, and to benchmark codes capable of computing RREA characteristics for further use, we calculated the probability for an electron to accelerate into the runaway regime (see section 3), which is closely related to the quantity ~~$\epsilon_2^{\min}(E)$~~$\epsilon_2^{\min}$. From this probability study, it is directly clear that it is safe to choose the low energy cutoff ε_c higher than previously expected by Skeltved et al. (2014) and Rutjes et al. (2016), ~~even higher than $F(\varepsilon_c) > E$~~given an electric field

30　$E < E_k$. ~~The probability for these particles below ε_c~~ In section 3, we will demonstrate that the probability for particles below 10 keV to accelerate and participate in the penetrating radiation is actually negligible. ~~In~~Thus, in practice an energy threshold value of ~~about $\varepsilon_c =$~~$\varepsilon_c \approx$ 10 keV can be used for any electric field below ~~the conventional breakdown field. Nevertheless, we found out~~ E_k. However, in section 2.4, we will show that step-length restrictions are of major importance (e.g. it can lead to an underestimation of a factor of 10 ~~underestimation~~ of the probability to produce a RREA~~), as will be described in section 2.4.~~

9

in some cases). The results of the comparison of several parameters of the ~~RREA~~ RREAs produced by the four tested codes is then presented in section ~~4.3.~~ 4. We conclude in section 5.

The test set-ups of ~~both~~ the two types of simulations (RREA probability, and RREA characteristics) are described in ~~detail in~~ the Supplementary Material, together with ~~data we obtained, and~~ the data we generated, and supplementary figures comparing several ~~different characteristics~~ characteristics of the showers. The Geant4 source codes used in this study are also provided (see sections 6 and 7).

2   Model descriptions

~~For this work, the~~ The data we discuss in the next sections ~~was provided~~ were produced by the general-purpose code Geant4 (with several set-ups) and two custom-made codes (GRRR and REAM) which we describe below. However, we will not describe comprehensively all the processes, models or cross-sections used by the different codes, and a table summarizing it is provided in the supplementary material document, section 13 (including all references).

2.1   Geant4

Geant4 is a software toolkit developed by the European Organization for Nuclear Research (CERN) and a worldwide collaboration (Agostinelli et al., 2003; Allison et al., 2006, 2016). We use version 10.2.3. The electro-magnetic models can simulate the propagation of photons, electrons and positrons including all the relevant processes, and the effect of electric and magnetic fields. Geant4 uses steps in distance, whereas REAM and GRRR use time step. In the context of this study, three main different electro-magnetic cross-section sets implementation are included : one based on analytical of semi-analytical models (e.g. uses the Møller cross section for ionisation and Klein-Nishina cross section for Compton scattering), one based on the Livermore data set (Perkins et al., 1991), and one based on the Penelope models (Salvat et al., 2011). Each of them can be implemented with a large number of different electro-magnetic parameters (binning of the cross section tables, energy thresholds, production cuts, maximum energies, multiple scattering factors, accuracy of the electro-magnetic field stepper, among others), and some processes have multiple models in addition to the main three, e.g. the Monash University model for Compton scattering (Brown et al., 2014). Skeltved et al. (2014) used two different physics list : LHEP and LBE. The first one, based on ~~parametrization~~ parametrisation on measurement data and optimized for speed, was deprecated since the 10.0 version of the toolkit. The LBE physics list is based on the Livermore data, but it is not considered as the most accurate electro-magnetic physics list in the Geant4 documentation, which is given by the Option 4 physics list (O4). This last uses a mix of different models, and in particular uses the Penelope model for the the impact ionisation of electrons. For this study, we will use two GEANT4 physics list options : Option 4 (referred as simply O4 hereafter) that is the most accurate one according to the documentation, and the Option 1 (referred as simply O1 hereafter) that is less accurate, but runs faster. In practice, O1 and O4 give very similar results for simulations without electric field and energies above 50 keV, as produced in our previous code comparison study (Rutjes et al., 2016).

~~Concerning how low the energy threshold is handled,~~ By default, Geant4 ~~, by default,~~ is following all primary particles down to zero energy. A primary particle is defined as a particle with more energy than a threshold energy ~~ϵ_c^p~~ ε_c^g (that is different from ~~ϵ_c~~ ε_c described before). ~~The default~~ϵ_c^p ~~By default,~~ ε_c^g is set to 990 eV and ~~is not changed in this study~~was not changed to obtain the results presented in the next sections. The LBE Physics list used ~~in (Skeltved et al., 2014)~~ by Skeltved et al. (2014) uses a threshold down to 250 eV ~~, and this parameters~~ (i.e. more accurate than using 990 eV, in principle) and this parameter was thought to be responsible for a major change in the ~~simulated~~ accuracy of the obtained RREA energy spectra. In section 3, we will argue that the ~~main parameter governing the spectrum~~ most important factor able to effect the spectra obtained from Geant4 simulations is the accuracy of the stepping method for the tracking of the ~~particles. The interpretation of (Skeltved et al., 2014) was possible because reducing the value of ϵ_c^p also indirectly reduces the average step that is used by the simulation~~electrons, and not the low energy threshold. Actually, we found that the stepping accuracy of the simulation is indirectly improved by reducing ε_c^g, that explains why Skeltved et al. (2014) could make this interpretation.

2.2 GRRR

The GRRR (GRanada Relativistic Runaway simulator) is a time-oriented code for the simulation of energetic electrons propagating in air, and can handle self-consistent electric fields. It is described in detail in the supplement of Luque (2014) and its source code is fully available in a public repository (see section 7 about code availability). In the scope of this work, we want to point out three important features : 1. Electron ionisation and scattering processes are simulated discretely, and the friction is uniform and without a way to mimic the straggling effect. 2. Bremsstrahlung collisions are not explicit and are simulated as continuous radiative losses, without straggling. 3. GRRR uses a constant time-step Δt both for the integration of the continuous interactions using a fourth-order Runge-Kutta scheme and for determining the collision probability of each discrete process k as $\nu_k \Delta t$, where ν_k is the collision rate of process k. This expression assumes that $\nu_k \Delta t \ll 1$ and therefore that the probability of a particle experiencing two collisions within Δt is negligibly small. The collisions are sampled at the beginning of each time step and therefore the rate ν_k is calculated using the energy at that instant. In this work we used $\Delta t = 0.25$ ps for the avalanche probabilities simulations, and $\Delta t = 1$ ps for the simulations used to characterise the RREA. For both cases, the time steps are small enough to guarantee a very accurate integration.

2.3 REAM

The REAM (Runaway Electron Avalanche Model) is a three dimension Monte Carlo simulation of Relativistic Runaway Electron Avalanche (also refeed as Runaway Breakdown), including electric and magnetic fields (Dwyer, 2003, 2007; Cramer et al., 2016). This code is inspired by earlier work by Lehtinen et al. (1999) and takes accurately into account all the important interactions involving runaway electrons, including energy losses through ionisation, atomic excitation and Møller scattering. A shielded-Coulomb potential is implemented in order to fully model elastic scattering, and it also includes the production of X/gamma-rays from radiation energy loss (bremsstrahlung) and the propagation of the photons, by including photoelectric absorption, Compton scattering and electron/positron pair production. The positron propagation is also simulated, including

the generation of energetic seed electrons through Bhabha scattering. The bremsstrahlung photon emissions from the newly produced electrons and positron are also included.

In the scope of this study, it is important to point out that REAM limits the time step size of the particles so that the energy change within one time step cannot be more than 10 %. The effect of reducing this factor down to 1 % was tested and did not make any noticeable difference in the resulting spectra. The comparative curves are presented in the Supplementary Material, section 4. 10.

2.4 Stepping methodology

2.4.1 General method

In Monte Carlo simulations, particles propagate in steps, collide and interact with surrounding media by means of cross sections (and their derivatives). A step is defined by the displacement of a particle between two collisions. As it is presented in sections 3 and 4, ~~this~~ the stepping methodology is responsible for most of the differences we observed between the codes we tested. Simulations can be either *space-oriented* or *time-oriented*, if the stepping is done in space or in time. By construction, space-oriented simulations are thus not synchronous in time. Usually, a single particle is simulated ~~over its entire life-time before going to the next particle~~until it goes below the low energy threshold (ε_c), chosen by the user. But there are exceptions, like Geant4, that by default follows all primary particles down to zero energy. The advantage of asynchronous simulations is the ability to easily include boundaries, to have particles step as far as possible in the same material (minimizing the overhead due to null collisions), and smaller memory usage since there is no need to store all the particles alive at a given time (that may be a million or more). However, asynchronous simulations makes it impossible to incorporate particle to particle interactions, such as a space charge electric field, or self-consistent electric fields.

During steps, charged particles can ~~loose~~ lose energy (and momentum) by collisions, and also change in energy (and momentum) when an electric fields is present. To guarantee accuracy, energies should be updated frequently enough. An accurate method would be to exponentially sample step lengths with

$$\delta\ell = \min_{\epsilon}\{(\sigma_t(\epsilon)N)^{-1}\}, \tag{12}$$

in space-oriented perspective, or

$$\delta t = \min_{\epsilon}\{(v(\epsilon)\sigma_t(\epsilon)N)^{-1}\}, \tag{13}$$

in time-oriented perspective. With v the velocity, σ_t the total cross section and N the number density of the medium. Then at each updated location (and energy), the type of collision must be sampled from probability distributions. The probability of doing a collision of the given process (pr) can be calculated with:

$$p_{pr} = 1 - \exp\left(-N\int_{i}^{f}\sigma_{pr}\left(\epsilon(\ell)\right)d\ell\right) \tag{14}$$

Where the index i refers to the beginning of the step, f to its end, ℓ is the step length variable along the trajectory, and $d\ell$ is an infinitesimal step length. For time oriented simulations, we have equivalently :

$$p_{pr} = 1 - \exp\left(-N \int_i^f v(\epsilon(t))\, \sigma_{pr}(\epsilon(t))\; dt\right) \tag{15}$$

Using these probabilities along a given step length or duration, there is a chance that no interactions happens, but the energy of the particle is guaranteed to be updated correctly.

2.4.2 The case of Geant4

In the Geant4 documentation, the stepping method presented in the previous section is referred as the "the integral approach to particle transport". This method is set up by default in Geant4 for impact ionisation and bremsstrahlung. However, the way it is implemented is not exactly following what was described in the previous section. The description of the exact implementation is out of the scope of this article, but is presented into details in Ivanchenko et al. (1991) and Apostolakis et al. (2009). The method relies on determining the maximum of the cross section over the step (σ_{max}), using a parameter ~~ξ, that is based on another parameter~~ α_R (called "dR over Range" in the Geant4 documentation), that is also used to determine the step lengths. Another related parameter is the maximum range parameter (ρ_{max}), set to the default values of 1 millimeter and 0.1 millimeter for O1 and O4 respectively, and was never changed in the scope of this study. The exact definition of these parameters is given in Allison et al. (2016) and in the online Geant4 documentation (available at http://geant4.cern.ch/support/userdocuments.shtml). The default value of α_R is set to 0.80 for O1 and to 0.20 for O4. We found ~~out~~ that both values are not low enough to be able to produce accurate results for the RREA probability simulations presented in the next section. To make Geant4 able to produce accurate RREA simulations using the multiple scattering algorithm, two methods are possible.

The first method is to tweak the value of the α_R parameter. Its value is set to 0.80 by default for O1, and 0.20 by default for O4. We found that these default values are way too high to be able to produce accurate RREA simulations, and values of $\alpha_R < 5.0 \times 10^{-3}$ should be used, as presented in the next section.

The second method is to implement a step limiter process (or maximum acceptable step). By default, this max step ($\delta\ell_{max}$) is set to one kilometer, and such a large value has no effect in practice, since the mean free path of energetic electrons in STP air is orders of magnitude smaller. Acceptable values of $\delta\ell_{max}$ depend on the electric field, and we found ~~out~~ that it should be set to 1 millimeter or less to produce accurate RREA simulations, as presented in the next section. However, using this method results in relatively long simulation time required to achieve an acceptable accuracy, as the step is not adapted to the energy of the electrons. For information, the relative impact on performance (in terms of requirements of computation time) of tweaking the $\delta\ell_{max}$ and α_R parameters is presented in Appendix A.

3 Probability of generating RREA

As a first comparison test, we estimated the probability for an electron to accelerate into the runaway regime and produce a RREA, given its initial energy ϵ and some electric field magnitude E. Note that the momentum of the initial electrons is aligned along the opposite direction of the electric field, so that it gets accelerated. That gives maximum RREA probabilities, as other alignments reduce the chance to produce a shower (see, e.g., (Lehtinen et al., 1999, Figure 2.6)). We defined this probability as the fraction of initial (seed) electrons that created an avalanche of at least 20 electrons above 1 MeV. Once this state is reached, there is no doubt the RREA is triggered and can go on forever if no limits are set. The number 20 is arbitrary, to be well above 1 but small enough for computational reasons. For some initial conditions, we also tested requirements of 30 and 50 electrons above 1 MeV, that resulted in very similar probabilities. This study is somehow similar to the works presented in Lehtinen et al. (1999); Li et al. (2009); Liu et al. (2016); Chanrion et al. (2016), but they all looked at the probability to have only one single runaway electron, whereas we used the criterion of ~~20~~ $N = 20$ electrons above 1 MeV, that is a stricter constraint. The difference between the two criteria is mainly noticeable for low electric field (< 0.4 MV/m) and high seed energies (> 700 keV). A figure illustrating how the probability can change with N is presented in the supplementary material, section 5.3.

As a test case, we calculated the probability to produce ~~RREA as~~ RREAs as a function of α_R and $\delta\ell_{max}$ (these parameters are presented in the previous section), for the configuration $\epsilon = 75$ keV, $E = 0.80$ MV/m. This case was chosen because it showed a particularly large sensitivity to the stepping methodology, as discussed later. The results are presented in figure 1. Although this configuration has a very low RREA probability for O1 ~~f~~and O4 by default (where α_R respectively equal to 0.80 and 0.20, and $\delta\ell_{max}$ is one kilometer for both), the probability increases as α_R decreases and converges to a value between 10 and 12 % for both models when $\alpha_R < 5.0 \times 10^{-3}$. The same effect is observed when reducing $\delta\ell_{max}$. In this case, the user should not set $\delta\ell_{max}$ below the maximum range parameter, set to 1 millimeter for O1 and 0.1 millimeter for O4 by default (and never changed in the scope of this article). When reducing the α_R parameter to arbitrarily small values, both Geant4 models converge to slightly different probabilities : 10.7 % for O1 and 11.7 % for O4. We think this small difference is not due to the stepping method, as reducing ρ_{max} or α_R further does not produce a significant difference. It is probability due to other factors, in particular the difference in the physical models and cross section sets used.

As explained in section 1.2, the final electron spectrum is essentially driven by the minimum energy $\epsilon_2^{\min}$ of electrons that can create a RREA. Here we can clearly see this probability is strongly affected by the choice of the α_R and $\delta\ell_{max}$ simulation parameters, affecting the accuracy of the stepping method, and that the values set by default for these parameters are not ~~correct for correctly handling this problem~~precise enough to obtain correct RREA probabilities. In order to help future researchers, we provide example Geant4 source codes where the α_R and $\delta\ell_{max}$ parameters can be changed and their effect to be tested (see sections 6 and 7).

In figure 2.a, we compare the contour lines of the 10%, 50% and 90% probability of triggering a RREA as function ϵ and E, for ~~three codes~~ the four models : Geant4 O4 ($\alpha_R = 1.0 \times 10^{-3}$), Geant4 O1 ($\alpha_R = 1.0 \times 10^{-3}$)~~and GRRR . For most of the~~

~~domain,the level curves are consistent between O1, O4 and GRRR.~~, GRRR and REAM. The full RREA probability results in the (ϵ,E) domain for each model are presented in the supplementary material, section 5.

The most important difference between Geant4 and GRRR is present for energies > 200 keV and ~~low E-field (~~E-fields < 0.5 MV/m~~)~~. At 1 MeV, the level curves are ~~quite~~ significantly different between the Geant4 models and GRRR: the 50% probability to trigger RREA for GRRR is approximately located at the 10 % probability for O4, and the 90 % probability to for GRRR is located at the 50 % probability for O1. The reason is probably similar to a point we raised in our previous study (Rutjes et al., 2016) : GRRR does not include a way to simulate the straggling effect for the ionisation process. By looking at figure 2 of Rutjes et al. (2016), we can see that 200 keV is roughly the energy from where the difference in the spectrum of GRRR, compared to codes that simulate straggling, starts to become significant.

For low electron energy (< 40 keV) and high electric field (> 2 MV/m), GRRR and O4 present a good agreement, however O1 deviates significantly from O4. We ~~double checked~~ investigated the effects of the stepping parameters (α_R, $\delta\ell_{max}$ and ρ_{max}) and it is clear that they were not involved in this case. We think the Møller differential cross section (with respect to the energy of the secondary electron) used by O1 and extrapolated down to low energies leads to the production of secondary electrons with average energies lower than the Penelope model (used by O4), that includes the effects of the atomic electron shells, hence is probably more accurate. This hypothesis is confirmed by looking at the shape of the differential cross sections of impact ionisation, which plots are presented in the Supplementary Material, section ~~8.4~~11.4.

The RREA probability data for REAM is also displayed in figure 2.a, as the red curves. The three REAM level curves show a significantly higher noise than the Geant4 data, mainly because the latter used 1000 electrons seeds whereas the former used only 100. The algorithms used to calculate the levels curves were also found to impact the noise level. Nevertheless, the noise level is low enough to be able to evaluate the consistency between the codes. REAM shows a consistency with Geant4 (O1 and O4) within less than 12% in the full parameter range, and less than 5 % in some part of it. The most apparent deviations between REAM and Geant4 O1/O4 can be noticed for a seed electron energy range between 50 and 300 keV, for the 50 % and 90% level curves, where there is a systematic, statistically significant difference in the probability for REAM compared to Geant4 (REAM requiring about 10% larger electric field or primary electron energy to reach the 90% or the 50% contour level). However, we do not expect such a small difference to significantly affect the characteristics of the RREA showers, such as the multiplication factors or the mean energies of the RREA electrons. To test this quantitatively, a detailed comparison of the most important characteristics of the RREA showers obtained with the four models is presented in the following section.

In figure 2.b we show the 0 %, 10 %, 50 %, 90 % and 100 % probability contour lines for the Geant4 O4 model where we could run a very large number of initial electrons ("seeds") to obtain curves with a very low noise level. These are the most accurate probabilities we could obtain. From this figure, it is clear that the RREA probability for an electron of less than ≈ 10 keV is null for any electric field below $E_k \approx 3.0$ MV/m. Therefore 10 keV is a reasonable a lower boundary of $\epsilon_2^{\min}$ (the minimum energy at which a secondary electron can runaway), and any simulation with an electric field below $E_k \approx 3.0$ MV/m could use an energy threshold (ε_c) of this value while keeping accurate results. If electric fields with lower magnitude are used, it is also reasonable to increase this energy threshold by following the 0% level curve showed in Figure 2.b.
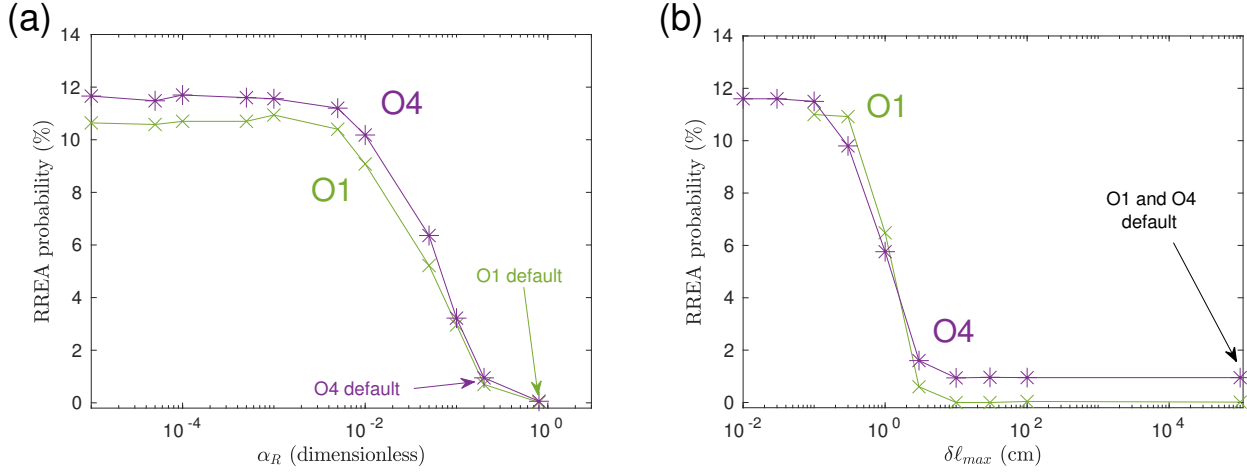
Figure 1. Relativistic avalanches probabilities calculated from Geant4 simulations, for specific point $\{\epsilon = 75\,\text{keV}, \text{E} = 0.80\,\text{MV/m}\}$ (illustrated by a cross in figure 2) and for two stepping settings. **(a)**: Avalanche probability versus α_R setting for Geant4 O4 and Geant4 O1. $\delta\ell_{max}$ is set to the default value of 1 kilometer. **(b)**: Avalanche probability versus maximum step setting ($\delta\ell_{max}$) for Geant4 O4 and Geant4 O1. The parameter α_R is set to the default value of the models, that is 0.8 for O1 and 0.2 for O4.

4 Characteristisation of RREA showers

We compared the output of the four models over 12 different electric field magnitudes from $E = 0.60\,\text{MV/m}$ to ~~$E = 2.8$~~ $E = 3.0\,\text{MV/m}$. Two types of simulation were set : record in time, and record in distance (or space). This last choice was made because the resulting spectra can change significantly depending on the record method, as presented in figure 10 of Skeltved et al. (2014). All the curves presenting the simulation results are presented in the Supplementary Material, as well as the complete details on how the simulation should be set up. In the following section, we discuss only the most important differences we found between the four codes. We show the comparison of avalanche scales in space and time in section 4.1 and in section 4.2 the evolution to self-similar state. Finally, in section 4.3 we show the comparison of the self-similar energy spectra of electrons and photons of the RREA.

4.1 Avalanche time and length scales

~~Figure~~ Figures 3 and 4 show the avalanche length and time scales as function of electric fields, for the four models, together with their relative difference with respect to REAM. Note that we could not compute any values for electric fields below 0.60 MV/m, as we ~~used only~~ only used 200 initial electron seeds of 100 keV, which ~~have a very low probability to trigger RREA for such fields. All the models agree well,~~ could not produced enough showers. The choice of 200 initial electrons is purely due to computational limitations. The avalanches length and times of the different models agree within $\pm 10\%$. There is also a systematic shift of about 7 % between the two Geant4 models for both time and length scales. The Geant4 O4 model is in principle more accurate than the O1 model, since it includes more advanced models. For most of the electric fields, O1

16

(a)

Electric field (V/m)

Geant4 O1: 10%, 50% and 90%

Geant4 O4: 10%, 50% and 90%

REAM: 10%, 50% and 90%

GRRR: 10%, 50% and 90%

Primary energy (keV)

(b)

Electric field (V/m)

≈100%

90%

50%

10%

≈0%
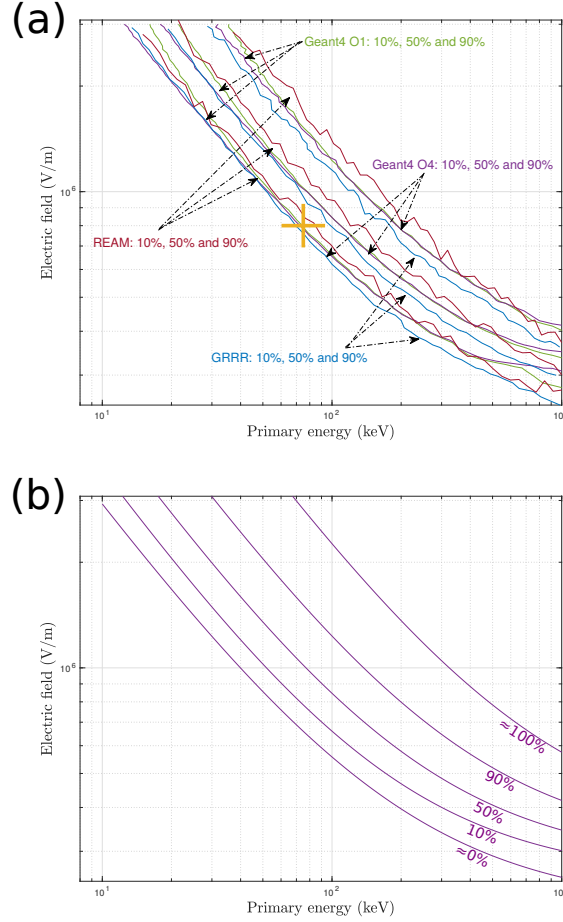
Primary energy (keV)

Figure 2. ~~Avalanche~~ **(a)**: Relativistic avalanche probability comparison between ~~O4, O1 and~~ GRRR, ~~with~~ REAM, O4 and O1. It shows three contour ~~probabilities~~ lines at 10%, 50% and 90%, as function of seed (primary) energy ϵ and electric field magnitude E. These contours are derived from the full probability scan, that are presented in the Supplementary Material (section 5). The cross at $\{\epsilon = 75 \text{ keV}, E = 0.80 \text{ MV/m}\}$ highlights the point where we studied the ~~behaviour~~ effect of the ~~stepping~~ simulation stepping parameters (for the O4 and O1) on the probability, see figure 1. **(b)**: Five contour lines indicating the 0%, 10%, 50%, 90% and 100% probabilities to generate a relativistic electron avalanche (RREA) as function of ϵ and E, for the Geant4 O4 model for which we could run a very large number of initial electrons ($> 50,000$) to obtain curves with a very low noise level.

tends to be closer to REAM and O4 tends to be closer to GRRR. Following Coleman and Dwyer (2006), the avalanche length and time can be fitted by the empirical models,

$$\lambda(E) = \frac{c_1}{E - c_2}, \tag{16}$$

$$\tau(E) = \frac{c_3}{E - c_4} \tag{17}$$

where c_1 is in V, c_2 and c_4 in V/m and and c_3 in s .·V/m. The c_2 and c_4 parameters can be seen as two estimates of the magnitude of the electric field of the minimum of ionisation for electrons along the avalanche direction, and also of the electric field magnitude of the RREA threshold; both values being close. However, we note that these fits neglect the sensitivity of the mean energy and velocity to the electric field. These empirical fits are motivated from the relations presented in equation 9 and 10, derived for the one dimensional case. First results of such fits were presented in ~~Coleman and Dwyer (2006) .~~ Babich et al. (2004b) and Coleman and Dwyer (2006) ; and they obtained consistent results. Here we will compare our results against Coleman and Dwyer.

The best fit values of the two models to the simulation data are given in table 1. The c_1 parameter is directly linked to the average energy of the RREA spectrum, though the definition of this average energy can be ambiguous as energy spectra change significantly if recorded in time or in space. The values given by all the code are located between 6.8 and 7.61 MV, and are all consistent with each other within a 95 % confidence interval, with the exception of O4 that slightly deviates from O1. Combining ~~all the~~ the four values gives :

$$\overline{c_1} = 7.28 \pm 0.10 \text{ MV} \tag{18}$$

~~That~~ By "combining", we mean that the four values are averaged and the rule $\sigma_{comb} = \sqrt{\sigma_1^2 + \sigma_2^2 + \sigma_3^2 + \sigma_4^2}/4$ is used to "combine" the four uncertainty ranges. The value $\overline{c_1}$ is consistent with the value of 7.3 ± 0.06 MV given in Coleman and Dwyer (2006). And all the estimated values of the c_2 and c_4 are consistent with each other within a 95 % confidence interval. Combining all the values of c_2 and c_4 gives :

$$\overline{c_2} = 279 \pm 5.6 \text{ kV/m}$$

$$\overline{c_4} = 288 \pm 4.8 \text{ kV/m}$$

And both value are also consistent with each other, leading to the final value of $\overline{c_{2,4}} = 283.5 \pm 3.69$ kV/m. These values slightly deviates from the value of 276.5 ± 2.24 obtained from Coleman and Dwyer (2006) if the values they obtained for the fits of λ and τ are combined. The work of Coleman and Dwyer (2006) used the REAM model too, in a version that should not have significantly changed compared to the one used here. Thus, we think this difference is purely attributed to differences in the methodology that was used to make these estimates from the output data of the code. Concerning the c_3 parameter,
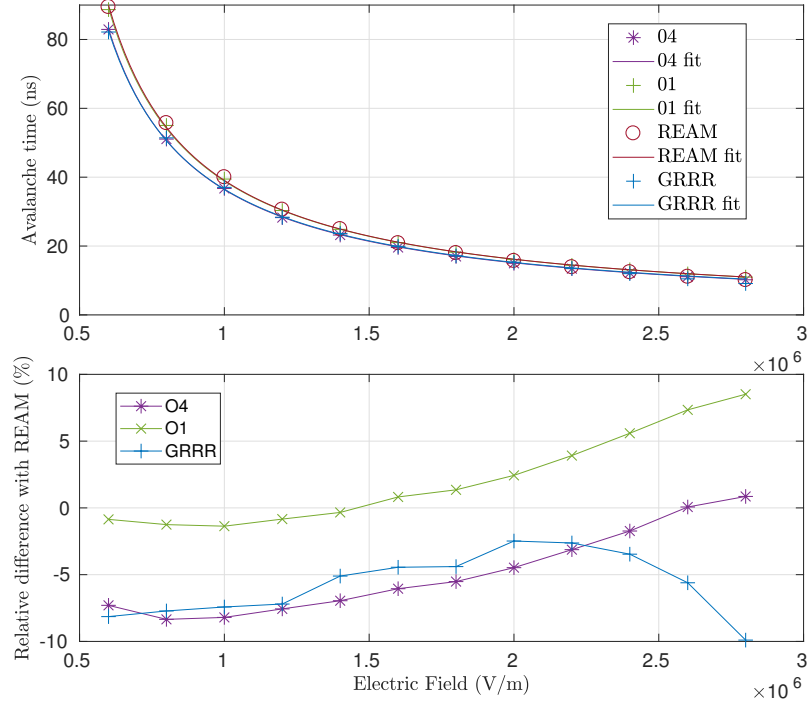
18

Figure 3. Top : Avalanche multiplication length as function of ambient electric field, for each of the codes included in this study. **Bottom** : The relative difference of all other models with respect to REAM. Table 1 indicates the values of the fit parameters.

Table 1. Values of the parameters of the fits (with 95 % confidence intervals) for the simulations data for avalanche scale in space and time, using the models described by equations 16 and 17. See figure 3 and 4 for the corresponding curves.

Code	Avalanche length		Avalanche time	
	c_1 (MV)	c_2 (kV/m)	c_3 (ns MV/m)	c_4 (kV/m)
REAM	7.43 ± 0.18	290 ± 9.5	27.6 ± 0.91	293 ± 13
G4 O1	7.50 ± 0.10	276 ± 5.6	27.6 ± 0.44	290 ± 6.3
G4 O4	6.93 ± 0.13	285 ± 7.5	25.9 ± 0.28	288 ± 4.2
GRRR	7.25 ± 0.30	266 ± 18	26.2 ± 0.76	282 ± 12

combining all the estimates gives $\overline{c_3} = 26.8 \pm 0.32$ ns MV/m, that is slightly lower than the value of 27.3 ± 0.1 ns MV/m of Coleman and Dwyer (2006), but none of the values are consistent within the 95 % confidence interval. For this case, we also think the slight difference can be attributed to differences in methodology. Furthermore, the ratio $\overline{c_1}/\overline{c_3}$ can also be used to determine an average speed of the avalanche $\approx \beta_{\parallel} c$ along the direction of the electric field (that also corresponds to the z direction), and we can estimate $\beta_{\parallel} \approx 0.90$, that is very close to what was found in previous studies.

5

19

Figure 4. Top : Avalanche multiplication time as function of ambient electric field, for each of the codes included in this study. **Bottom** : The relative difference of all other models with respect to REAM. Table 1 indicates the values of the fit parameters.

4.2 Evolution to self-similar state

The photon and electron energy spectra of a relativistic runaway electron avalanche (RREA) is known to converge in time to a self-similar solution, where its shape is not evolving anymore, even if the number of particles continues growing exponentially. It may also be referred as the "self-sustained state", or the "steady state" in the literature. At least 5 avalanche lengths (or avalanche times) are required to be able to ~~reasonably~~ assert that this state is reached. We propose to estimate this time by looking ~~to~~ at the mean electron energy evolution as a function of time. Notice that, as already mentioned in the beginning of Section 4, this mean energy recorded in time is different from the one recorded in distance, used in the next section. We arbitrarily choose to evaluate this mean by averaging all the ~~energy~~ energies of each individually recorded ~~electrons~~ electron from 10 keV and above. This choice of a 10 keV energy threshold (instead of a higher value, like 511 keV or 1 MeV) does not affect significantly the final estimate of this time to self-similar state. We started with a mono-energetic beam of 100 keV

20

electrons, which ~~are~~ is considered low enough compared to the self-similar state mean energy of 6 to 9 MeV. To define the time to self-similar state (T_s), we fitted the time evolution of the mean electron energy $\bar\epsilon$ with the model

$$\bar\epsilon(t) = b_1 - b_2 \times \exp(-t/b_3), \tag{19}$$

where b_1 and b_2 have dimension of energy, b_3 dimension of time, and we define $T_\mathrm{s} = 5\, b_3$, that is five e-folding times, i.e.

5   converged to 99.3%. The evolution of ~~electrons~~ electron spectra to self-similar state are illustrated for the Geant4 O4 model in the supplementary material (section ~~11.4~~12.4). The values of T_s we estimated for the different models are presented in figure 5, together with relative differences of the models with respect to REAM. The relatively high uncertainty (within 95 % confidence intervals) that can be seen on the estimate of T_s is due to a combination of the confidence interval from the exponential fit, from the statistics of the number of seed electrons that could produce a RREA, and from the statistics of the particle counts.

10   For most case, 200 initial seed were used, but for REAM, only 16 seeds were simulated for $E \geq 2.2$ MV/m, and for GRRR, only 20 seeds were simulated above $E \geq 2.0$ MV/m, because of computation time limitations.

In figure 5, Geant O1, O4, GRRR and REAM show consistent times to reach the self-similar state, for all the E-fields. Notice that for them, $T(= T_\mathrm{s}/5)$ is close to the avalanche time value τ given in the top panel of figure 4. For the low electric field of 0.60 MV/m, it seems to take about 5 times more to reach self-similar state. For this field, there were only three electrons

15   seeds that could produce a RREA, giving a large uncertainty on the estimate of T_s, making it impossible to conclude on an inconsistency. From 0.60 MV/m to 1.8 MV/m, where all data from codes have good statistics, the times to self-similar state are consistent. From 2.0 MV/m to 2.4 MV/m, the two Geant4 models and REAM are consistent, but GRRR present lower times by about -20% to -50 %, but it is impossible to conclude ~~to~~ an inconsistency, given the large confidence intervals. For E-field magnitudes of 2.6 MV/m to 2.8 MV/m, O1 and O4 present times to self-similar state lower than REAM by about 50 %, that is

20   significant given the uncertainty intervals, whereas GRRR and REAM are consistent. We could not find a clear explanation for it.

4.3   RREA spectra

The supplementary material (section 6) presents all the comparison spectra we obtained for ~~photon~~photons, electrons and positrons, for the electric field between ~~0.80~~ 0.60 MV/m and ~~2.8~~ 3.0 MV/m. In this section, we discuss the most important

25   differences we could find ~~out~~ between the four models.

4.3.1   Electrons

After the RREA electron spectra has reached self-similar state (that requires at least 5 avalanche lengths or times), we recorded the energy spectrum in a plane at a given distance (that is different for each electric field). Then we fitted it with an exponential spectrum model $\propto \exp(-\epsilon/\bar\epsilon)$ (see also equation 8). Note that for an exponential distribution, the mean of the energy

30   distribution is an estimator of its parameter $\bar\epsilon$, justifying the bar notation. We chose to evaluate the mean energy $\bar\epsilon$ for record at distances because, contrary to time records, it produces spectra that can be perfectly fit with an exponential distribution over

Figure 5. Top : time to self-similar state as function of ambient electric field, for each of the codes included in this study. **Bottom** : relative difference with respect to REAM.

the whole energy range (0 to 100 MeV). Therefore, in this case only the mean RREA electron energy is uniquely defined, and does not depend on an arbitrarily chosen energy threshold, or fitting method. The mean energy $\bar{\epsilon}$ of the exponential spectrum is calculated for the several codes as a function of electric field E, as presented in figure 6. For Geant4 O1 the whole simulations and analysis were done twice, for ~~max~~ maximum allowed step length settings of $\delta\ell_{\max} = 1$ cm and $\delta\ell_{\max} = 1$ mm, to show

5 that the first case generates totally incorrect spectra~~. The final data was fitted again by three parameters a_1, a_2 and a_3,~~ that is consistent with having incorrect RREA probabilities (presented in section 3). In addition, values of the mean energy $\bar{\epsilon}$ for O1 with $\alpha_R = 1.0 \times 10^{-3}$ and $\delta\ell_{\max} = 1$ cm are presented in the supplementary material, section 7.

The data of figure 6 was fit following the model,
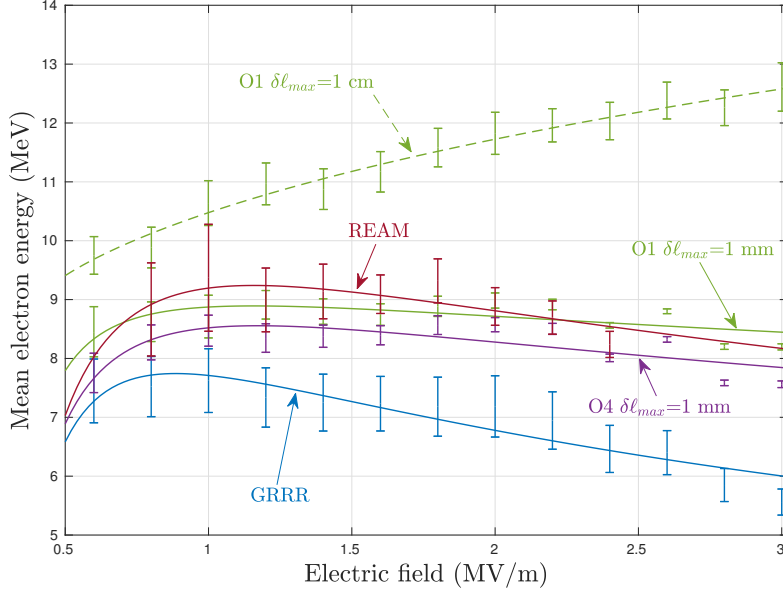
$$\bar{\epsilon}_{\text{fit}}(E) = \lambda(E)(qE - F), \quad \lambda(E) = \beta c \left[a_1 \left(\frac{qE}{F} \right)^{a_2} + a_3 \right]^{-1}, \tag{20}$$

22

Figure 6. Mean electron energies at self-similar state (for distance record), for different electric field magnitudes. The data points are fitted with the model presented in section 4.3.1, equation 20. The values of the fitted parameters are presented in Table 2. To highlight the importance of including step limitations, Geant4 O1 values are presented for two different max step ($\delta\ell_{max}$) settings: one that is not acceptable (1 cm) and one that is acceptable (1 mm). The parameter α_R is set to its default value of 0.8 for O1 and 0.2 for O4.

motivated by the facts that $\epsilon_2^{\min}$ is roughly a power-law of E (see figure 2) and λ is a power-law of $\epsilon_2^{\min}$ (see equation 3). It has three adjustable parameters a_1, a_2 and a_3. We set $F = 0.28$ ~~MV~~MeV/m, that is approximately the RREA threshold. The speed β is ~~chosen~~ set constant, equal to 0.90, because the RREA velocity does not change of more than 5 % over the range of electric fields we tested. ~~The fits are~~ This model is in general agreement with the calculations of Celestin et al. (2012), where

5    $\lambda(E)$ presents an approximately linear relation with the electric field. ~~Figure 6 shows the corresponding plots, and table 2 the corresponding parameters of the fits~~Table 2 gives the parameters' best fits (with confidence intervals) for the different models, and figure 6 shows the corresponding curves.

     In figure 6, it is clear that the Geant4 O1 model with $\delta\ell_{\max} = 1$ cm presents a significantly higher $\bar{\epsilon}(E)$ than the other codes, with values ranging from 9.5 MeV to 12.5 MeV. From the previous RREA probability simulations (see section 3), we know

10   that this $\delta\ell_{\max}$ parameter is not low enough, and so the results of this model can be disqualified. However, when $\delta\ell_{\max}$ is reduced to 1 mm, the results of both Geant4 model are close. There seems to be a consensus between Geant4 (O1 and O4) and REAM, that gives a mean energy that is between 8 and 9 MeV and can vary up to 10 % depending on the electric field. For all electric field magnitudes, GRRR shows a smaller average energy, from about 10 % less at 1 MV/m to about 20 % less at 2.8 MV/m. The reason is certainly because GRRR only includes radiative energy looses as a continuous friction. This is actually a

Table 2. Mean energy variation with electric field. For evaluated codes we fitted by equation 20, with $F = 0.28$ MV/m. Figure 6 shows the corresponding curves.

Parameter / Code	a_1 $[10^6\mathrm{s}^{-1}]$	a_2	a_3 $[10^6\mathrm{s}^{-1}]$
Geant4 O1 ($\delta l_{max} = 1$ mm)	~~5.96~~ 6.17 ± 2.15	~~1.14~~ $1.14 \pm 7.3 \times 10^{-2}$	~~-4.15~~ -4.31 ± 2.0
Geant4 O4 ($\delta l_{max} = 1$ mm)	~~4.99~~ 5.17 ± 1.8	~~1.23~~ $1.23 \pm 8.2 \times 10^{-2}$	~~-1.85~~ -1.93 ± 1.5
Geant4 O1 ($\delta l_{max} = 1$ cm)	~~6.96~~ 10.8 ± 3.4	~~0.929~~ $0.782 \pm 3.9 \times 10^{-2}$	~~-5.15~~ -10.7 ± 3.6
REAM	~~3.82~~ 3.98 ± 2.1	~~1.3175~~ 1.31 ± 0.20	~~-3.25×10^{-3}~~ $-8.41 \times 10^{-2} \pm 2.1$
GRRR	~~6.87~~ 4.24 ± 1.6	~~1.1760~~ 1.42 ± 0.11	~~-5.63~~ -0.639 ± 1.16

similar difference to what has been observed and discussed in Rutjes et al. (2016) concerning the high energy electron beams, and one can read the discussion therein for more details.

Figure 7 compares the electron spectra recorded at ~~128 meters~~ $z = 128$ meters (the electric field has a non-null component only in the z direction, so that electrons are accelerated towards positive z), for an electric field magnitude $E = 0.80$ MV/m, for a RREA generated from 200 ~~seed~~ initial ("seed") electrons with $\epsilon = 100$ keV. ~~The~~ This record distance was chosen because it corresponds to about 8.5 avalanche lengths, giving a maximum multiplication factor of about 5000, for which there is not doubt the RREA is fully developed and has reached self-similar state. This electric field of $E = 0.80$ MV/m was chosen because it is were we could observe the most interesting differences between the models, and it also happens to be the lowest for which we could build spectra with enough statistics on all the models to be able to present a precise comparison. The choice of 200 initial electrons is purely due to computational limitations.

In Figure 7, the error bars on the bottom panel represent the uncertainty due to the Poisson statistics inherent when counting particles. The four models are consistent within 10 % between 20 keV and 7 MeV. Below 20 keV, we think the discrepancy is not physical, and can be attributed to the recording methods set up for the different codes, that are not perfect and have a more or less important uncertainty range (that is not included in the display errors bars, only based on Poisson statistics). Above 7 MeV, O1 remains consistent with REAM overall, but O4 and O1 deviate significantly : up to 50 % for O4 and up to 90 % for GRRR. For the last bin between 58 and 74 MeV, O4 and GRRR are inconsistent, that is explained by the fact that GRRR does not include straggling for Bremsstrahlung (i.e. either explicit bremsstrahlung collision or some stochastic fluctuations mimicking straggling). The deviations for the high energy part (>7 MeV) in the electron spectrum are significant for this particular field ($E = 0.80$ MV/m), however this is not true for all electric fields, where the codes are overall roughly consistent, as seen in the Supplementary Material (section 6). In principle O4 should be more precise than O1 (Allison et al., 2006), as it includes more advanced models, yet we cannot argue that O4 is more accurate than REAM. One way of deciding which model is the most accurate might be to compare these results with experimental measurements. but in the context of ~~TGF~~ TGFs and Gamma-ray
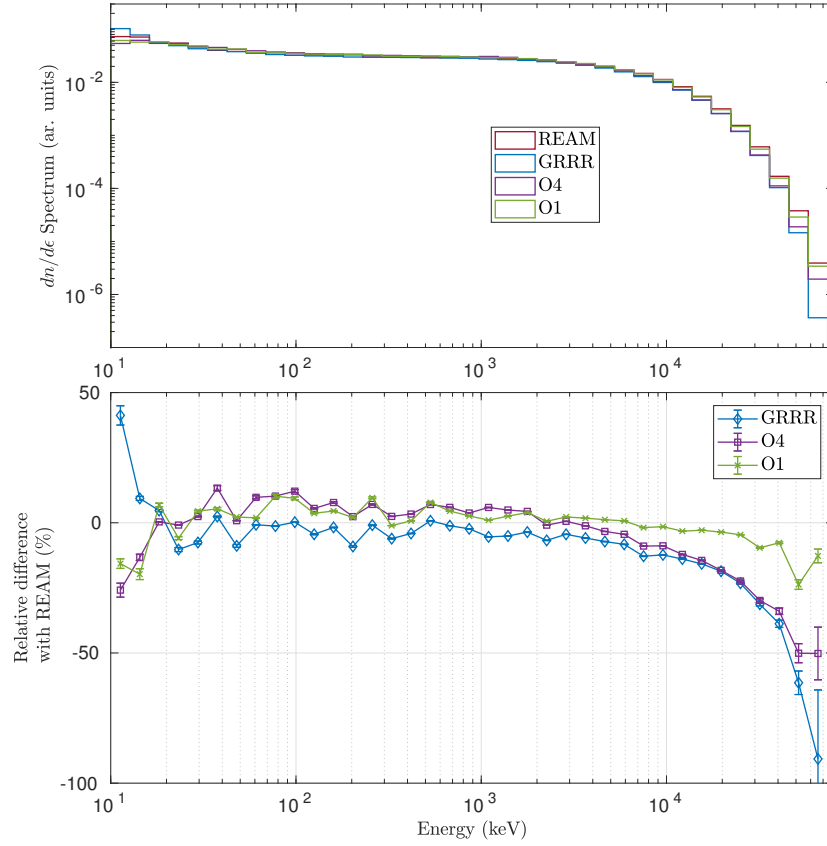
Figure 7. Top : Electron (kinetic) energy spectra of Geant4 (O4 and O1), REAM and GRRR, for $E = 0.80$ MV/m, recorded at ~~128~~ $z = 128$ m. The RREA is generated from 200 seed electrons of $\epsilon = 100$ keV. **Bottom** : relative difference between REAM and the three other models. The error bars are calculated from the Poisson statistics.

glows it is complicated to get a proper measurement of electron spectra produced by RREA. However, photons have much longer attenuation lengths than electron and can be more easily detected, e.g. from mountains, planes, balloons or satellites. In the next section we present and discuss the corresponding photon spectra.

4.3.2 Photons

5   In figure 8, the photon spectra recorded at ~~128 m for~~ $z = 128$ m (the electric field has a non-null component only in the z direction) for a magnitude $E = 0.80$ MV/m are given for Geant4 ~~O4~~O1/O4 and REAM, together with the relative difference with respect to REAM. The reasons why these z and E values were chosen is given in the previous section.

The error bars in the relative differences represent the uncertainty due to the inherent Poisson statistics when evaluating particle counts. The Geant4 O1 and O4 models are consistent for the full energy range, except a small discrepancy below 20

10   keV, that can be attributed to different physical models, O4 being more accurate in principle. In this case, it cannot be attributed

25

to recording methods, since they are exactly the same for both Geant4 models. At 10 keV the two Geant4 spectra are about 80 % larger than REAM. With increasing energy, the discrepancy reduces and reaches 0 % at 100 keV. Above 100 keV, the three models show consistent spectra. There may be some discrepancy above 30 MeV, but it is hard to conclude since the uncertainty interval is relatively large~~large~~.

5   As just presented, the main noticeable discrepancy between O1/O4 and REAM is present below 100 keV. As far as we know, there is no reason to argue that Geant4 gives a better result than REAM in this range, or vice-versa. One way to find out which model is the most accurate could be to compare these results with real measurements. Are such measurement possible to obtain? Any photon that an instrument could detect has to travel in a significant amount of air before reaching detectors. The average path ~~travelled~~ traveled in the atmosphere by a 100 keV photon in 12 km altitude air is 1540 ± 806 meters. It decreases

10   for lower energies and is 671 ± 484 meters at 50 keV, and 63.0 ± 61.5 meters at 20 keV. ~~Therefore these photons have no~~ Note that these lengths have been evaluated from precise Geant4 simulations, and are smaller than the attenuation lengths at the same energies, because photons gradually loose energy due to stochastic collisions. These average traveled paths are too small for the photons to have a reasonable chance to escape the atmosphere and to be detected by a satellite~~, but~~. But we cannot exclude that they may reach an airborne detector located inside or close to a thunderstorm. As a side note, we want to indicate

15   that the vast majority (if not all) of the photons observed from space with energies below a few hundred of kilo-electronvolts (e.g., by the Fermi space telescope, see Mailyan et al. (2016)) had very likely more than 1 MeV when they were emitted. They lost some part of their energy by collisions (with air molecules in the atmosphere or/and with some part of the satellite) before being detected by the satellite. For information, a figure presenting the probability of a photon to escape the atmosphere as function of its primary energy for a typical TGF is presented in the supplementary material, section 14.

20   **4.4   Other differences**

In addition to what is presented so far in this article, the following points should also be mentioned when comparing the results of the codes. The corresponding plots are available in the Supplementary Material.

– The ~~parallel velocity $\beta_\parallel$~~ mean parallel (to the E-field direction) velocity $\beta_\parallel$ of the avalanche is shown in section ~~9.2~~ 4.2 of the Supplementary Material (labeled "mean Z velocity"). We observe that GRRR is giving $\beta_\parallel$ faster than all the other

25   codes, and O4 is systematically slower than REAM and O1, though the differences are less than 2 %. The variation of $\beta_\parallel$ towards the electric field E is small, about 10 % for all codes. For increasing E-fields, electrons are less scattered and more focused in the field direction, hence slightly increasing $\beta_\parallel$.

– The electron to (bremsstrahlung) photon ratio $r_{e/p}$ was also calculated and compared for different distance record in the RREA shower, and the corresponding plots are presented in the Supplementary Material, section ~~7.~~ 3. GRRR is

30   excluded because it does not include photons. For any electric field, the same discrepancy is observed. At the beginning of the shower (<4 avalanche lengths), $r_{e/p}$ appears to be about 20 % larger for REAM compared to O1 and O4, then the three models are consistent at a given distance, and finally for more than about 4 avalanche lengths, the tendency is inverted and REAM presents a $r_{e/p}$ about 20 % smaller than Geant4. The magnitude of this discrepancy is largely
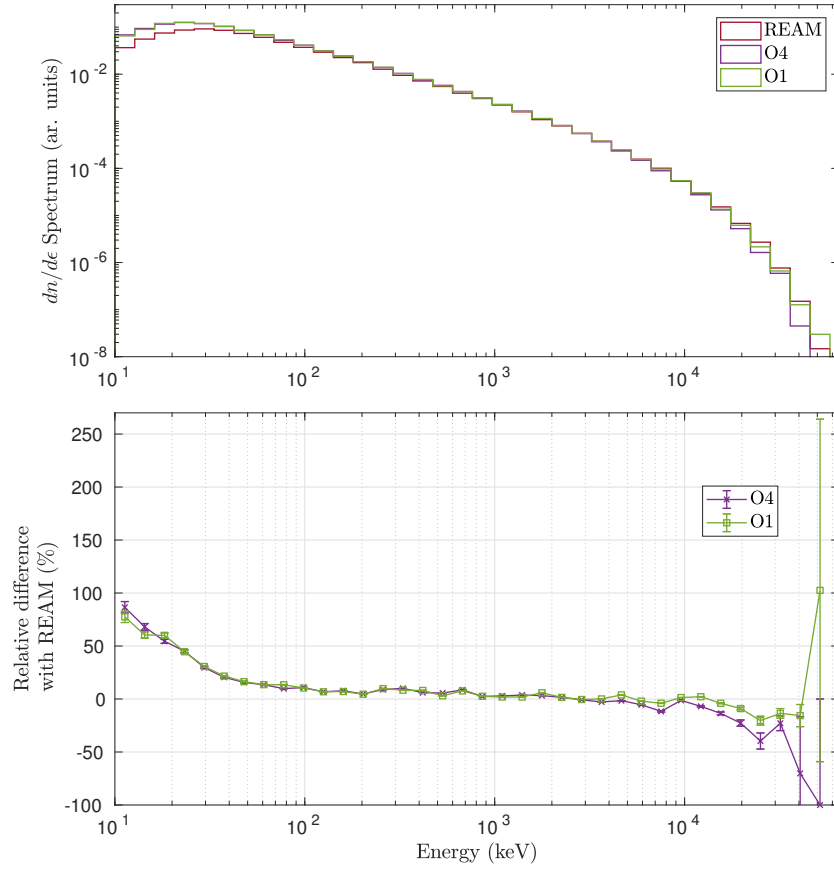
Figure 8. Top : Photon energy spectra of Geant4 (O4 and O1) and REAM for $E = 0.80$ MV/m, recorded at ~~128 m~~$z = 128\ m$. **Bottom** : relative difference between Geant4 (O1 and O4) and REAM. The error bars are calculated from the Poisson statistics.

reduced for increasing electric fields. We did not fully understand the reasons of these differences, and it may be due to the bremsstrahlung models used are involved. More investigations are required.

– The positron spectra have relatively low statistics (in the order of few hundreds particles recorded) and are all quite consistent within the relatively large uncertainties.

5 – In the photon spectra obtained from particle records at fixed times, REAM seems to show significantly less (at least a factor of 10) photon counts than the two Geant4 models for most of the electric fields magnitudes. For some fields, it even shows a lack of high energy photons, with a sharp cut at about 30 MeV. It seems to point out to a problem in the record method, explaining why we chose not to discuss these spectra in the main article. The spectra produced by the Geant4 O1 and O4 models for this case are consistent with one another for all the E-fields.

27

5 ~~Conclusion~~Conclusions

We have investigated the results of three Monte Carlo codes able to simulate Relativistic Runaway Electron Avalanches (RREA), including the effects of electric fields up to the classical breakdown field, which is $E_k \approx 3$ MV/m at STP. The Monte-Carlo codes REAM, GRRR and Geant4 (two models: O1 and O4) were compared. The main difference between the Geant4 O4 and O1 ~~is due to~~ models is the inclusion of more precise cross sections for low energy interactions (< 10 keV) ~~.~~ for O4.

~~From analytical considerations, we have shown first that the full characterisation~~ We first proposed a theoretical description of the RREA ~~(such as the avalanche length or the mean energy)~~ process, that is based and incremented over previous published works. Our analysis confirmed that the relativistic avalanche is mainly driven by electric fields and the ionisation and scattering processes determining $\epsilon_2^{\min}$ ~~(~~, the minimum energy of electrons that can runaway~~) and the associated probabilities. The exact value of $\epsilon_2^{\min}$ depends on the electric field magnitude, but a reasonable lower boundary can be set to $\epsilon_2^{\min} = 10$ keV for any electric field below 3 MV/m (at STP)~~. This is different from some of the previous works that speculated that the low energy threshold (ε_c), when changed from 1 keV to 250 eV, was the most important factor affecting the electron energy spectra (Skeltved et al., 2014; Rutjes et al., 2016) .

~~To investigate this point further~~Then, we estimated the probability to produce a RREA from a given electron energy (ϵ) and a given electric field magnitude (E). We found that the stepping methodology is of major importance, and the stepping parameters are not set up satisfactorily in Geant4 by default. We pointed out which settings should be adjusted and provided example codes to the community (see sections 6 and 7). When properly set-up, the two Geant4 models showed a good overall agreement (within ≈ 10 %) with REAM and GRRR. From the Geant4~~and GRRR~~, GRRR and REAM simulations, we found that the probability for the particles below ~~10~~≈ 10 keV to accelerate and participate in the penetrating radiation is actually negligible for the full range of electric field we tested ($E < 3$ MV/m). ~~In practice, an energy threshold~~ It results that a reasonable lower boundary of the low energy threshold (ε_c~~of about of 10 keV or higher (for lower fields~~) can be ~~used, making~~ set to ≈ 10 keV for any electric field below $E_k \approx 3$ MV/m (at STP), making it possible to have relatively fast simulations. For lower electric fields, it is possible to use larger ε_c, following a curve we provided (Figure 2.b).

The advantage of using more sophisticated cross sections able to accurately ~~track~~ take into account low energy particles could be probed by comparing directly the O1 and O4 ~~: it~~models. They showed minor differences that are mainly visible only for high E-fields ($E > 2$ MV/m), where ~~particles with lower energies~~low energy particles have more chance to runaway.

In a second part, we produced RREA simulations from the four models, and compared the physical characteristics of the produced ~~RREA~~showers. The two Geant4 models and REAM showed a good agreement on all the parameters we tested. GRRR also showed an overall good agreement with the other codes, except for the electron energy spectra. ~~As far as we know, it~~ That is probably because GRRR does not include straggling for the radiative and ionisation energy losses, hence implementing these two processes is of primary importance to produce accurate RREA spectra. By comparing O1 and O4, we also pointed out that including precise modelling of the interactions of particles below ~~10~~≈ 10 keV provided only small differences; the most important being a $\approx$ ~~5%~~ 5% change in the avalanche multiplication times and lengths. We also pointed out a discrepancy from Geant4 (O1 and O4) compared REAM, that is a 10% to 100% relative difference in the low energy part (< 100 keV) of the

photon energy spectrum for an electric field of $E = 0.80$ MV/m. But we argued that it is unlikely to have an impact on spectra detected from satellites.

6 Recommendations

From the experience of this study, we give the following general recommendations concerning RREA simulations :

- Codes should be checked / tested / benchmarked using standard test set-ups. In the supplementary material, we provide a precise description of such tests. In section ~~6~~7 of this article, we provide links to download the full ~~dataset~~ data-set we obtained for the codes we tested (Geant4 with two set-ups, REAM and GRRR), as well as processing scripts. We also provide the source code of the Geant4 codes.

- Custom-made codes should be make available to other researchers, or at least the results they give for standard tests.

- In order to make it possible to compare results from different studies, the methodology used to derive a given quantity should be rigorously chosen, and presented ~~somewhere (in the main article, in the supplementary material, on a webpage, or other)~~clearly somewhere.

- Extending the recommendations of Rutjes et al. (2016), we concluded that to get an accurate RREA electron spectra above 10 MeV, radiative loss (bremsstrahlung) should not be implemented with uniform friction only: straggling should be included. Straggling should also be included for ionisation energy ~~looses below~~ loses below the energy threshold.

Concerning the usage of Geant4 for simulating RREA :

- Default settings are not able to simulate RREA accurately. To get accurate RREA results, one of the following tweaks is possible :

    - Changing the α_R ("dR over Range") parameter of the electron/positron ionisation process to 5.0×10^{-3} or less. This solution gives the best ratio between accuracy and computation time. Leave the "final range" parameter to one millimeter (default value) or less.

    - Setting up a step limitation process (or a maximum acceptable step) to one millimeters or less. This will significantly increase the required computation time.

    - Using the single (Coulomb) scattering model instead of multiple scattering (the two previous tweaks relying on the multiple scattering algorithm). This will ~~quite~~ substantially increase the necessary computation time. This is because multiple scatterings algorithms were invented to make the simulation run faster by permitting to use substantially larger (usually >10 times) step lengths compared to a pure single scattering strategy, while keeping a similar accuracy.

- In section 7, we provide a link to Geant4 example source codes implementing these three methods.

29

- Compared to using the default Møller/Bhabha scattering models for ionisation, the usage of more accurate cross sections, e.g. taking into account the electrons' molecular ~~biding~~ binding energies (like done for the Livermore or Penelope models), only leads to minor differences.

7 Code and/or data availability

The full simulation output data of the four models is available though the following link:

https://filesender.uninett.no/?s=download&token=738a8663-a457-403a-991e-ae8d3fca3dc3

The scripts used to process this data to make the ~~figure~~ figures of the supplementary material are available in the following repository:

https://gitlab.com/dsarria/HEAP2_matlab_codes.git

The full GRRR source code is available in the following repository :

https://github.com/aluque/grrr/tree/avalanches

The Geant4 source code for the RREA probability simulations is available in the following repository :

https://gitlab.com/dsarria/av_prob.git

The Geant4 source code for the RREA characterisation simulations is available in the following repository :

https://gitlab.com/dsarria/RREA_characteristics.git

Model $\delta\ell_{\max}$	Option 1 (O1)	Option 4 (O4)
10 cm	**1**	**6.49**
1 cm	**11.5**	**27.2**
1 mm	**222**	**393**
0.1 mm	**2100**	**3740**
α_R (default)	0.80	0.20

Model α_R	Option 1 (O1)	Option 4 (O4)
0.80	**≈1**	**2.44**
0.20	**2.61**	**7.66**
0.050	**7.12**	**36.5**
0.0050	**21.0**	**126**
0.0010	**41.7**	**224**
$\delta\ell_{\max}$ (default)	1 km	1 km

Table 3. Computation time needed by different Geant4 configurations for the simulation of the same physical problem, relatively to the Geant4 O1 $\delta\ell_{\max} = 10$ cm case. Two parameters are tested : the maximum allowed step ($\delta\ell_{\max}$) and the "~~dRoverRange~~dR over Range" (α_R).

Appendix A: Geant4 relative performance

Table ~~A1~~ 3 presents the relative computation times it takes to complete the simulation with an ~~Electric~~ electric field magnitude of 1.2 MV/m, and 100 ~~seed~~ initial ("seed") electrons with initial energy $\epsilon = 100$ keV, and a stop time (physical) of 233 nanoseconds. The fastest simulation uses Geant4 with the O1 physics list and $\delta\ell_{\max} = 10$ cm and took 4.53 seconds to complete on one thread with the microprocessor we used. The simulations with the O4 physics list with $\delta\ell_{\max} = 1$ mm requires about 400 times more computation time. Setting up $\delta\ell_{\max} = 1$ mm, or lower, is necessary to achieve correct simulation of the RREA process, as argued in section 3. To achieve it for the full range of electric fields we tested (in a reasonable amount of time), it required the use of the Norwegian FRAM computer cluster. The simulations with $\delta\ell_{\max} = 0.1$ mm for all electric fields could not be achieved in a reasonable amount of time, even by using the computer cluster.

On the other hand, if $\delta\ell_{\max}$ is left at its default value (1 kilometer) and α_R parameter is tweaked instead, accurate simulations can be achieved with a value of $\alpha_R = 5.0 \times 10^{-3}$ or lower. It requires almost an order of magnitude less computation time compared to using $\delta\ell_{\max} = 1$ mm.

References

Adachi, T., Takahashi, Y., Ohya, H., Tsuchiya, F., Yamashita, K., Yamamoto, M., and Hashiguchi, H.: Monitoring of Lightning Activity in Southeast Asia: Scientific Objectives and Strategies, Kyoto Working Papers on Area Studies: G-COE Series, 2008.

Agostinelli, S. et al.: GEANT4: A simulation toolkit, Nucl. Instrum. Meth., A506, 250–303, doi:10.1016/S0168-9002(03)01368-8, 2003.

5   Allison, J., Amako, K., Apostolakis, J., Araujo, H., Dubois, P. A., Asai, M., Barrand, G., Capra, R., Chauvie, S., Chytracek, R., Cirrone, G. A. P., Cooperman, G., Cosmo, G., Cuttone, G., Daquino, G. G., Donszelmann, M., Dressel, M., Folger, G., Foppiano, F., Generowicz, J., Grichine, V., Guatelli, S., Gumplinger, P., Heikkinen, A., Hrivnacova, I., Howard, A., Incerti, S., Ivanchenko, V., Johnson, T., Jones, F., Koi, T., Kokoulin, R., Kossov, M., Kurashige, H., Lara, V., Larsson, S., Lei, F., Link, O., Longo, F., Maire, M., Mantero, A., Mascialino, B., McLaren, I., Lorenzo, P. M., Minamimoto, K., Murakami, K., Nieminen, P., Pandola, L., Parlati, S., Peralta, L., Perl, J., Pfeiffer, A.,

10   Pia, M. G., Ribon, A., Rodrigues, P., Russo, G., Sadilov, S., Santin, G., Sasaki, T., Smith, D., Starkov, N., Tanaka, S., Tcherniaev, E., Tome, B., Trindade, A., Truscott, P., Urban, L., Verderi, M., Walkden, A., Wellisch, J. P., Williams, D. C., Wright, D., and Yoshida, H.: Geant4 developments and applications, IEEE Transactions on Nuclear Science, 53, 270–278, doi:10.1109/TNS.2006.869826, 2006.

Allison, J., Amako, K., Apostolakis, J., et al.: Recent developments in Geant4, Nuclear Instruments and Methods in Physics Research Section A: Accelerators, Spectrometers, Detectors and Associated Equipment, 835, 186 – 225, doi:https://doi.org/10.1016/j.nima.2016.06.125,

15   http://www.sciencedirect.com/science/article/pii/S0168900216306957, 2016.

Apostolakis, J., Asai, M., Bogdanov, A., Burkhardt, H., Cosmo, G., Elles, S., Folger, G., Grichine, V., Gumplinger, P., Heikkinen, A., Hrivnacova, I., Ivanchenko, V., Jacquemier, J., Koi, T., Kokoulin, R., Kossov, M., Kurashige, H., McLaren, I., Link, O., Maire, M., Pokorski, W., Sasaki, T., Starkov, N., Urban, L., and Wright, D.: Geometry and physics of the Geant4 toolkit for high and medium energy applications, Radiation Physics and Chemistry, 78, 859 – 873, doi:https://doi.org/10.1016/j.radphyschem.2009.04.026, http://www.

20   sciencedirect.com/science/article/pii/S0969806X09001650, workshop on Use of Monte Carlo Techniques for Design and Analysis of Radiation Detectors, 2009.

Babich, L., Donskoy, E., Kutsyk, I., and Roussel-Dupré, R.: The feedback mechanism of runaway air breakdown, Geophysical research letters, 32, L09809, doi:10.1029/2004GL021744, 2005.

Babich, L. P.: Generation of neutrons in giant upward atmospheric discharges, JETP letters, 84, 285–288, 2006.

25   Babich, L. P., Donskoy, E. N., Kutsyk, I. M., Kudryavtsev, A. Y., Roussel-Dupre, R. A., Shamraev, B. N., and Symbalisty, E. M.: Comparison of relativistic runaway electron avalanche rates obtained from Monte Carlo simulations and kinetic equation solution, IEEE transactions on plasma science, 29, 430–438, 2001.

Babich, L. P., Bakhov, K. I., Balakin, V. A., Donskoi, E. N., Zavada, N. I., Zelenskii, K. F., Il'kaev, R. I., Kutsyk, I. M., Loiko, T. V., Nedoikash, Y. M., Pavlovskaya, N. G., Roussel-Dupre, R. A., Symbalisty, E. M. D., and Shamraev, B. N.: An Experi-

30   mental Investigation of an Avalanche of Relativistic Runaway Electrons under Normal Conditions, High Temperature, 42, 1–11, doi:10.1023/B:HITE.0000020085.61526.40, https://doi.org/10.1023/B:HITE.0000020085.61526.40, 2004a.

Babich, L. P., Donskoy, E. N., Il'kaev, R. I., Kutsyk, I. M., and Roussel-Dupre, R. A.: Fundamental parameters of a relativistic runaway electron avalanche in air, Plasma Physics Reports, 30, 616–624, doi:10.1134/1.1778437, https://doi.org/10.1134/1.1778437, 2004b.

Bethe, H. and Heitler, W.: On the stopping of fast particles and on the creation of positive electrons, Proceedings of the Royal Society of

35   London A: Mathematical, Physical and Engineering Sciences, 146, 83–112, 1934.

Bowers, G. S., Smith, D. M., Martinez-McKinney, G., Kamogawa, M., Cummer, S., Dwyer, J., Wang, D., Stock, M., and Kawasaki, Z.: Gamma Ray Signatures of Neutrons From a Terrestrial Gamma Ray Flash, Geophysical Research Letters, 2017.

Briggs, M. S., Fishman, G. J., Connaughton, V., Bhat, P. N., Paciesas, W. S., Preece, R. D., Wilson-Hodge, C., Chaplin, V. L., Kippen, R. M., von Kienlin, A., Meegan, C. A., Bissaldi, E., Dwyer, J. R., Smith, D. M., Holzworth, R. H., Grove, J. E., and Chekhtman, A.: First results on terrestrial gamma ray flashes from the Fermi Gamma-ray Burst Monitor, Journal of Geophysical Research (Space Physics), 115, A07323, doi:10.1029/2009JA015242, 2010.

5 Briggs, M. S., Connaughton, V., Wilson-Hodge, C., Preece, R. D., Fishman, G. J., Kippen, R. M., Bhat, P., Paciesas, W. S., Chaplin, V. L., Meegan, C. A., et al.: Electron-positron beams from terrestrial lightning observed with Fermi GBM, Geophysical research letters, 38, L02808, doi:10.1029/2010GL046259, 2011.

Brown, J. M. C., Dimmock, M. R., Gillam, J. E., and Paganin, D. M.: A low energy bound atomic electron Compton scattering model for Geant4, Nuclear Instruments and Methods in Physics Research B, 338, 77–88, doi:10.1016/j.nimb.2014.07.042, 2014.

10 Carlson, B., Lehtinen, N. G., and Inan, U. S.: Neutron production in terrestrial gamma ray flashes, Journal of Geophysical Research: Space Physics, 115, A00E19, doi:10.1029/2009JA014696, 2010.

Celestin, S. and Pasko, V. P.: Soft collisions in relativistic runaway electron avalanches, Journal of Physics D: Applied Physics, 43, 315206, doi:10.1088/0022-3727/43/31/315206, 2010.

Celestin, S. and Pasko, V. P.: Energy and fluxes of thermal runaway electrons produced by exponential growth of streamers during

15 the stepping of lightning leaders and in transient luminous events, Journal of Geophysical Research: Space Physics, 116, A03315, doi:10.1029/2010JA016260, 2011.

Celestin, S., Xu, W., and Pasko, V. P.: Terrestrial gamma ray flashes with energies up to 100 MeV produced by nonequilibrium acceleration of electrons in lightning, Journal of Geophysical Research (Space Physics), 117, A05315, doi:10.1029/2012JA017535, http://dx.doi.org/ 10.1029/2012JA017535, a05315, 2012.

20 Chanrion, O. and Neubert, T.: Production of runaway electrons by negative streamer discharges, J. Geophys. Res. (Space Phys), 115, A00E32, doi:10.1029/2009JA014774, 2010.

Chanrion, O., Bonaventura, Z., Çinar, D., Bourdon, A., and Neubert, T.: Runaway electrons from a "beam-bulk" model of streamer: application to TGFs, Environmental Research Letters, 9, 055003, doi:10.1088/1748-9326/9/5/055003, 2014.

Chanrion, O., Bonaventura, Z., Bourdon, A., and Neubert, T.: Influence of the angular scattering of electrons on the runaway threshold in air,

25 Plasma Physics and Controlled Fusion, 58, 044001, doi:10.1088/0741-3335/58/4/044001, 2016.

Chilingarian, A., Daryan, A., Arakelyan, K., Hovhannisyan, A., Mailyan, B., Melkumyan, L., Hovsepyan, G., Chilingaryan, S., Reymers, A., and Vanyan, L.: Ground-based observations of thunderstorm-correlated fluxes of high-energy electrons, gamma rays, and neutrons, Physical Review D, 82, 043009, doi:10.1103/PhysRevD.82.043009, 2010.

Chilingarian, A., Hovsepyan, G., and Hovhannisyan, A.: Particle bursts from thunderclouds: Natural particle accelerators above our heads,

30 Physical review D, 83, 062001, doi:10.1103/PhysRevD.83.062001, 2011.

Chilingarian, A., Mailyan, B., and Vanyan, L.: Recovering of the energy spectra of electrons and gamma rays coming from the thunderclouds, Atmospheric Research, 114, 1–16, doi:10.1016/j.atmosres.2012.05.008, 2012.

Chilingarian, A., Hovsepyan, G., Khanikyanc, G., Reymers, A., and Soghomonyan, S.: Lightning origination and thunderstorm ground enhancements terminated by the lightning flash, EPL (Europhysics Letters), 110, 49 001, 2015.

35 Coleman, L. M. and Dwyer, J. R.: Propagation speed of runaway electron avalanches, Geophysical Research Letters, 33, L11810, doi:10.1029/2006GL025863, 2006.

Cooray, V., Arevalo, L., Rahman, M., Dwyer, J., and Rassoul, H.: On the possible origin of X-rays in long laboratory sparks, J. Atm. Sol.-Terr. Phys., 71, 1890, doi:10.1016/j.jastp.2009.07.010, 2009.

Cramer, E. S., Dwyer, J. R., Arabshahi, S., Vodopiyanov, I., Liu, N., and Rassoul, H.: An analytical approach for calculating energy spectra of relativistic runaway electron avalanches in air, Journal of Geophysical Research: Space Physics, 119, 7794–7823, 2014.

Cramer, E. S., Dwyer, J. R., and Rassoul, H. K.: Magnetic field modification to the relativistic runaway electron avalanche length, Journal of Geophysical Research (Space Physics), 121, 11, doi:10.1002/2016JA022891, 2016.

5 Dubinova, A., Rutjes, C., Ebert, U., Buitink, S., Scholten, O., and Trinh, G. T. N.: Prediction of Lightning Inception by Large Ice Particles and Extensive Air Showers, Physical Review Letters, 115, 015 002, doi:10.1103/PhysRevLett.115.015002, https://link.aps.org/doi/10. 1103/PhysRevLett.115.015002, 2015.

Dwyer, J., Saleh, Z., Rassoul, H., Concha, D., Rahman, M., Cooray, V., Jerauld, J., Uman, M., and Rakov, V.: A study of X-ray emission from laboratory sparks in air at atmospheric pressure, Journal of Geophysical Research: Atmospheres, 113, D23207,

10   doi:10.1029/2008JD010315, 2008.

Dwyer, J. R.: A fundamental limit on electric fields in air, Geophysical Research Letters, 30, 2055, doi:10.1029/2003GL017781, http: //www.agu.org/pubs/crossref/2003/2003GL017781.shtml, 2003.

Dwyer, J. R.: Relativistic breakdown in planetary atmospheres, Physics of Plasmas, 14, 042 901, doi:10.1063/1.2709652, 2007.

Dwyer, J. R.: Source mechanisms of terrestrial gamma-ray flashes, Journal of Geophysical Research: Atmospheres, 113, n/a–n/a,

15   doi:10.1029/2007JD009248, http://dx.doi.org/10.1029/2007JD009248, d10103, 2008.

Dwyer, J. R.: The relativistic feedback discharge model of terrestrial gamma ray flashes, J. Geophys. Res. (Space Phys), 117, A02308, doi:10.1029/2011JA017160, 2012.

Dwyer, J. R., Grefenstette, B. W., and Smith, D. M.: High-energy electron beams launched into space by thunderstorms, Geophysical Research Letters, 35, L02815, doi:10.1029/2007GL032430, http://dx.doi.org/10.1029/2007GL032430, 2008.

20 Dwyer, J. R., Smith, D. M., and Cummer, S. A.: High-Energy Atmospheric Physics: Terrestrial Gamma-Ray Flashes and Related Phenomena, Space Science Review, 173, 133–196, doi:10.1007/s11214-012-9894-0, 2012.

Dwyer, J. R., Smith, D. M., Hazelton, B. J., Grefenstette, B. W., Kelley, N. A., Lowell, A. W., Schaal, M. M., and Rassoul, H. K.: Positron clouds within thunderstorms, Journal of Plasma Physics, 81, 475810405, doi:10.1017/S0022377815000549, 2015.

Eack, K. B., Beasley, W. H., Rust, W. D., Marshall, T. C., and Stolzenburg, M.: Initial results from simultaneous observation of X-rays and

25   electric fields in a thunderstorm, Journal of Geophysical Research: Atmospheres, 101, 29 637–29 640, doi:10.1029/96JD01705, 1996.

Ferrari, A., Sala, P. R., Fasso, A., and Ranft, J.: FLUKA: A multi-particle transport code (Program version 2005), Tech. rep., 2005.

Fishman, G. J., Bhat, P. N., Mallozzi, R., Horack, J. M., Koshut, T., Kouveliotou, C., Pendleton, G. N., Meegan, C. A., Wilson, R. B., Paciesas, W. S., Goodman, S. J., and Christian, H. J.: Discovery of Intense Gamma-Ray Flashes of Atmospheric Origin, Science, 264, 1313–1316, doi:10.1126/science.264.5163.1313, 1994.

30 Grefenstette, B. W., Smith, D. M., Hazelton, B. J., and Lopez, L. I.: First RHESSI terrestrial gamma ray flash catalog, Journal of Geophysical Research (Space Physics), 114, A02314, doi:10.1029/2008JA013721, 2009.

Gurevich, A.: On the theory of runaway electrons, Sov. Phys. JETP, 12, 904–912, 1961.

Gurevich, A. and Zybin, K.: Kinetic equation for high energy electrons in gases, Physics Letters A, 237, 240–246, 1998.

Gurevich, A., Milikh, G., and Roussel-Dupre, R.: Runaway electron mechanism of air breakdown and preconditioning during a thunderstorm,

35   Physics Letters A, 165, 463–468, doi:10.1016/0375-9601(92)90348-P, http://linkinghub.elsevier.com/retrieve/pii/037596019290348P, 1992.

Hirayama, H., Namito, Y., Nelson, W. R., Bielajew, A. F., Wilderman, S. J., and Michigan, U.: The EGS5 code system, Tech. rep., United States. Department of Energy, 2005.

34

Ihaddadene, M. A. and Celestin, S.: Increase of the electric field in head-on collisions between negative and positive streamers, grl, 42, 5644–5651, doi:10.1002/2015GL064623, 2015.

Ivanchenko, V. N., Bukin, A. D., Dubrovin, M. S., Eidelman, S. I., Grozina, N. A., and Tayursky, V. A.: UNIMOD2: Universal Monte Carlo code for simulation of e+ e- experiments, in: MC 91: Detector and event simulation in high-energy physics. Proceedings, Workshop, Amsterdam, Netherlands, April 8-12, 1991, pp. 79–85, 1991.

Kelley, N. A., Smith, D. M., Dwyer, J. R., Splitt, M., Lazarus, S., Martinez-McKinney, F., Hazelton, B., Grefenstette, B., Lowell, A., and Rassoul, H. K.: Relativistic electron avalanches as a thunderstorm discharge competing with lightning, Nature communications, 6, 2015.

Kochkin, P., Köhn, C., Ebert, U., and van Deursen, L.: Analyzing x-ray emissions from meter-scale negative discharges in ambient air, Plasma Sources Science and Technology, 25, 044 002, 2016.

Kochkin, P., van Deursen, A. P. J., Marisaldi, M., Ursi, A., de Boer, A. I., Bardet, M., Allasia, C., Boissin, J.-F., Flourens, F., and Østgaard, N.: In-flight observation of gamma-ray glows by ILDAS, Journal of Geophysical Research: Atmospheres, doi:10.1002/2017JD027405, http://dx.doi.org/10.1002/2017JD027405, 2017.

Kochkin, P., Sarria, D., Skeie, C., Deursen, A. P. J., Boer, A. I., Bardet, M., Allasia, C., Flourens, F., and Østgaard, N.: In-Flight Observation of Positron Annihilation by ILDAS, Journal of Geophysical Research: Atmospheres, 0, doi:10.1029/2018JD028337, https://agupubs. onlinelibrary.wiley.com/doi/abs/10.1029/2018JD028337, 2018.

Köhn, C. and Ebert, U.: Calculation of beams of positrons, neutrons, and protons associated with terrestrial gamma ray flashes, Journal of Geophysical Research: Atmospheres, 120, 1620–1635, 2015.

Köhn, C., Ebert, U., and Mangiarotti, A.: The importance of electron–electron bremsstrahlung for terrestrial gamma-ray flashes, electron beams and electron–positron beams, Journal of Physics D: Applied Physics, 47, 252 001, http://stacks.iop.org/0022-3727/47/i=25/a= 252001, 2014.

Köhn, C., Diniz, G., and Harakeh, M. N.: Production mechanisms of leptons, photons, and hadrons and their possible feedback close to lightning leaders, Journal of Geophysical Research: Atmospheres, 122, 1365–1383, 2017.

Landau, L. D., Bell, J., Kearsley, M., Pitaevskii, L., Lifshitz, E., and Sykes, J.: Electrodynamics of continuous media, vol. 8, elsevier, 2013.

Lefeuvre, F., Blanc, E., and Pinçon, J. L.: TARANIS-a Satellite Project Dedicated to the Physics of TLEs and TGFs, in: American Institute of Physics Conference Series, vol. 1118 of *American Institute of Physics Conference Series*, pp. 3–7, doi:10.1063/1.3137711, 2009.

Lehtinen, N. G. and Østgaard, N.: X-ray Emissions in a Multiscale Fluid Model of a Streamer Discharge, Journal of Geophysical Research: Atmospheres, 123, 6935–6953, doi:10.1029/2018JD028646, https://agupubs.onlinelibrary.wiley.com/doi/abs/10.1029/2018JD028646, 2018.

Lehtinen, N. G., Bell, T. F., and Inan, U. S.: Monte Carlo simulation of runaway MeV electron breakdown with application to red sprites and terrestrial gamma ray flashes, jgr, 104, 24 699–24 712, doi:10.1029/1999JA900335, 1999.

Li, C., Ebert, U., and Hundsdorfer, W.: 3D hybrid computations for streamer discharges and production of runaway electrons, Journal of Physics D: Applied Physics, 42, 202003, doi:10.1088/0022-3727/42/20/202003, 2009.

Liu, C., Brennan, D. P., Bhattacharjee, A., and Boozer, A. H.: Adjoint Fokker-Planck equation and runaway electron dynamics, Physics of Plasmas, 23, 010 702, 2016.

Luque, A.: Relativistic Runaway Ionization Fronts, Physical Review Letters, 112, 045003, doi:10.1103/PhysRevLett.112.045003, 2014.

Luque, A.: Radio Frequency Electromagnetic Radiation From Streamer Collisions, Journal of Geophysical Research (Atmospheres), 122, 10, doi:10.1002/2017JD027157, 2017.

Mailyan, B. G., Briggs, M. S., Cramer, E. S., Fitzpatrick, G., Roberts, O. J., Stanbro, M., Connaughton, V., McBreen, S., Bhat, P. N., and Dwyer, J. R.: The spectroscopy of individual terrestrial gamma-ray flashes: Constraining the source properties, Journal of Geophysical Research (Space Physics), 121, 11, doi:10.1002/2016JA022702, 2016.

Marisaldi, M., Fuschino, F., Tavani, M., Dietrich, S., Price, C., Galli, M., et al.: Properties of terrestrial gamma ray flashes detected by AGILE MCAL below 30 MeV, Journal of Geophysical Research (Space Physics), 119, 1337–1355, doi:10.1002/2013JA019301, 2014.

McCarthy, M. and Parks, G.: Further observations of X-rays inside thunderstorms, Geophysical Research Letters, 12, 393–396, doi:10.1029/GL012i006p00393, 1985.

Moss, G. D., Pasko, V. P., Liu, N., and Veronis, G.: Monte Carlo model for analysis of thermal runaway electrons in streamer tips in transient luminous events and streamer zones of lightning leaders, Journal of Geophysical Research (Space Physics), 111, A02307, doi:10.1029/2005JA011350, 2006.

Neubert, T., Kuvvetli, I., Budtz-Jørgensen, C., Østgaard, N., Reglero, V., and Arnold, N.: The atmosphere-space interactions monitor (ASIM) for the international space station, in: Proceedings of the ILWS Workshop, edited by Gopalswamy, N. and Bhattacharyya, A., p. 448, 2006.

Østgaard, N., Gjesteland, T., Stadsnes, J., Connell, P., and Carlson, B.: Production altitude and time delays of the terrestrial gamma flashes: Revisiting the Burst and Transient Source Experiment spectra, Journal of Geophysical Research: Space Physics, 113, A02307, doi:10.1029/2007JA012618, 2008.

Parks, G. K., Mauk, B. H., Spiger, R., and Chin, J.: X-ray enhancements detected during thunderstorm and lightning activities, Geophysical Research Letters, 8, 1176–1179, doi:10.1029/GL008i011p01176, https://agupubs.onlinelibrary.wiley.com/doi/abs/10.1029/GL008i011p01176, 1981.

Perkins, S., Cullen, D., and Seltzer, S.: Tables and graphs of electron-interaction cross sections from 10 eV to 100 GeV derived from the LLNL Evaluated Electron Data Library (EEDL), Z = 1–100, Tech. rep., doi:10.2172/5691165, https://doi.org/10.2172/5691165, 1991.

Rahman, M., Cooray, V., Azlinda Ahmad, N., Nyberg, J., Rakov, V. A., and Sharma, S.: X rays from 80-cm long sparks in air, grl, 35, L06 805, doi:10.1029/2007GL032678, 2008.

Raizer, Y. P.: Gas discharge physics, vol. 2, Springer Berlin, 1997.

Roberts, O. J., Fitzpatrick, G., Stanbro, M., McBreen, S., Briggs, M. S., Holzworth, R. H., Grove, J. E., Chekhtman, A., Cramer, E. S., and Mailyan, B. G.: The First Fermi-GBM Terrestrial Gamma Ray Flash Catalog, Journal of Geophysical Research (Space Physics), 123, 4381–4401, doi:10.1029/2017JA024837, 2018.

Roussel-Dupre, R. A., Gurevich, A. V., Tunnell, T., and Milikh, G. M.: Kinetic theory of runaway air breakdown, Physical Review E, 49, 2257–2271, doi:10.1103/PhysRevE.49.2257, 1994.

Rutjes, C., Sarria, D., Skeltved, A. B., Luque, A., Diniz, G., Østgaard, N., and Ebert, U.: Evaluation of Monte Carlo tools for high energy atmospheric physics, Geoscientific Model Development, 9, 3961, doi:10.5194/gmd-9-3961-2016, http://www.geosci-model-dev.net/9/3961/2016/, 2016.

Rutjes, C., Diniz, G., Ferreira, I. S., and Ebert, U.: TGF afterglows: a new radiation mechanism from thunderstorms, Geophysical Research Letters, doi:10.1002/2017GL075552, 2017.

Salvat, F., Fernández-Varea, J. M., and Sempau, J.: PENELOPE-2011: A Code System for Monte Carlo Simulation of Electron and Photon Transport, 2011.

Sarria, D., Blelly, P.-L., and Forme, F.: MC-PEPTITA: a Monte Carlo model for Photon, Electron and Positron Tracking In Terrestrial Atmosphere. Application for a Terrestrial Gamma-ray Flash, Journal of Geophysical Research: Space Physics, pp. n/a–n/a, doi:10.1002/2014JA020695, http://dx.doi.org/10.1002/2014JA020695, 2014JA020695, 2015.

Sarria, D., Blelly, P.-L., Briggs, M. S., and Forme, F.: Studying the time histogram of a terrestrial electron beam detected from the opposite hemisphere of its associated TGF, Journal of Geophysical Research: Space Physics, pp. n/a–n/a, doi:10.1002/2015JA021881, http://dx.doi.org/10.1002/2015JA021881, 2016.

Sarria, D., Lebrun, F., Blelly, P.-L., Chipaux, R., Laurent, P., Sauvaud, J.-A., Prech, L., Devoto, P., Pailot, D., Baronick, J.-P., and Lindsey-Clark, M.: TARANIS XGRE and IDEE detection capability of terrestrial gamma-ray flashes and associated electron beams, Geoscientific Instrumentation, Methods and Data Systems, 6, 239–256, doi:10.5194/gi-6-239-2017, https://www.geosci-instrum-method-data-syst.net/6/239/2017/, 2017.

Shao, T., Zhang, C., Niu, Z., Yan, P., Tarasenko, V. F., Baksht, E. K., Burahenko, A. G., and Shut'ko, Y. V.: Diffuse discharge, runaway electron, and x-ray in atmospheric pressure air in an inhomogeneous electrical field in repetitive pulsed modes, Applied Physics Letters, 98, 021503, doi:10.1063/1.3540504, 2011.

Skeltved, A. B., Østgaard, N., Carlson, B., Gjesteland, T., and Celestin, S.: Modeling the relativistic runaway electron avalanche and the feedback mechanism with GEANT4, Journal of Geophysical Research: Space Physics, 119, 9174–9191, doi:10.1002/2014ja020504, http://dx.doi.org/10.1002/2014JA020504, 2014.

Teruaki, E., Wada, Y., et al.: Photonuclear reactions triggered by lightning discharge, Nature, 551, doi:10.1038/nature24630, https://www.nature.com/articles/nature24630, 2017.

Torii, T., Takeishi, M., and Hosono, T.: Observation of gamma-ray dose increase associated with winter thunderstorm and lightning activity, Journal of Geophysical Research: Atmospheres, 107, 4324, doi:10.1029/2001JD000938, 2002.

Tsuchiya, H., Enoto, T., Yamada, S., Yuasa, T., Kawaharada, M., Kitaguchi, T., Kokubun, M., Kato, H., Okano, M., Nakamura, S., et al.: Detection of high-energy gamma rays from winter thunderclouds, Physical review letters, 99, 165002, doi:10.1103/PhysRevLett.99.165002, 2007.

Williams, E. R.: Origin and context of C. T. R. Wilson's ideas on electron runaway in thunderclouds, Journal of Geophysical Research (Space Physics), 115, A00E50, doi:10.1029/2009JA014581, 2010.

Wilson, C. T. R.: The Acceleration of β-particles in Strong Electric Fields such as those of Thunderclouds, Proceedings of the Cambridge Philosophical Society, 22, 534, doi:10.1017/S0305004100003236, 1925.

4   Revised manuscript

Evaluation of Monte Carlo tools for high energy atmospheric physics II : relativistic runaway electron avalanches

David Sarria[1], Casper Rutjes[2], Gabriel Diniz[2,3], Alejandro Luque[4], Kevin M. A. Ihaddadene[5], Joseph R. Dwyer[5], Nikolai Østgaard[1], Alexander B. Skeltved[1], Ivan S. Ferreira[3], and Ute Ebert[2,6]

[1]Birkeland Centre for Space Science, Department of Physics and Technology, University of Bergen, Bergen, Norway
[2]Centrum Wiskunde & Informatica (CWI), Amsterdam, The Netherlands
[3]Instituto de Física, Universidade de Brasília, Brazil
[4]Instituto de Astrofísica de Andalucía (IAA-CSIC), P.O. Box 3004, Granada, Spain
[5]University of New Hampshire Main Campus, Department of Physics, Durham, NH, United States
[6]Eindhoven University of Technology, Eindhoven, The Netherlands

Correspondence to: David Sarria (david.sarria@uib.no)

Abstract.

The emerging field of High Energy Atmospheric Physics studies how high energy particles are produced in thunderstorms, in the form of terrestrial gamma-ray flashes and gamma-ray glows (also referred as thunderstorm ground enhancements). Understanding these phenomena requires appropriate models of the interaction of electrons, positrons and photons with air molecules and electric fields. We investigated the results of three codes used in the community (Geant4, GRRR and REAM) to simulate Relativistic Runaway Electron Avalanches (RREAs). This work continues the study of Rutjes et al. (2016), now also including the effects of electric fields, up to the classical breakdown field, which is about 3.0 MV/m at standard temperature and pressure.

We first present our theoretical description of the RREA process, that is based and incremented over previous published works. This analysis confirmed that the avalanche is mainly driven by electric fields and the ionisation and scattering processes determining the minimum energy of electrons that can runaway, that was found to be above ≈ 10 keV for any fields up to the classical breakdown field.

To investigate this point further, we then evaluated the probability to produce a RREA as a function of the initial electron energy and of the magnitude of the electric field. We found that the stepping methodology in the particle simulation has to be set up very carefully in Geant4. For example, a too large step size can lead to an avalanche probability reduced by a factor of 10, or to a 40% over-estimation of the average electron energy. When properly set-up, both Geant4 models show an overall good agreement (within ≈ 10 %) with REAM and GRRR. Furthermore, the probability that particles below 10 keV accelerate and participate in the high energy radiation is found negligible for electric fields below the classical breakdown value. The added value of accurately tracking low energy particles (< 10 keV) is minor, and mainly visible for fields above 2 MV/m.

In a second simulation set-up, we compared the physical characteristics of the avalanches produced by the four models: avalanche (time and length) scales, convergence time to a self-similar state and energy spectra of photons and electrons. The two Geant4 models and REAM showed a good agreement on all parameters we tested. GRRR was also found to be consistent

1

with the other codes, except for the electron energy spectra. That is probably because GRRR does not include straggling for the radiative and ionisation energy losses, hence implementing these two processes is of primary importance to produce accurate RREA spectra. Including precise modelling of the interactions of particles below 10 keV (e.g. by taking into account molecular binding energy of secondary electrons for impact ionisation) also produced only small differences in the recorded spectra.

1   Introduction

1.1   Phenomena and observations in high energy atmospheric physics

In 1925, C.T.R. Wilson proposed that thunderstorms could emit a "measurable amount of extremely penetrating radiation of β or γ type" (Wilson, 1925), about 60 years before such radiation was observed from the atmosphere and from space (Parks et al., 1981; Fishman et al., 1994; Williams, 2010). This, and subsequent observations and modeling are now being investigated withing the field of High Energy Atmospheric Physics (HEAP). A review is provided by Dwyer et al. (2012).

Observationally different types of high energy emissions have been identified coming from thunderclouds, naturally categorized by duration. Microsecond-long burst of photons, which were first observed from space (Fishman et al., 1994; Grefenstette et al., 2009; Marisaldi et al., 2014; Roberts et al., 2018), are known as Terrestrial Gamma-ray Flashes (TGFs). TGFs also produce bursts of electron and positrons (Dwyer et al., 2008; Briggs et al., 2011; Sarria et al., 2016) that follow the geomagnetic field lines into space and show longer durations. Two space missions specifically designed to study TGFs and related phenomena will provide new observations in the near future : ASIM (Atmosphere-Space Interaction Monitor) (Neubert et al., 2006), successfully launched in April 2018; and TARANIS (Tool for the Analysis of Radiation from lightning and Sprites) (Lefeuvre et al., 2009; Sarria et al., 2017) to be launched at the end of 2019.

Seconds to minutes or even hours long X and gamma radiation have been observed on ground, from balloons and aircraft, by McCarthy and Parks (1985); Eack et al. (1996); Torii et al. (2002); Tsuchiya et al. (2007); Adachi et al. (2008); Chilingarian et al. (2010, 2011); Kelley et al. (2015); Dwyer et al. (2015); Kochkin et al. (2017, 2018), which are called gamma-ray glows or thunderstorm ground enhancements. Some modeling attempts of both gamma ray and electron observations are also presented in Chilingarian et al. (2012).

TGFs were predicted to create a neutron emission on the millisecond duration, with associated isotope production (Babich, 2006). Such emission was observed from the ground (Bowers et al., 2017; Teruaki et al., 2017). A similar phenomenon was modeled at higher altitudes by Rutjes et al. (2017), that also proposed to call it "TGF afterglow".

Following the idea of Wilson (1925), high energy X and gamma radiation is created by runaway electrons, which may further grow by the effect of Møller scattering in the form of so called relativistic runaway electron avalanches (RREAs) (Gurevich et al., 1992). For the multiplication to occurre, a threshold electric field of $E_{\mathrm{th}} = 0.28$ MV/m (at STP) is required (Babich et al., 2004a; Dwyer, 2003).

The difference in duration between TGFs and gamma-ray glows can be explained by two possible scenarios to create runaway electrons, which is traditionally illustrated using the average energy-loss or friction curve (see, e.g., figure 1 of Dwyer et al. (2012)). In this curve, there is a maximum at around $\varepsilon \approx 123$ eV, illustrating the scenario that for electric fields higher

2

than a critical electric field, of $E_c \approx 26$ MV/m at standard temperature and pressure (STP), thermal electrons can be accelerated into runaway regime, described in the so-called Cold Runaway theory (Gurevich, 1961). The effective value of E_c may be significantly lower, as electrons could overcome the friction barrier due to their intrinsic random interactions (Lehtinen et al., 1999; Li et al., 2009; Liu et al., 2016; Chanrion et al., 2016). Cold Runaway could happen in the streamer phase (Moss et al., 2006; Li et al., 2009; Chanrion and Neubert, 2010) or leader phase (Celestin and Pasko, 2011; Celestin et al., 2012; Chanrion et al., 2014; Köhn et al., 2014; Köhn and Ebert, 2015; Köhn et al., 2017) of a transient discharge, explaining the high energy electron seeding that will evolve to RREAs and produce gamma-rays by bremsstrahlung emission from the accelerated electrons. The cold runaway mechanism may be further investigated with laboratory experiments, in high voltage and pulsed plasma technology, and may be linked to the not fully understood x-ray emissions that have been observed during nanosecond pulsed discharges and the formation of long sparks, (Rahman et al. (2008); Dwyer et al. (2008); Shao et al. (2011); Kochkin et al. (2016), and references therein), with different possible production mechanism that were proposed and tested using analytical modeling (Cooray et al., 2009) and computer simulations (Ihaddadene and Celestin, 2015; Luque, 2017; Lehtinen and Østgaard, 2018). Alternatively, the relativistic feedback discharge model is also proposed to explain TGF production using large scale and high potential electric fields (Dwyer, 2012), where the RREA initial seeding may be provided by cosmic-ray secondaries, background radiation, or cold runaway (Dwyer, 2008).

For fields significantly below the thermal runaway critical electric field $E_c \approx 26$ MV/m but above the RREA threshold electric field of $E_{\mathrm{th}} = 0.28$ MV/m (at STP), runaway behaviour is still observed in detailed Monte Carlo studies (see Dwyer et al. (2012), and references therein). At thundercloud altitudes, cosmic particles create energetic electrons that could runaway in patches of the thundercloud where the electric field satisfies this criterion. RREAs are then formed if space permits and could be sustained with feedback of photons and positrons creating new avalanches (Babich et al., 2005; Dwyer, 2007, 2012). Gamma-ray glows could be explained by this mechanism, as they are observed irrespectively of lightning or observed to be terminated by lightning (McCarthy and Parks, 1985; Chilingarian et al., 2015; Kelley et al., 2015; Kochkin et al., 2017). The fact that gamma-ray glows are not (necessarily) accompanied by classical discharges, results in the conclusion that the electric fields causing them are usually also below the conventional breakdown. The conventional (or classical) breakdown field, of $E_k \approx 3.0$ MV/m (at STP), is where low energy electrons (< 123 eV) exponentially grow in number, as ionisation overcomes attachment. This exponential growth of charged particles will affect the electric field, which requires a self-consistent simulation to be properly taken into account. That is not something we want to test in this study, since Geant4 is not capable of simulating it. Therefore we will focus on electric fields below the breakdown field $E_k \approx 3.0$ MV/m, and above the RREA threshold $E_{\mathrm{th}} \approx 0.28$ MV/m.

As a note, one can find in the literature that E_k can be given between 2.36 MV/m and 3.2 MV/m (Raizer, 1997), the theoretical lowest breakdown field being between 2.36 and 2.6 MV/m (see Raizer, 1997, page 338). The value of ≈ 3.2 MV/m is the measured breakdown field in centimeter gaps in laboratory spark experiments (see Raizer, 1997, page 135), that can be lower for longer gaps.

1.2 Theoretical understanding of RREAs

In the energy regime of a kilo-electronvolt (keV) to a hundred of mega-electronvolts (MeV), the evolution of electrons is mostly driven by electron impact ionisation (Landau et al., 2013), as this energy loss channel is much larger than the radiative (bremsstrahlung) energy loss. However, the bremsstrahlung process does impact the shape of the electron energy spectrum, that can be understood by the straggling effect, that is discussed in the next section. When the electric field is below the classical breakdown $E_k \approx 3.0$ MV/m (at STP), the system can be simplified, because the effect of the electrons below a certain energy can be neglected, in particular the population that would otherwise (if $E > E_k$) multiply exponentially and have an important effect on the electric field. The part of the electron population that decelerates, and eventually attaches, cannot contribute to the production of the high energy radiation. Let $\epsilon_2^{\min}$ be the minimum energy for a secondary electron to have a chance to runaway, thus participate to the production of high energy radiation. The subscript index $i = 2$ indicates a secondary electron. A precise value of $\epsilon_2^{\min}$ will be evaluated in section 3 with the help of simulations, but, by looking at the friction curve, one can guess it is located in the keV to tens of keV energy regime (see Dwyer et al., 2012, Figure 1). As almost all energy loss of ionisation is going into producing secondary electrons of lower energy ($\epsilon_2 \lesssim 200$ eV), it is reasonable to approximate that channel as a continuous energy loss, or friction.

In the case of electric fields above the RREA threshold ($E_{\text{th}} = 0.28$ MV/m at STP), the electrons, when considered as a population, will undergo avalanche multiplication. Some individual electrons do not survive (because there can be hard bremsstrahlung or ionisation collisions that will remove enough energy to get below $\epsilon_2^{\min}$), but the ensemble grows exponentially as new electrons keep being generated from the ionisation collisions on air molecules, including a fraction with energy larger than $\epsilon_2^{\min}$. The production of secondaries with energies much larger than the ionisation threshold (a few kilo-electronvolts being a reasonable value), can be described using the Møller cross section, which is the exact solution for a free-free electron-electron interaction (see, e.g., Landau et al. (2013, page 321)) :

$$
\begin{aligned}
\frac{\mathrm{d}\sigma_{\text{M}}}{\mathrm{d}\delta_2} \;=\;& Z \frac{2\pi r_e^2}{\gamma_1^2 - 1}\left[\frac{(\gamma_1 - 1)^2 \gamma_1^2}{\delta_2^2(\gamma_1 - 1 - \delta_2)^2}\right. \\
& \left. - \frac{2\gamma_1^2 + 2\gamma_1 - 1}{\delta_2(\gamma_1 - 1 - \delta_2)} + 1 \right],
\end{aligned}
\tag{1}
$$

where Z is the number of electrons in the molecule, the index $i = 1$ indicates the primary electron, $i = 2$ the secondary, γ_i is the Lorentz factor, $\delta_i = \gamma_i - 1 = \epsilon_i/(m_e c^2)$ is the kinetic energy divided by the electron rest energy (with rest mass m_e) and $r_e = \frac{1}{4\pi\epsilon_0}\frac{e^2}{m_e c^2} \approx 2.8 \times 10^{-15}$ m is the classical electron radius. In the case $\delta_2 \ll \gamma_1 - 1$ and $\delta_2 \ll 1$, we observe that the term $\propto 1/\delta_2^2$ is dominating. Thus, we can write equation 1 as:

$$
\frac{\mathrm{d}\sigma_{\text{M}}}{\mathrm{d}\delta_2} \approx Z \frac{2\pi r_e^2}{\beta_1^2}\frac{1}{\delta_2^2},
\tag{2}
$$

with $\beta_1 = v_1/c$ the velocity of the primary particle. Integrating equation (2) from δ_2 to the maximum energy ($\epsilon_1/2$) yields a production rate

$$
\sigma_{\text{prod}} \approx Z \frac{2\pi r_e^2}{\beta_1^2}\frac{1}{\delta_2} \propto \frac{1}{\epsilon_2},
\tag{3}
$$

4

using again $\epsilon_2 \ll \epsilon_1$. The remaining sensitivity of σ_{prod} in units of area to the primary particle is given by the the factor β_1^2 which converges strongly to 1 as the mean energy of the primary electrons exceeds 1 MeV. In other words, as the mean energy of the electrons grows towards even more relativistic energies, the production rate σ_{prod} becomes independent of the energy spectrum.

For illustrative purposes, we now consider the one dimensional deterministic case, which results in an analytical solution of the electron energy spectrum. We make the system deterministic by assuming that the differential cross section is a delta-function at $\epsilon_2^{\mathrm{min}}$ (the minimum energy at which a secondary electron can runaway) and use $\Lambda_{\mathrm{prod}} = \frac{1}{N\sigma_{\mathrm{prod}}}$ as the constant collision length, with N the air number density. In other words, every length Λ_{prod} a secondary electron of energy $\epsilon_2^{\mathrm{min}}$ is produced. The derivation below is close to what was presented by Celestin and Pasko (2010); Dwyer et al. (2012); Skeltved et al. (2014) and references therein.

Consider a population of electrons in one dimension with space-coordinate z, a homogeneous and constant electric field E above the RREA threshold and a friction force $F(\epsilon)$. The minimum energy $\epsilon_2^{\mathrm{min}}$ at which an electron can runaway is given by the requirement $F(\epsilon_2^{\mathrm{min}}) \approx qE$ (where q is the elementary charge), that is to say $\epsilon_2^{\mathrm{min}} = \mathrm{function}(F, E)$ is constant. Assuming that the mean energy of the ensemble is relativistic results in a constant production rate $\Lambda_{\mathrm{prod}} = \Lambda_{\mathrm{prod}}(\epsilon_{\mathrm{min}})$. Thus, in space, the distribution f_e grows exponentially as,

$$\frac{\partial f_e}{\partial z} = \frac{1}{\Lambda_{\mathrm{prod}}} f_e. \tag{4}$$

While in energy, the differential equation is given by the net force,

$$\frac{\mathrm{d}\epsilon}{\mathrm{d}z} = qE - F(\epsilon). \tag{5}$$

Solving for steady state means,

$$\frac{\mathrm{d}f_e}{\mathrm{d}z} = \frac{\partial f_e}{\partial z} + \frac{\partial f_e}{\partial \epsilon} \frac{\mathrm{d}\epsilon}{\mathrm{d}z} = 0, \tag{6}$$

and using equation 4 and 5 results in,

$$\frac{\partial f_e}{\partial \epsilon} = -\frac{1}{\Lambda_{\mathrm{prod}}(qE - F(\epsilon))} f_e. \tag{7}$$

For the largest part of the energy spectrum, specifically above 0.511 MeV and below 100 MeV, $F(\epsilon)$ is not sensitive to ϵ (e.g. see Rutjes et al. (2016)). Only at around $\epsilon \approx 100$ MeV electron energy $F(\epsilon)$ starts increasing again because of the bremsstrahlung process. Thus, one may assume $F(\epsilon) \approx F$ constant, which yields that the RREA energy spectrum $f(\epsilon)$ at steady state is given by,

$$f_e(\epsilon) = \frac{1}{\bar{\epsilon}} \exp\left(-\frac{\epsilon}{\bar{\epsilon}}\right), \tag{8}$$

with the exponential shape parameter and approximated average energy $\bar{\epsilon}(E)$ given by,

$$\bar{\epsilon}(E) = \Lambda_{\mathrm{prod}}(qE - F). \tag{9}$$

Equivalently, in terms of collision frequency $\nu_{\mathrm{prod}} = \frac{\beta c}{\Lambda_{\mathrm{prod}}}$, equation 9 can be written as,

$$\bar{\epsilon}(E) = \frac{\beta c}{\nu_{\mathrm{prod}}}(qE - F), \tag{10}$$

with β the velocity v/c of the RREA avalanche front. For the 1-d case there is no momentum-loss or diffusion, so $\beta \approx 1$. Note that Λ_{prod} depends on $\epsilon_2^{\mathrm{min}}$ (the minimum energy at which a secondary electron can runaway), which depends on the electric field E as that determines the minimum electron energy that can go into runaway. In this analysis, we illustrate with equations 8 and 9, that the full RREA characteristics, such as the mean energy $\bar{\epsilon}$ or the collision length Λ_{prod} (directly related to the avalanche length scale λ discussed in section 4.1) are driven by processes determining $\epsilon_2^{\mathrm{min}}$.

In reality there are important differences compared to the one dimensional deterministic case described previously, which we propose to discuss qualitatively for understanding the Monte Carlo simulations evaluated in this study. During collisions, electrons deviate from the path parallel to E. Therefore in general, electrons experience a reduced net electric field as the cosine function of the opening angle θ, which reduces the net force to $qE\cos(\theta) - F$ and thereby the mean energy $\bar{\epsilon}$ of equation 9. In reality the 3D scattering (with angle parameter θ) changes of the path of the particle. Although the velocity remains still close to c (as the mean energy is still larger than several MeV), the RREA front velocity parallel to the electric field (**E**) is reduced again because of the opening angle as function of its cosine:

$$\beta_{\parallel} = \beta\cos(\theta), \tag{11}$$

which also reduces the mean energy $\bar{\epsilon}$. Note that θ is not a constant and may change with each collision. Equivalently the avalanche scale length Λ_{prod} in 3-D changes to $\approx \Lambda_{\mathrm{prod}} \times \cos(\theta)$. However, most importantly, the momentum-loss of the lower energetic electrons results in a significant increase of $\epsilon_2^{\mathrm{min}}$, as it is much harder for electrons to runaway. The increase of $\epsilon_2^{\mathrm{min}}$ significantly increases Λ_{prod} and thereby increases the characteristic mean energy $\bar{\epsilon}$. On the other hand, the stochasticity creates an interval of possible energies $\epsilon_2^{\mathrm{min}}$ that can runaway with a certain probability and for thin targets a straggling effect (Rutjes et al., 2016). A recent article discussed the influence of the angular scattering of electrons on the runaway threshold in air (Chanrion et al., 2016).

The effects discussed above prevent a straight forward analytical derivation of the RREA characteristics in 3 dimensions, but what remains is the important notion that the physics is completely driven by the intermediate energy electron production. "Intermediate" means they are far above ionisation threshold ($\gg 123\,\mathrm{eV}$) but much below relativistic energies ($\ll 1\,\mathrm{MeV}$). The parametrisation of the electron energy spectrum, given by equation 9 turns out to be an accurate empirical fit, as it was already shown in Celestin and Pasko (2010); Dwyer et al. (2012); Skeltved et al. (2014) and references therein. Nevertheless in these works $\lambda^{\mathrm{min}}(E)$, or equivalently the velocity over collision frequency $\beta c/\nu_{\mathrm{prod}}$, is fitted by numerical Monte Carlo studies and the final direct relation to $\epsilon_2^{\mathrm{min}}$ is not executed. Celestin and Pasko (2010) calculated that $\nu^{\mathrm{prod}}(E) \propto E$, thus explains why $\bar{\epsilon}(E)$ must saturate to constant value. Celestin and Pasko (2010) argue that $\epsilon_2^{\mathrm{min}}(E)$ is given by the deterministic friction curve F, for which they use the Bethe's formula and an integration of a more sophisticated electron impact ionisation cross section (RBEB) including molecular effects, but that is only true in one dimension without stochastic fluctuations. Other attempts to simulate RREA by solving the kinetic equation instead of using Monte-Carlo methods are presented in Roussel-Dupre et al.

6

(1994); Gurevich and Zybin (1998); Babich et al. (2001) and references therein. An analytical approach is provided by Cramer et al. (2014).

1.3   Model reductions and previous study

Apart from analytical calculations, the physics behind TGFs, TGF afterglows and gamma-ray glows are also studied with the help of experimental data, computer simulations, and often a combination of both. Simulations necessarily involves model reduction and assumptions. As we argued in the previously, in scenarios where the electric field is below the classical breakdown field ($E_k \approx 3.0$ MV/m at STP), electrons below a certain energy can be neglected, because they will decelerate and eventually attach, thus not contributing to the production of the hard radiation. In Monte Carlo simulations it is therefore common to apply a so-called "low energy cutoff" (or threshold), noted ε_c, that is a threshold where particles with lower energy can be discarded (or not produced), to improve code performance. It is different from $\epsilon_2^{\min}$ (the minimum energy at which a secondary electron can runaway) as one is a simulation parameter and the other is a physical value. Ideally, ε_c should be set as close as possible to $\epsilon_2^{\min}$. A second simplification can be made for the energetic enough particles that stay in the ensemble, by treating collisions that would produce particles below the low energy cutoff as a friction.

Both simplifications can be implemented in different ways, leading to different efficiencies and accuracies. Rutjes et al. (2016) benchmarked the performance of the Monte Carlo codes Geant4 (Agostinelli et al., 2003), EGS5 (Hirayama et al., 2005), FLUKA (Ferrari et al., 2005) developed in other fields of physics, and of the custom-made codes GRRR (Luque, 2014) and MC-PEPTITA (Sarria et al., 2015) within the parameter regime relevant for HEAP, in the absence of electric and magnetic fields. In that study they focused on basic tests of electrons, positrons and photons with kinetic energies between 100 keV and 40 MeV through homogeneous air using a low energy cutoff of 50 keV and found several differences between the codes and invited other researchers to test their codes on the provided test configurations. We found that the usage of an average friction fails in the high energy regime ($\gtrsim 100$ keV), as the energy loss is too much averaged, resulting in an incorrect energy distribution (Rutjes et al., 2016).

As we indicated in section 1.2, the ionisation energy loss channel is much larger than the radiative (bremsstrahlung) energy loss, by a few orders of magnitude. However, this is only true for the average, and bremsstrahlung does have a significant effect on the electron spectrum because of straggling (Rutjes et al., 2016). This straggling effect was first studied by Bethe and Heitler (1934). If it is not taken into account in the implementation of the low energy cut-off, the primary particle suffers a uniform (and deterministic) energy loss. This means that only the energy of the primary particle is altered, but not its direction. The accuracy of the assumed uniform energy loss is a matter of length scale : on a small length scale, the real energy loss distribution (if all interactions are considered explicitly) among the population would have a large spread. One way to obtain an accurate energy distribution is by implementing a stochastic friction mimicking the straggling effect.

Rutjes et al. (2016) also indicated that including electric fields in the simulations would potentially enhance the differences found by introducing new errors, the simulation results being supposingly sensitive to the low energy cutoff. This effect is believed to be responsible of the observed differences between the two Geant4 physics lists tested in Skeltved et al. (2014): for all fields between 0.4 and 2.5 MV/m (at STP), they found that the energy the spectrum and the mean energy of runaway

electrons depended on the low energy cutoff, even when it was chosen between 250 eV and 1 keV. In the following, this interpretation is challenged.

1.4 Content and order of the present study

In the context of High Energy Atmospheric Physics, the computer codes that were used are either general purpose codes developed by large collaborations, or custom made codes programmed by smaller groups or individuals. Examples of general purpose codes that were used are Geant4 (e.g., Østgaard et al., 2008; Carlson et al., 2010; Bowers et al., 2017; Sarria et al., 2015, 2017; Skeltved et al., 2014) and FLUKA (e.g., Dubinova et al., 2015; Rutjes et al., 2017). Custom made codes were used in Roussel-Dupre et al. (1994); Lehtinen et al. (1999); Dwyer (2003); Babich et al. (2004b); Østgaard et al. (2008); Celestin and Pasko (2011); Luque (2014); Köhn et al. (2014); Chanrion et al. (2014); Sarria et al. (2015), among others. Rutjes et al. (2016) presented in their section 1.3 the reasons why different results between codes (or models) can be obtained and why defining a comparison standard (based on the physical outputs produced by the codes) is the easiest way (if not the only) to compare and verify the codes. Here we continue the work of Rutjes et al. (2016), now with electric fields up to the classical breakdown field ($E_k \approx 3.0$ MV/m). As mentioned previously, we chose not to use larger electric fields because that would produce an exponential growth of low energy electrons (< 123 eV) which would affect the electric field and therefore require a self-consistent simulation, that Geant4 is not capable of. We aim to provide a comparison standard for the particle codes able to simulate Relativistic Runaway Electron Avalanches, as simple and informative as possible, by only considering their physical outputs. These comparison standards are described in the Supplementary Material (Sections 1 and 2).

In section 1.2, we illustrated that the full RREA characteristics, such as the mean energy $\bar{\epsilon}$ or the collision length Λ_{prod} are driven by processes determining $\epsilon_2^{\mathrm{min}}$ (the minimum energy at which a secondary electron can runaway). To prove this insight, and to benchmark codes capable of computing RREA characteristics for further use, we calculated the probability for an electron to accelerate into the runaway regime (see section 3), which is closely related to the quantity $\epsilon_2^{\mathrm{min}}$. From this probability study, it is directly clear that it is safe to choose the low energy cutoff ε_c higher than previously expected by Skeltved et al. (2014) and Rutjes et al. (2016), given an electric field $E < E_k$. In section 3, we will demonstrate that the probability for particles below 10 keV to accelerate and participate in the penetrating radiation is actually negligible. Thus, in practice an energy threshold value of $\varepsilon_c \approx 10$ keV can be used for any electric field below E_k. However, in section 2.4, we will show that step-length restrictions are of major importance (e.g. it can lead to an underestimation of a factor of 10 of the probability to produce a RREA, in some cases). The results of the comparison of several parameters of the RREAs produced by the four tested codes is then presented in section 4. We conclude in section 5.

The test set-ups of the two types of simulations (RREA probability, and RREA characteristics) are described in the Supplementary Material, together with the data we generated, and supplementary figures comparing several characteristics of the showers. The Geant4 source codes used in this study are also provided (see sections 6 and 7).

2 Model descriptions

The data we discuss in the next sections were produced by the general-purpose code Geant4 (with several set-ups) and two custom-made codes (GRRR and REAM) which we describe below. However, we will not describe comprehensively all the processes, models or cross-sections used by the different codes, and a table summarizing it is provided in the supplementary material document, section 13 (including all references).

2.1 Geant4

Geant4 is a software toolkit developed by the European Organization for Nuclear Research (CERN) and a worldwide collaboration (Agostinelli et al., 2003; Allison et al., 2006, 2016). We use version 10.2.3. The electro-magnetic models can simulate the propagation of photons, electrons and positrons including all the relevant processes, and the effect of electric and magnetic fields. Geant4 uses steps in distance, whereas REAM and GRRR use time step. In the context of this study, three main different electro-magnetic cross-section sets implementation are included : one based on analytical of semi-analytical models (e.g. uses the Møller cross section for ionisation and Klein-Nishina cross section for Compton scattering), one based on the Livermore data set (Perkins et al., 1991), and one based on the Penelope models (Salvat et al., 2011). Each of them can be implemented with a large number of different electro-magnetic parameters (binning of the cross section tables, energy thresholds, production cuts, maximum energies, multiple scattering factors, accuracy of the electro-magnetic field stepper, among others), and some processes have multiple models in addition to the main three, e.g. the Monash University model for Compton scattering (Brown et al., 2014). Skeltved et al. (2014) used two different physics list : LHEP and LBE. The first one, based on parametrisation on measurement data and optimized for speed, was deprecated since the 10.0 version of the toolkit. The LBE physics list is based on the Livermore data, but it is not considered as the most accurate electro-magnetic physics list in the Geant4 documentation, which is given by the Option 4 physics list (O4). This last uses a mix of different models, and in particular uses the Penelope model for the the impact ionisation of electrons. For this study, we will use two GEANT4 physics list options : Option 4 (referred as simply O4 hereafter) that is the most accurate one according to the documentation, and the Option 1 (referred as simply O1 hereafter) that is less accurate, but runs faster. In practice, O1 and O4 give very similar results for simulations without electric field and energies above 50 keV, as produced in our previous code comparison study (Rutjes et al., 2016).

By default, Geant4 is following all primary particles down to zero energy. A primary particle is defined as a particle with more energy than a threshold energy ε_c^g (that is different from ε_c described before). By default, ε_c^g is set to 990 eV and was not changed to obtain the results presented in the next sections. The LBE Physics list used by Skeltved et al. (2014) uses a threshold down to 250 eV (i.e. more accurate than using 990 eV, in principle) and this parameter was thought to be responsible for a major change in the accuracy of the obtained RREA energy spectra. In section 3, we will argue that the most important factor able to effect the spectra obtained from Geant4 simulations is the accuracy of the stepping method for the tracking of the electrons, and not the low energy threshold. Actually, we found that the stepping accuracy of the simulation is indirectly improved by reducing ε_c^g, that explains why Skeltved et al. (2014) could make this interpretation.

9

2.2 GRRR

The GRRR (GRanada Relativistic Runaway simulator) is a time-oriented code for the simulation of energetic electrons propagating in air, and can handle self-consistent electric fields. It is described in detail in the supplement of Luque (2014) and its source code is fully available in a public repository (see section 7 about code availability). In the scope of this work, we want to point out three important features : 1. Electron ionisation and scattering processes are simulated discretely, and the friction is uniform and without a way to mimic the straggling effect. 2. Bremsstrahlung collisions are not explicit and are simulated as continuous radiative losses, without straggling. 3. GRRR uses a constant time-step Δt both for the integration of the continuous interactions using a fourth-order Runge-Kutta scheme and for determining the collision probability of each discrete process k as $\nu_k \Delta t$, where ν_k is the collision rate of process k. This expression assumes that $\nu_k \Delta t \ll 1$ and therefore that the probability of a particle experiencing two collisions within Δt is negligibly small. The collisions are sampled at the beginning of each time step and therefore the rate ν_k is calculated using the energy at that instant. In this work we used $\Delta t = 0.25$ ps for the avalanche probabilities simulations, and $\Delta t = 1$ ps for the simulations used to characterise the RREA. For both cases, the time steps are small enough to guarantee a very accurate integration.

2.3 REAM

The REAM (Runaway Electron Avalanche Model) is a three dimension Monte Carlo simulation of Relativistic Runaway Electron Avalanche (also refereed as Runaway Breakdown), including electric and magnetic fields (Dwyer, 2003, 2007; Cramer et al., 2016). This code is inspired by earlier work by Lehtinen et al. (1999) and takes accurately into account all the important interactions involving runaway electrons, including energy losses through ionisation, atomic excitation and Møller scattering. A shielded-Coulomb potential is implemented in order to fully model elastic scattering, and it also includes the production of X/gamma-rays from radiation energy loss (bremsstrahlung) and the propagation of the photons, by including photoelectric absorption, Compton scattering and electron/positron pair production. The positron propagation is also simulated, including the generation of energetic seed electrons through Bhabha scattering. The bremsstrahlung photon emissions from the newly produced electrons and positron are also included.

In the scope of this study, it is important to point out that REAM limits the time step size of the particles so that the energy change within one time step cannot be more than 10 %. The effect of reducing this factor down to 1 % was tested and did not make any noticeable difference in the resulting spectra. The comparative curves are presented in the Supplementary Material, section 10.

2.4 Stepping methodology

2.4.1 General method

In Monte Carlo simulations, particles propagate in steps, collide and interact with surrounding media by means of cross sections (and their derivatives). A step is defined by the displacement of a particle between two collisions. As it is presented in

sections 3 and 4, the stepping methodology is responsible for most of the differences we observed between the codes we tested. Simulations can be either *space-oriented* or *time-oriented*, if the stepping is done in space or in time. By construction, space-oriented simulations are thus not synchronous in time. Usually, a single particle is simulated until it goes below the low energy threshold (ε_c), chosen by the user. But there are exceptions, like Geant4, that by default follows all primary particles down to zero energy. The advantage of asynchronous simulations is the ability to easily include boundaries, to have particles step as far as possible in the same material (minimizing the overhead due to null collisions), and smaller memory usage since there is no need to store all the particles alive at a given time (that may be a million or more). However, asynchronous simulations makes it impossible to incorporate particle to particle interactions, such as a space charge electric field, or self-consistent electric fields.

During steps, charged particles can lose energy (and momentum) by collisions, and also change in energy (and momentum) when an electric fields is present. To guarantee accuracy, energies should be updated frequently enough. An accurate method would be to exponentially sample step lengths with

$$\delta\ell = \min_{\epsilon}\{(\sigma_t(\epsilon)N)^{-1}\}, \tag{12}$$

in space-oriented perspective, or

$$\delta t = \min_{\epsilon}\{(v(\epsilon)\sigma_t(\epsilon)N)^{-1}\}, \tag{13}$$

in time-oriented perspective. With v the velocity, σ_t the total cross section and N the number density of the medium. Then at each updated location (and energy), the type of collision must be sampled from probability distributions. The probability of doing a collision of the given process (pr) can be calculated with:

$$p_{pr} = 1 - \exp\left(-N\int_i^f \sigma_{pr}\left(\epsilon(\ell)\right)d\ell\right) \tag{14}$$

Where the index i refers to the beginning of the step, f to its end, ℓ is the step length variable along the trajectory, and $d\ell$ is an infinitesimal step length. For time oriented simulations, we have equivalently :

$$p_{pr} = 1 - \exp\left(-N\int_i^f v(\epsilon(t))\,\sigma_{pr}\left(\epsilon(t)\right)dt\right) \tag{15}$$

Using these probabilities along a given step length or duration, there is a chance that no interactions happens, but the energy of the particle is guaranteed to be updated correctly.

2.4.2 The case of Geant4

In the Geant4 documentation, the stepping method presented in the previous section is referred as the "the integral approach to particle transport". This method is set up by default in Geant4 for impact ionisation and bremsstrahlung. However, the way it is

implemented is not exactly following what was described in the previous section. The description of the exact implementation is out of the scope of this article, but is presented into details in Ivanchenko et al. (1991) and Apostolakis et al. (2009). The method relies on determining the maximum of the cross section over the step (σ_{max}), using a parameter α_R (called "dR over Range" in the Geant4 documentation), that is also used to determine the step lengths. Another related parameter is the maximum range parameter (ρ_{max}), set to the default values of 1 millimeter and 0.1 millimeter for O1 and O4 respectively, and was never changed in the scope of this study. The exact definition of these parameters is given in Allison et al. (2016) and in the online Geant4 documentation (available at http://geant4.cern.ch/support/userdocuments.shtml). The default value of α_R is set to 0.80 for O1 and to 0.20 for O4. We found that both values are not low enough to be able to produce accurate results for the RREA probability simulations presented in the next section. To make Geant4 able to produce accurate RREA simulations using the multiple scattering algorithm, two methods are possible.

The first method is to tweak the value of the α_R parameter. Its value is set to 0.80 by default for O1, and 0.20 by default for O4. We found that these default values are way too high to be able to produce accurate RREA simulations, and values of $\alpha_R < 5.0 \times 10^{-3}$ should be used, as presented in the next section.

The second method is to implement a step limiter process (or maximum acceptable step). By default, this max step ($\delta \ell_{max}$) is set to one kilometer, and such a large value has no effect in practice, since the mean free path of energetic electrons in STP air is orders of magnitude smaller. Acceptable values of $\delta \ell_{max}$ depend on the electric field, and we found that it should be set to 1 millimeter or less to produce accurate RREA simulations, as presented in the next section. However, using this method results in relatively long simulation time required to achieve an acceptable accuracy, as the step is not adapted to the energy of the electrons. For information, the relative impact on performance (in terms of requirements of computation time) of tweaking the $\delta \ell_{max}$ and α_R parameters is presented in Appendix A.

3 Probability of generating RREA

As a first comparison test, we estimated the probability for an electron to accelerate into the runaway regime and produce a RREA, given its initial energy ϵ and some electric field magnitude E. Note that the momentum of the initial electrons is aligned along the opposite direction of the electric field, so that it gets accelerated. That gives maximum RREA probabilities, as other alignments reduce the chance to produce a shower (see, e.g., (Lehtinen et al., 1999, Figure 2.6)). We defined this probability as the fraction of initial (seed) electrons that created an avalanche of at least 20 electrons above 1 MeV. Once this state is reached, there is no doubt the RREA is triggered and can go on forever if no limits are set. The number 20 is arbitrary, to be well above 1 but small enough for computational reasons. For some initial conditions, we also tested requirements of 30 and 50 electrons above 1 MeV, that resulted in very similar probabilities. This study is somehow similar to the works presented in Lehtinen et al. (1999); Li et al. (2009); Liu et al. (2016); Chanrion et al. (2016), but they all looked at the probability to have only one single runaway electron, whereas we used the criterion of $N = 20$ electrons above 1 MeV, that is a stricter constraint. The difference between the two criteria is mainly noticeable for low electric field (< 0.4 MV/m) and high seed energies (> 700 keV). A figure illustrating how the probability can change with N is presented in the supplementary material, section 5.3.

As a test case, we calculated the probability to produce RREAs as a function of α_R and $\delta\ell_{max}$ (these parameters are presented in the previous section), for the configuration $\epsilon = 75$ keV, $E = 0.80$ MV/m. This case was chosen because it showed a particularly large sensitivity to the stepping methodology, as discussed later. The results are presented in figure 1. Although this configuration has a very low RREA probability for O1 and O4 by default (where α_R respectively equal to 0.80 and 0.20,

5   and $\delta\ell_{max}$ is one kilometer for both), the probability increases as α_R decreases and converges to a value between 10 and 12 % for both models when $\alpha_R < 5.0 \times 10^{-3}$. The same effect is observed when reducing $\delta\ell_{max}$. In this case, the user should not set $\delta\ell_{max}$ below the maximum range parameter, set to 1 millimeter for O1 and 0.1 millimeter for O4 by default (and never changed in the scope of this article). When reducing the α_R parameter to arbitrarily small values, both Geant4 models converge to slightly different probabilities : 10.7 % for O1 and 11.7 % for O4. We think this small difference is not due to the stepping

10 method, as reducing ρ_{max} or α_R further does not produce a significant difference. It is probability due to other factors, in particular the difference in the physical models and cross section sets used.

As explained in section 1.2, the final electron spectrum is essentially driven by the minimum energy $\epsilon_2^{\min}$ of electrons that can create a RREA. Here we can clearly see this probability is strongly affected by the choice of the α_R and $\delta\ell_{max}$ simulation parameters, affecting the accuracy of the stepping method, and that the values set by default for these parameters are not precise

15 enough to obtain correct RREA probabilities. In order to help future researchers, we provide example Geant4 source codes where the α_R and $\delta\ell_{max}$ parameters can be changed and their effect to be tested (see sections 6 and 7).

In figure 2.a, we compare the contour lines of the 10%, 50% and 90% probability of triggering a RREA as function ϵ and E, for the four models : Geant4 O4 ($\alpha_R = 1.0 \times 10^{-3}$), Geant4 O1 ($\alpha_R = 1.0 \times 10^{-3}$), GRRR and REAM. The full RREA probability results in the (ϵ,E) domain for each model are presented in the supplementary material, section 5.

20 The most important difference between Geant4 and GRRR is present for energies > 200 keV and E-fields < 0.5 MV/m. At 1 MeV, the level curves are significantly different between the Geant4 models and GRRR: the 50% probability to trigger RREA for GRRR is approximately located at the 10 % probability for O4, and the 90 % probability to for GRRR is located at the 50 % probability for O1. The reason is probably similar to a point we raised in our previous study (Rutjes et al., 2016) : GRRR does not include a way to simulate the straggling effect for the ionisation process. By looking at figure 2 of Rutjes et al.

25 (2016), we can see that 200 keV is roughly the energy from where the difference in the spectrum of GRRR, compared to codes that simulate straggling, starts to become significant.

For low electron energy (< 40 keV) and high electric field (> 2 MV/m), GRRR and O4 present a good agreement, however O1 deviates significantly from O4. We investigated the effects of the stepping parameters (α_R, $\delta\ell_{max}$ and ρ_{max}) and it is clear that they were not involved in this case. We think the Møller differential cross section (with respect to the energy of the

30 secondary electron) used by O1 and extrapolated down to low energies leads to the production of secondary electrons with average energies lower than the Penelope model (used by O4), that includes the effects of the atomic electron shells, hence is probably more accurate. This hypothesis is confirmed by looking at the shape of the differential cross sections of impact ionisation, which plots are presented in the Supplementary Material, section 11.4.

The RREA probability data for REAM is also displayed in figure 2.a, as the red curves. The three REAM level curves show

35 a significantly higher noise than the Geant4 data, mainly because the latter used 1000 electrons seeds whereas the former used
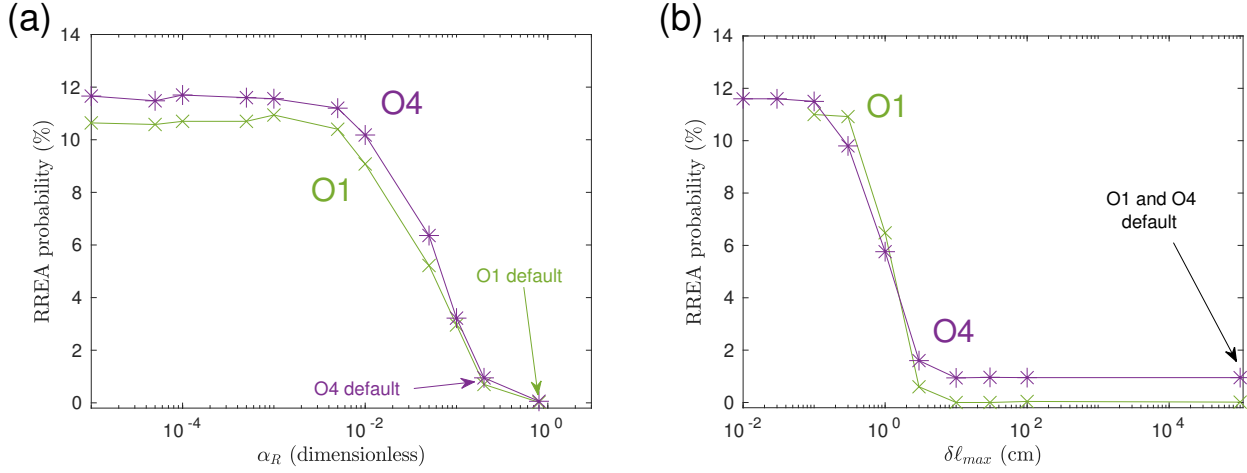
Figure 1. Relativistic avalanches probabilities calculated from Geant4 simulations, for specific point $\{\epsilon = 75 \text{ keV}, \text{E} = 0.80 \text{ MV/m}\}$ (illustrated by a cross in figure 2) and for two stepping settings. **(a)**: Avalanche probability versus α_R setting for Geant4 O4 and Geant4 O1. $\delta\ell_{max}$ is set to the default value of 1 kilometer. **(b)**: Avalanche probability versus maximum step setting ($\delta\ell_{max}$) for Geant4 O4 and Geant4 O1. The parameter α_R is set to the default value of the models, that is 0.8 for O1 and 0.2 for O4.

only 100. The algorithms used to calculate the levels curves were also found to impact the noise level. Nevertheless, the noise level is low enough to be able to evaluate the consistency between the codes. REAM shows a consistency with Geant4 (O1 and O4) within less than 12% in the full parameter range, and less than 5 % in some part of it. The most apparent deviations between REAM and Geant4 O1/O4 can be noticed for a seed electron energy range between 50 and 300 keV, for the 50 %

5   and 90% level curves, where there is a systematic, statistically significant difference in the probability for REAM compared to Geant4 (REAM requiring about 10% larger electric field or primary electron energy to reach the 90% or the 50% contour level). However, we do not expect such a small difference to significantly affect the characteristics of the RREA showers, such as the multiplication factors or the mean energies of the RREA electrons. To test this quantitatively, a detailed comparison of the most important characteristics of the RREA showers obtained with the four models is presented in the following section.

10   In figure 2.b we show the 0 %, 10 %, 50 %, 90 % and 100 % probability contour lines for the Geant4 O4 model where we could run a very large number of initial electrons ("seeds") to obtain curves with a very low noise level. These are the most accurate probabilities we could obtain. From this figure, it is clear that the RREA probability for an electron of less than ≈ 10 keV is null for any electric field below $E_k \approx 3.0$ MV/m. Therefore 10 keV is a reasonable a lower boundary of $\epsilon_2^{\min}$ (the minimum energy at which a secondary electron can runaway), and any simulation with an electric field below $E_k \approx 3.0$ MV/m

15   could use an energy threshold (ε_c) of this value while keeping accurate results. If electric fields with lower magnitude are used, it is also reasonable to increase this energy threshold by following the 0% level curve showed in Figure 2.b.
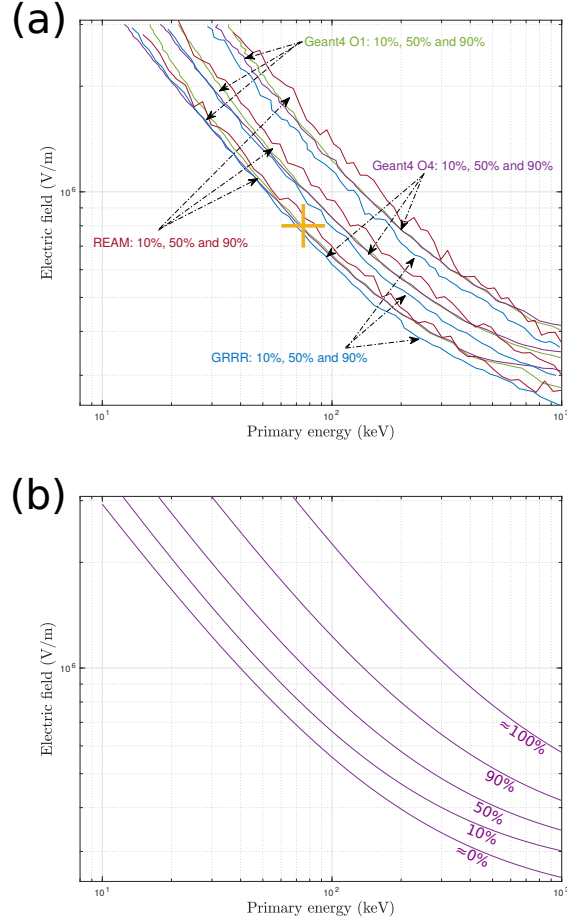
Figure 2. (a): Relativistic avalanche probability comparison between GRRR, REAM, O4 and O1. It shows three contour lines at 10%, 50% and 90%, as function of seed (primary) energy ϵ and electric field magnitude E. These contours are derived from the full probability scan, that are presented in the Supplementary Material (section 5). The cross at $\{\epsilon = 75 \text{ keV}, E = 0.80 \text{ MV/m}\}$ highlights the point where we studied the effect of the simulation stepping parameters (for the O4 and O1) on the probability, see figure 1. **(b)**: Five contour lines indicating the 0%, 10%, 50%, 90% and 100% probabilities to generate a relativistic electron avalanche (RREA) as function of ϵ and E, for the Geant4 O4 model for which we could run a very large number of initial electrons ($> 50,000$) to obtain curves with a very low noise level.

4 Characteristisation of RREA showers

We compared the output of the four models over 12 different electric field magnitudes from $E = 0.60$ MV/m to $E = 3.0$ MV/m. Two types of simulation were set : record in time, and record in distance (or space). This last choice was made because the resulting spectra can change significantly depending on the record method, as presented in figure 10 of Skeltved et al. (2014). All the curves presenting the simulation results are presented in the Supplementary Material, as well as the complete details on how the simulation should be set up. In the following section, we discuss only the most important differences we found between the four codes. We show the comparison of avalanche scales in space and time in section 4.1 and in section 4.2 the evolution to self-similar state. Finally, in section 4.3 we show the comparison of the self-similar energy spectra of electrons and photons of the RREA.

4.1 Avalanche time and length scales

Figures 3 and 4 show the avalanche length and time scales as function of electric fields, for the four models, together with their relative difference with respect to REAM. Note that we could not compute any values for electric fields below 0.60 MV/m, as we only used 200 initial electron seeds of 100 keV, which could not produced enough showers. The choice of 200 initial electrons is purely due to computational limitations. The avalanches length and times of the different models agree within $\pm 10\%$. There is also a systematic shift of about 7 % between the two Geant4 models for both time and length scales. The Geant4 O4 model is in principle more accurate than the O1 model, since it includes more advanced models. For most of the electric fields, O1 tends to be closer to REAM and O4 tends to be closer to GRRR. Following Coleman and Dwyer (2006), the avalanche length and time can be fitted by the empirical models,

$$\lambda(E) = \frac{c_1}{E - c_2},$$ (16)

$$\tau(E) = \frac{c_3}{E - c_4}$$ (17)

where c_1 is in V, c_2 and c_4 in V/m and and c_3 in s ·V/m. The c_2 and c_4 parameters can be seen as two estimates of the magnitude of the electric field of the minimum of ionisation for electrons along the avalanche direction, and also of the electric field magnitude of the RREA threshold; both values being close. However, we note that these fits neglect the sensitivity of the mean energy and velocity to the electric field. These empirical fits are motivated from the relations presented in equation 9 and 10, derived for the one dimensional case. First results of such fits were presented in Babich et al. (2004b) and Coleman and Dwyer (2006); and they obtained consistent results. Here we will compare our results against Coleman and Dwyer.

The best fit values of the two models to the simulation data are given in table 1. The c_1 parameter is directly linked to the average energy of the RREA spectrum, though the definition of this average energy can be ambiguous as energy spectra change significantly if recorded in time or in space. The values given by all the code are located between 6.8 and 7.61 MV, and

16

Table 1. Values of the parameters of the fits (with 95 % confidence intervals) for the simulations data for avalanche scale in space and time, using the models described by equations 16 and 17. See figure 3 and 4 for the corresponding curves.

Code	Avalanche length		Avalanche time	
	c_1 (MV)	c_2 (kV/m)	c_3 (ns MV/m)	c_4 (kV/m)
REAM	7.43 ± 0.18	290 ± 9.5	27.6 ± 0.91	293 ± 13
G4 O1	7.50 ± 0.10	276 ± 5.6	27.6 ± 0.44	290 ± 6.3
G4 O4	6.93 ± 0.13	285 ± 7.5	25.9 ± 0.28	288 ± 4.2
GRRR	7.25 ± 0.30	266 ± 18	26.2 ± 0.76	282 ± 12

are all consistent with each other within a 95 % confidence interval, with the exception of O4 that slightly deviates from O1. Combining the four values gives :

$$\overline{c_1} = 7.28 \pm 0.10 \text{ MV} \tag{18}$$

By "combining", we mean that the four values are averaged and the rule $\sigma_{comb} = \sqrt{\sigma_1^2 + \sigma_2^2 + \sigma_3^2 + \sigma_4^2}/4$ is used to "com-
5   bine" the four uncertainty ranges. The value $\overline{c_1}$ is consistent with the value of 7.3 ± 0.06 MV given in Coleman and Dwyer (2006). And all the estimated values of the c_2 and c_4 are consistent with each other within a 95 % confidence interval. Combining all the values of c_2 and c_4 gives :

$$\overline{c_2} = 279 \pm 5.6 \text{ kV/m}$$

$$\overline{c_4} = 288 \pm 4.8 \text{ kV/m}$$

10   And both value are also consistent with each other, leading to the final value of $\overline{c_{2,4}} = 283.5 \pm 3.69$ kV/m. These values slightly deviates from the value of 276.5 ± 2.24 obtained from Coleman and Dwyer (2006) if the values they obtained for the fits of λ and τ are combined. The work of Coleman and Dwyer (2006) used the REAM model too, in a version that should not have significantly changed compared to the one used here. Thus, we think this difference is purely attributed to differences in the methodology that was used to make these estimates from the output data of the code. Concerning the c_3 parameter,
15   combining all the estimates gives $\overline{c_3} = 26.8 \pm 0.32$ ns MV/m, that is slightly lower than the value of 27.3 ± 0.1 ns MV/m of Coleman and Dwyer (2006), but none of the values are consistent within the 95 % confidence interval. For this case, we also think the slight difference can be attributed to differences in methodology. Furthermore, the ratio $\overline{c_1}/\overline{c_3}$ can also be used to determine an average speed of the avalanche $\approx \beta_{\parallel} c$ along the direction of the electric field (that also corresponds to the z direction), and we can estimate $\beta_{\parallel} \approx 0.90$, that is very close to what was found in previous studies.
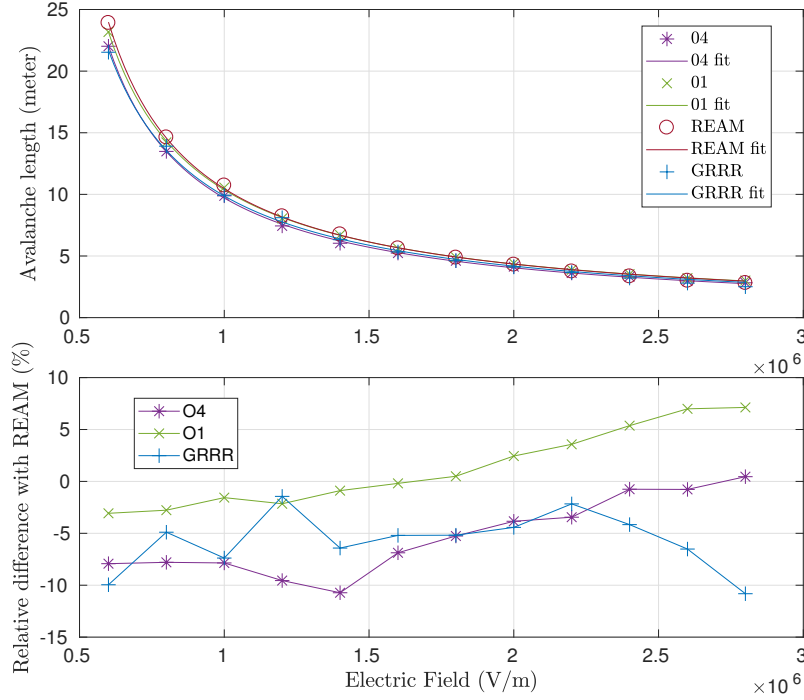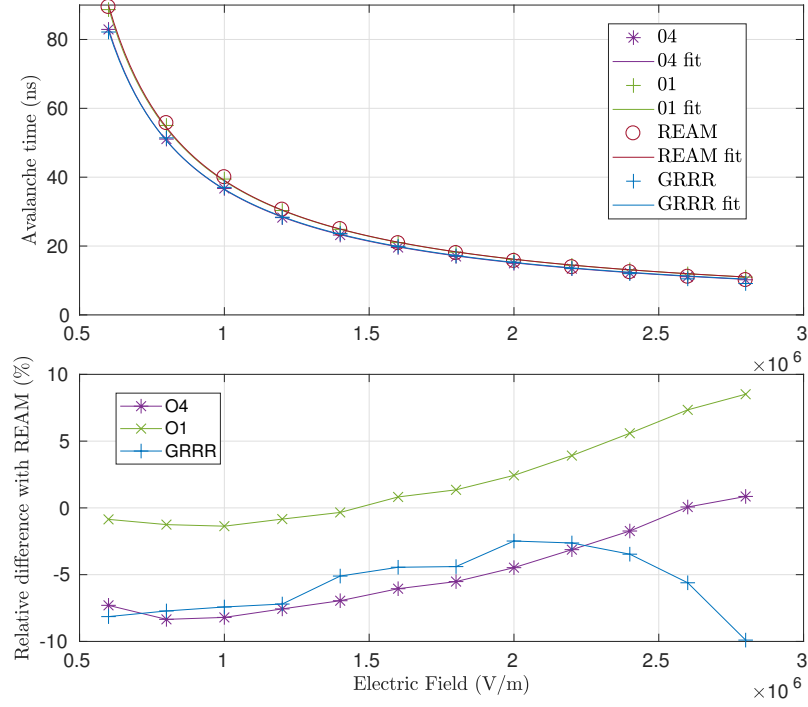
17

Figure 3. Top : Avalanche multiplication length as function of ambient electric field, for each of the codes included in this study. **Bottom** : The relative difference of all other models with respect to REAM. Table 1 indicates the values of the fit parameters.

4.2 Evolution to self-similar state

The photon and electron energy spectra of a relativistic runaway electron avalanche (RREA) is known to converge in time to a self-similar solution, where its shape is not evolving anymore, even if the number of particles continues growing exponentially. It may also be referred as the "self-sustained state", or the "steady state" in the literature. At least 5 avalanche lengths (or avalanche times) are required to be able to assert that this state is reached. We propose to estimate this time by looking at the mean electron energy evolution as a function of time. Notice that, as already mentioned in the beginning of Section 4, this mean energy recorded in time is different from the one recorded in distance, used in the next section. We arbitrarily choose to evaluate this mean by averaging all the energies of each individually recorded electron from 10 keV and above. This choice of a 10 keV energy threshold (instead of a higher value, like 511 keV or 1 MeV) does not affect significantly the final estimate of this time to self-similar state. We started with a mono-energetic beam of 100 keV electrons, which is considered low enough compared to the self-similar state mean energy of 6 to 9 MeV. To define the time to self-similar state (T_s), we fitted the time evolution of the mean electron energy $\bar{\epsilon}$ with the model

$$\bar{\epsilon}(t) = b_1 - b_2 \times \exp(-t/b_3), \tag{19}$$

18

Figure 4. Top : Avalanche multiplication time as function of ambient electric field, for each of the codes included in this study. **Bottom** : The relative difference of all other models with respect to REAM. Table 1 indicates the values of the fit parameters.

where b_1 and b_2 have dimension of energy, b_3 dimension of time, and we define $T_s = 5\,b_3$, that is five e-folding times, i.e. converged to 99.3%. The evolution of electron spectra to self-similar state are illustrated for the Geant4 O4 model in the supplementary material (section 12.4). The values of T_s we estimated for the different models are presented in figure 5, together with relative differences of the models with respect to REAM. The relatively high uncertainty (within 95 % confidence

5   intervals) that can be seen on the estimate of T_s is due to a combination of the confidence interval from the exponential fit, from the statistics of the number of seed electrons that could produce a RREA, and from the statistics of the particle counts. For most case, 200 initial seed were used, but for REAM, only 16 seeds were simulated for $E \geq 2.2$ MV/m, and for GRRR, only 20 seeds were simulated above $E \geq 2.0$ MV/m, because of computation time limitations.

In figure 5, Geant O1, O4, GRRR and REAM show consistent times to reach the self-similar state, for all the E-fields. Notice

10   that for them, $T(= T_s/5)$ is close to the avalanche time value τ given in the top panel of figure 4. For the low electric field of 0.60 MV/m, it seems to take about 5 times more to reach self-similar state. For this field, there were only three electrons seeds that could produce a RREA, giving a large uncertainty on the estimate of T_s, making it impossible to conclude on an inconsistency. From 0.60 MV/m to 1.8 MV/m, where all data from codes have good statistics, the times to self-similar state are consistent. From 2.0 MV/m to 2.4 MV/m, the two Geant4 models and REAM are consistent, but GRRR present lower times
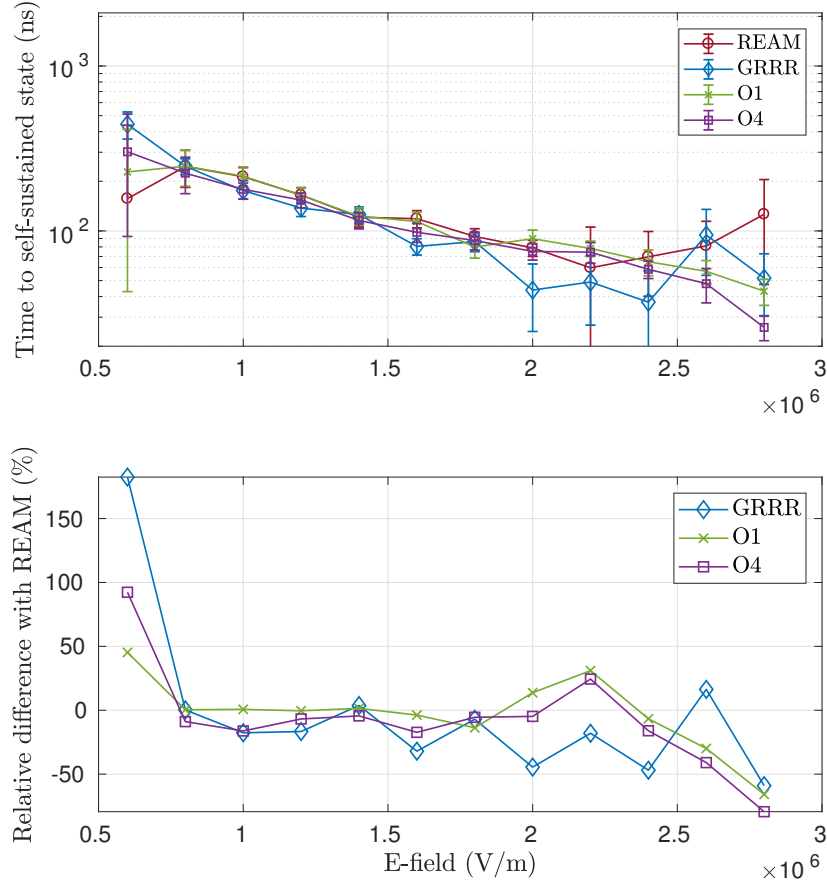
Figure 5. Top : time to self-similar state as function of ambient electric field, for each of the codes included in this study. **Bottom** : relative difference with respect to REAM.

by about -20% to -50 %, but it is impossible to conclude an inconsistency, given the large confidence intervals. For E-field magnitudes of 2.6 MV/m to 2.8 MV/m, O1 and O4 present times to self-similar state lower than REAM by about 50 %, that is significant given the uncertainty intervals, whereas GRRR and REAM are consistent. We could not find a clear explanation for it.

4.3   RREA spectra

The supplementary material (section 6) presents all the comparison spectra we obtained for photons, electrons and positrons, for the electric field between 0.60 MV/m and 3.0 MV/m. In this section, we discuss the most important differences we could find between the four models.
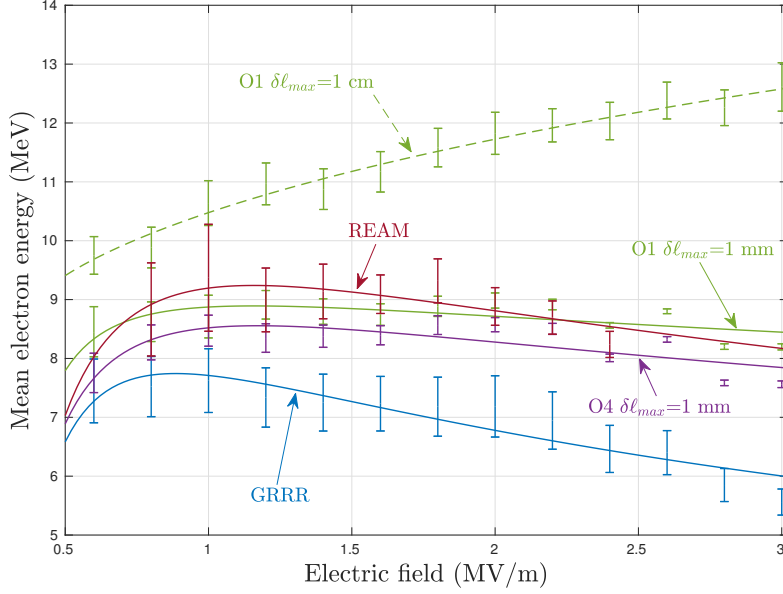
Figure 6. Mean electron energies at self-similar state (for distance record), for different electric field magnitudes. The data points are fitted with the model presented in section 4.3.1, equation 20. The values of the fitted parameters are presented in Table 2. To highlight the importance of including step limitations, Geant4 O1 values are presented for two different max step ($\delta\ell_{max}$) settings: one that is not acceptable (1 cm) and one that is acceptable (1 mm). The parameter α_R is set to its default value of 0.8 for O1 and 0.2 for O4.

4.3.1 Electrons

After the RREA electron spectra has reached self-similar state (that requires at least 5 avalanche lengths or times), we recorded the energy spectrum in a plane at a given distance (that is different for each electric field). Then we fitted it with an exponential spectrum model $\propto \exp(-\epsilon/\bar{\epsilon})$ (see also equation 8). Note that for an exponential distribution, the mean of the energy distribution is an estimator of its parameter $\bar{\epsilon}$, justifying the bar notation. We chose to evaluate the mean energy $\bar{\epsilon}$ for record at distances because, contrary to time records, it produces spectra that can be perfectly fit with an exponential distribution over the whole energy range (0 to 100 MeV). Therefore, in this case only the mean RREA electron energy is uniquely defined, and does not depend on an arbitrarily chosen energy threshold, or fitting method. The mean energy $\bar{\epsilon}$ of the exponential spectrum is calculated for the several codes as a function of electric field E, as presented in figure 6. For Geant4 O1 the whole simulations and analysis were done twice, for maximum allowed step length settings of $\delta\ell_{max} = 1$ cm and $\delta\ell_{max} = 1$ mm, to show that the first case generates totally incorrect spectra, that is consistent with having incorrect RREA probabilities (presented in section 3). In addition, values of the mean energy $\bar{\epsilon}$ for O1 with $\alpha_R = 1.0 \times 10^{-3}$ and $\delta\ell_{max} = 1$ cm are presented in the supplementary material, section 7.

Table 2. Mean energy variation with electric field. For evaluated codes we fitted by equation 20, with $F = 0.28$ MV/m. Figure 6 shows the corresponding curves.

Parameter / Code	a_1 [10^6s^{-1}]	a_2	a_3 [10^6s^{-1}]
Geant4 O1 (δl_{max} = 1 mm)	6.17 ± 2.15	$1.14 \pm 7.3 \times 10^{-2}$	-4.31 ± 2.0
Geant4 O4 (δl_{max} = 1 mm)	5.17 ± 1.8	$1.23 \pm 8.2 \times 10^{-2}$	-1.93 ± 1.5
Geant4 O1 (δl_{max} = 1 cm)	10.8 ± 3.4	$0.782 \pm 3.9 \times 10^{-2}$	-10.7 ± 3.6
REAM	3.98 ± 2.1	1.31 ± 0.20	$-8.41 \times 10^{-2} \pm 2.1$
GRRR	4.24 ± 1.6	1.42 ± 0.11	-0.639 ± 1.16

The data of figure 6 was fit following the model,

$$\bar{\epsilon}_{\text{fit}}(E) = \lambda(E)(qE - F), \quad \lambda(E) = \beta c \left[a_1 \left(\frac{qE}{F} \right)^{a_2} + a_3 \right]^{-1}, \tag{20}$$

motivated by the facts that $\epsilon_2^{\min}$ is roughly a power-law of E (see figure 2) and λ is a power-law of $\epsilon_2^{\min}$ (see equation 3). It has three adjustable parameters a_1, a_2 and a_3. We set $F = 0.28$ MeV/m, that is approximately the RREA threshold. The speed β is set constant, equal to 0.90, because the RREA velocity does not change of more than 5 % over the range of electric fields we tested. This model is in general agreement with the calculations of Celestin et al. (2012), where $\lambda(E)$ presents an approximately linear relation with the electric field. Table 2 gives the parameters' best fits (with confidence intervals) for the different models, and figure 6 shows the corresponding curves.

In figure 6, it is clear that the Geant4 O1 model with $\delta\ell_{\max} = 1$ cm presents a significantly higher $\bar{\epsilon}(E)$ than the other codes, with values ranging from 9.5 MeV to 12.5 MeV. From the previous RREA probability simulations (see section 3), we know that this $\delta\ell_{\max}$ parameter is not low enough, and so the results of this model can be disqualified. However, when $\delta\ell_{\max}$ is reduced to 1 mm, the results of both Geant4 model are close. There seems to be a consensus between Geant4 (O1 and O4) and REAM, that gives a mean energy that is between 8 and 9 MeV and can vary up to 10 % depending on the electric field. For all electric field magnitudes, GRRR shows a smaller average energy, from about 10 % less at 1 MV/m to about 20 % less at 2.8 MV/m. The reason is certainly because GRRR only includes radiative energy looses as a continuous friction. This is actually a similar difference to what has been observed and discussed in Rutjes et al. (2016) concerning the high energy electron beams, and one can read the discussion therein for more details.

Figure 7 compares the electron spectra recorded at $z = 128$ meters (the electric field has a non-null component only in the z direction, so that electrons are accelerated towards positive z), for an electric field magnitude $E = 0.80$ MV/m, for a RREA generated from 200 initial ("seed") electrons with $\epsilon = 100$ keV. This record distance was chosen because it corresponds to about 8.5 avalanche lengths, giving a maximum multiplication factor of about 5000, for which there is not doubt the RREA

is fully developed and has reached self-similar state. This electric field of $E = 0.80$ MV/m was chosen because it is were we could observe the most interesting differences between the models, and it also happens to be the lowest for which we could build spectra with enough statistics on all the models to be able to present a precise comparison. The choice of 200 initial electrons is purely due to computational limitations.

5   In Figure 7, the error bars on the bottom panel represent the uncertainty due to the Poisson statistics inherent when counting particles. The four models are consistent within 10 % between 20 keV and 7 MeV. Below 20 keV, we think the discrepancy is not physical, and can be attributed to the recording methods set up for the different codes, that are not perfect and have a more or less important uncertainty range (that is not included in the display errors bars, only based on Poisson statistics). Above 7 MeV, O1 remains consistent with REAM overall, but O4 and O1 deviate significantly : up to 50 % for O4 and up to 90 % for GRRR.

10   For the last bin between 58 and 74 MeV, O4 and GRRR are inconsistent, that is explained by the fact that GRRR does not include straggling for Bremsstrahlung (i.e. either explicit bremsstrahlung collision or some stochastic fluctuations mimicking straggling). The deviations for the high energy part (>7 MeV) in the electron spectrum are significant for this particular field ($E = 0.80$ MV/m), however this is not true for all electric fields, where the codes are overall roughly consistent, as seen in the Supplementary Material (section 6). In principle O4 should be more precise than O1 (Allison et al., 2006), as it includes more

15   advanced models, yet we cannot argue that O4 is more accurate than REAM. One way of deciding which model is the most accurate might be to compare these results with experimental measurements. but in the context of TGFs and Gamma-ray glows it is complicated to get a proper measurement of electron spectra produced by RREA. However, photons have much longer attenuation lengths than electron and can be more easily detected, e.g. from mountains, planes, balloons or satellites. In the next section we present and discuss the corresponding photon spectra.

20   **4.3.2   Photons**

In figure 8, the photon spectra recorded at $z = 128$ m (the electric field has a non-null component only in the z direction) for a magnitude $E = 0.80$ MV/m are given for Geant4 O1/O4 and REAM, together with the relative difference with respect to REAM. The reasons why these z and E values were chosen is given in the previous section.

The error bars in the relative differences represent the uncertainty due to the inherent Poisson statistics when evaluating

25   particle counts. The Geant4 O1 and O4 models are consistent for the full energy range, except a small discrepancy below 20 keV, that can be attributed to different physical models, O4 being more accurate in principle. In this case, it cannot be attributed to recording methods, since they are exactly the same for both Geant4 models. At 10 keV the two Geant4 spectra are about 80 % larger than REAM. With increasing energy, the discrepancy reduces and reaches 0 % at 100 keV. Above 100 keV, the three models show consistent spectra. There may be some discrepancy above 30 MeV, but it is hard to conclude since the uncertainty

30   interval is relatively large.

As just presented, the main noticeable discrepancy between O1/O4 and REAM is present below 100 keV. As far as we know, there is no reason to argue that Geant4 gives a better result than REAM in this range, or vice-versa. One way to find out which model is the most accurate could be to compare these results with real measurements. Are such measurement possible to obtain? Any photon that an instrument could detect has to travel in a significant amount of air before reaching detectors. The
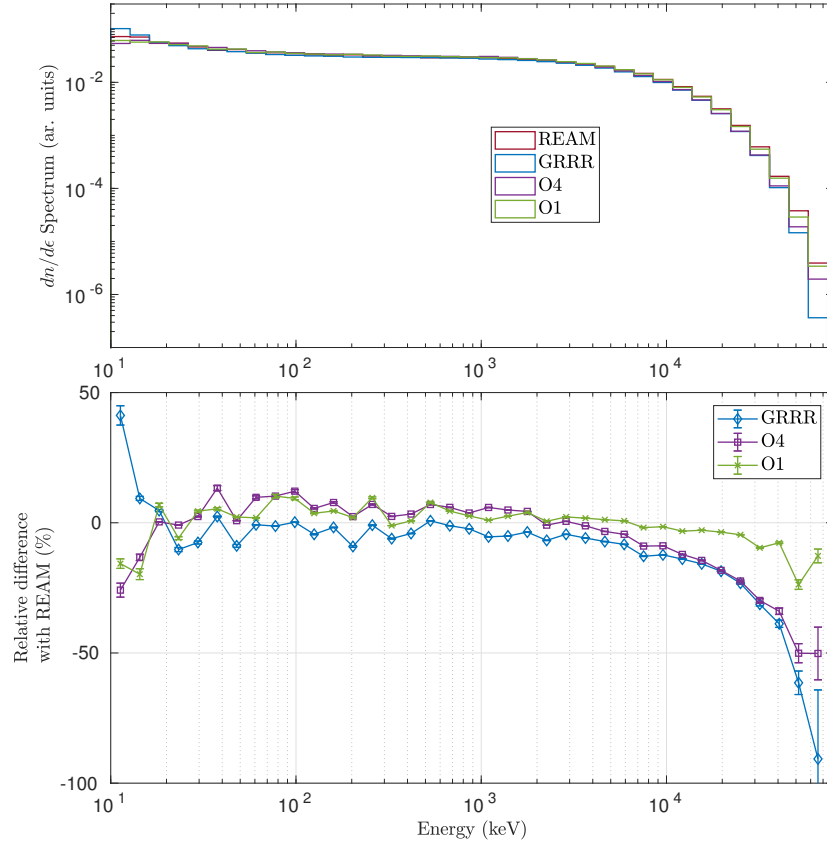
Figure 7. Top : Electron (kinetic) energy spectra of Geant4 (O4 and O1), REAM and GRRR, for $E = 0.80$ MV/m, recorded at $z = 128$ m. The RREA is generated from 200 seed electrons of $\epsilon = 100$ keV. **Bottom** : relative difference between REAM and the three other models. The error bars are calculated from the Poisson statistics.

average path traveled in the atmosphere by a 100 keV photon in 12 km altitude air is 1540 ± 806 meters. It decreases for lower energies and is 671 ± 484 meters at 50 keV, and 63.0 ± 61.5 meters at 20 keV. Note that these lengths have been evaluated from precise Geant4 simulations, and are smaller than the attenuation lengths at the same energies, because photons gradually loose energy due to stochastic collisions. These average traveled paths are too small for the photons to have a reasonable chance

5 to escape the atmosphere and to be detected by a satellite. But we cannot exclude that they may reach an airborne detector located inside or close to a thunderstorm. As a side note, we want to indicate that the vast majority (if not all) of the photons observed from space with energies below a few hundred of kilo-electronvolts (e.g., by the Fermi space telescope, see Mailyan et al. (2016)) had very likely more than 1 MeV when they were emitted. They lost some part of their energy by collisions (with air molecules in the atmosphere or/and with some part of the satellite) before being detected by the satellite. For information,

10 a figure presenting the probability of a photon to escape the atmosphere as function of its primary energy for a typical TGF is presented in the supplementary material, section 14.
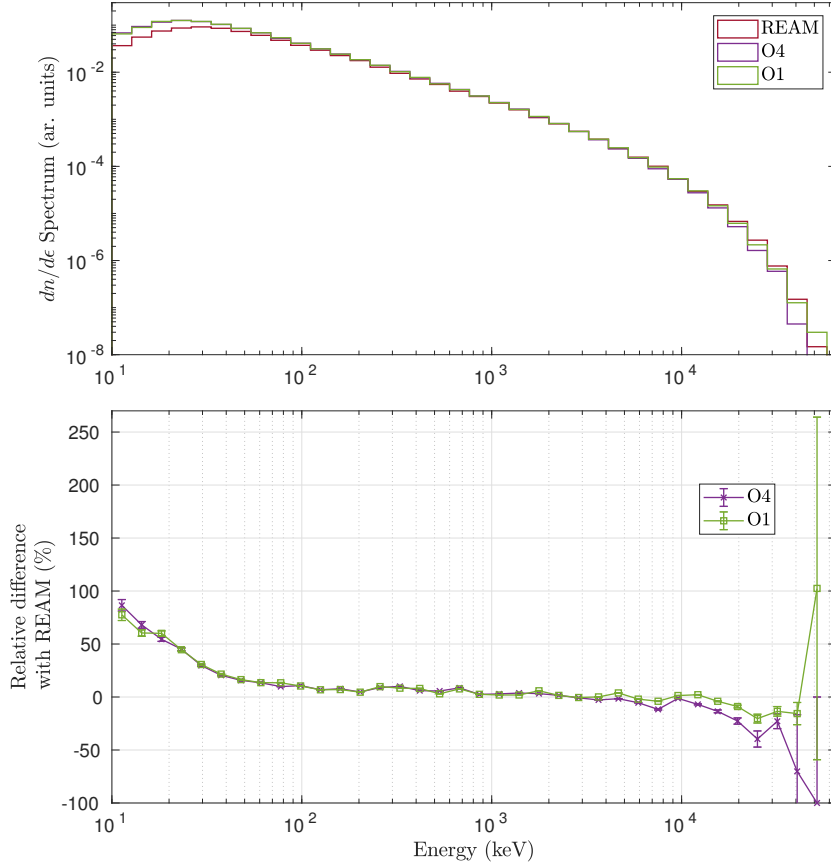
Figure 8. Top : Photon energy spectra of Geant4 (O4 and O1) and REAM for $E = 0.80$ MV/m, recorded at $z = 128\ m$. **Bottom** : relative difference between Geant4 (O1 and O4) and REAM. The error bars are calculated from the Poisson statistics.

4.4 Other differences

In addition to what is presented so far in this article, the following points should also be mentioned when comparing the results of the codes. The corresponding plots are available in the Supplementary Material.

- The mean parallel (to the E-field direction) velocity $\beta_\parallel$ of the avalanche is shown in section 4.2 of the Supplementary Material (labeled "mean Z velocity"). We observe that GRRR is giving $\beta_\parallel$ faster than all the other codes, and O4 is systematically slower than REAM and O1, though the differences are less than 2 %. The variation of $\beta_\parallel$ towards the electric field E is small, about 10 % for all codes. For increasing E-fields, electrons are less scattered and more focused in the field direction, hence slightly increasing $\beta_\parallel$.

- The electron to (bremsstrahlung) photon ratio $r_{e/p}$ was also calculated and compared for different distance record in the RREA shower, and the corresponding plots are presented in the Supplementary Material, section 3. GRRR is excluded because it does not include photons. For any electric field, the same discrepancy is observed. At the beginning of the

25

shower (<4 avalanche lengths), $r_{e/p}$ appears to be about 20 % larger for REAM compared to O1 and O4, then the three models are consistent at a given distance, and finally for more than about 4 avalanche lengths, the tendency is inverted and REAM presents a $r_{e/p}$ about 20 % smaller than Geant4. The magnitude of this discrepancy is largely reduced for increasing electric fields. We did not fully understand the reasons of these differences, and it may be due to the bremsstrahlung models used are involved. More investigations are required.

– The positron spectra have relatively low statistics (in the order of few hundreds particles recorded) and are all quite consistent within the relatively large uncertainties.

– In the photon spectra obtained from particle records at fixed times, REAM seems to show significantly less (at least a factor of 10) photon counts than the two Geant4 models for most of the electric fields magnitudes. For some fields, it even shows a lack of high energy photons, with a sharp cut at about 30 MeV. It seems to point out to a problem in the record method, explaining why we chose not to discuss these spectra in the main article. The spectra produced by the Geant4 O1 and O4 models for this case are consistent with one another for all the E-fields.

5 Conclusions

We have investigated the results of three Monte Carlo codes able to simulate Relativistic Runaway Electron Avalanches (RREA), including the effects of electric fields up to the classical breakdown field, which is $E_k \approx 3$ MV/m at STP. The Monte-Carlo codes REAM, GRRR and Geant4 (two models: O1 and O4) were compared. The main difference between the Geant4 O4 and O1 models is the inclusion of more precise cross sections for low energy interactions (< 10 keV) for O4.

We first proposed a theoretical description of the RREA process, that is based and incremented over previous published works. Our analysis confirmed that the relativistic avalanche is mainly driven by electric fields and the ionisation and scattering processes determining $\epsilon_2^{\min}$, the minimum energy of electrons that can runaway. This is different from some of the previous works that speculated that the low energy threshold (ε_c), when changed from 1 keV to 250 eV, was the most important factor affecting the electron energy spectra (Skeltved et al., 2014; Rutjes et al., 2016).

Then, we estimated the probability to produce a RREA from a given electron energy (ϵ) and a given electric field magnitude (E). We found that the stepping methodology is of major importance, and the stepping parameters are not set up satisfactorily in Geant4 by default. We pointed out which settings should be adjusted and provided example codes to the community (see sections 6 and 7). When properly set-up, the two Geant4 models showed a good overall agreement (within ≈ 10 %) with REAM and GRRR. From the Geant4, GRRR and REAM simulations, we found that the probability for the particles below ≈ 10 keV to accelerate and participate in the penetrating radiation is actually negligible for the full range of electric field we tested ($E < 3$ MV/m). It results that a reasonable lower boundary of the low energy threshold (ε_c) can be set to ≈ 10 keV for any electric field below $E_k \approx 3$ MV/m (at STP), making it possible to have relatively fast simulations. For lower electric fields, it is possible to use larger ε_c, following a curve we provided (Figure 2.b).

The advantage of using more sophisticated cross sections able to accurately take into account low energy particles could be probed by comparing directly the O1 and O4 models. They showed minor differences that are mainly visible only for high E-fields ($E > 2$ MV/m), where low energy particles have more chance to runaway.

In a second part, we produced RREA simulations from the four models, and compared the physical characteristics of the produced showers. The two Geant4 models and REAM showed a good agreement on all the parameters we tested. GRRR also showed an overall good agreement with the other codes, except for the electron energy spectra. That is probably because GRRR does not include straggling for the radiative and ionisation energy losses, hence implementing these two processes is of primary importance to produce accurate RREA spectra. By comparing O1 and O4, we also pointed out that including precise modelling of the interactions of particles below ≈ 10 keV provided only small differences; the most important being a 5% change in the avalanche multiplication times and lengths. We also pointed out a discrepancy from Geant4 (O1 and O4) compared REAM, that is a 10% to 100% relative difference in the low energy part (< 100 keV) of the photon energy spectrum for an electric field of $E = 0.80$ MV/m. But we argued that it is unlikely to have an impact on spectra detected from satellites.

6   Recommendations

From the experience of this study, we give the following general recommendations concerning RREA simulations :

- Codes should be checked / tested / benchmarked using standard test set-ups. In the supplementary material, we provide a precise description of such tests. In section 7 of this article, we provide links to download the full data-set we obtained for the codes we tested (Geant4 with two set-ups, REAM and GRRR), as well as processing scripts. We also provide the source code of the Geant4 codes.

- Custom-made codes should be make available to other researchers, or at least the results they give for standard tests.

- In order to make it possible to compare results from different studies, the methodology used to derive a given quantity should be rigorously chosen, and presented clearly somewhere.

- Extending the recommendations of Rutjes et al. (2016), we concluded that to get an accurate RREA electron spectra above 10 MeV, radiative loss (bremsstrahlung) should not be implemented with uniform friction only: straggling should be included. Straggling should also be included for ionisation energy loses below the energy threshold.

Concerning the usage of Geant4 for simulating RREA :

- Default settings are not able to simulate RREA accurately. To get accurate RREA results, one of the following tweaks is possible :

    - Changing the α_R ("dR over Range") parameter of the electron/positron ionisation process to 5.0×10^{-3} or less. This solution gives the best ratio between accuracy and computation time. Leave the "final range" parameter to one millimeter (default value) or less.

– Setting up a step limitation process (or a maximum acceptable step) to one millimeters or less. This will significantly increase the required computation time.

– Using the single (Coulomb) scattering model instead of multiple scattering (the two previous tweaks relying on the multiple scattering algorithm). This will substantially increase the necessary computation time. This is because multiple scatterings algorithms were invented to make the simulation run faster by permitting to use substantially larger (usually >10 times) step lengths compared to a pure single scattering strategy, while keeping a similar accuracy.

– In section 7, we provide a link to Geant4 example source codes implementing these three methods.

– Compared to using the default Møller/Bhabha scattering models for ionisation, the usage of more accurate cross sections, e.g. taking into account the electrons' molecular binding energies (like done for the Livermore or Penelope models), only leads to minor differences.

7 Code and/or data availability

The full simulation output data of the four models is available though the following link:

https://filesender.uninett.no/?s=download&token=738a8663-a457-403a-991e-ae8d3fca3dc3

The scripts used to process this data to make the figures of the supplementary material are available in the following repository:

https://gitlab.com/dsarria/HEAP2_matlab_codes.git

The full GRRR source code is available in the following repository :

https://github.com/aluque/grrr/tree/avalanches

The Geant4 source code for the RREA probability simulations is available in the following repository :

https://gitlab.com/dsarria/av_prob.git

The Geant4 source code for the RREA characterisation simulations is available in the following repository :

https://gitlab.com/dsarria/RREA_characteristics.git

Appendix A: Geant4 relative performance

Table 3 presents the relative computation times it takes to complete the simulation with an electric field magnitude of 1.2 MV/m, and 100 initial ("seed") electrons with initial energy $\epsilon = 100$ keV, and a stop time (physical) of 233 nanoseconds. The fastest simulation uses Geant4 with the O1 physics list and $\delta\ell_{\max} = 10$ cm and took 4.53 seconds to complete on one thread with the microprocessor we used. The simulations with the O4 physics list with $\delta\ell_{\max} = 1$ mm requires about 400 times more computation time. Setting up $\delta\ell_{\max} = 1$ mm, or lower, is necessary to achieve correct simulation of the RREA process, as argued in section 3. To achieve it for the full range of electric fields we tested (in a reasonable amount of time), it required the use of the Norwegian FRAM computer cluster. The simulations with $\delta\ell_{\max} = 0.1$ mm for all electric fields could not be achieved in a reasonable amount of time, even by using the computer cluster.

On the other hand, if $\delta\ell_{\max}$ is left at its default value (1 kilometer) and α_R parameter is tweaked instead, accurate simulations can be achieved with a value of $\alpha_R = 5.0 \times 10^{-3}$ or lower. It requires almost an order of magnitude less computation time compared to using $\delta\ell_{\max} = 1$ mm.

$\delta\ell_{\max}$ ╲ Model	Option 1 (O1)	Option 4 (O4)
10 cm	**1**	**6.49**
1 cm	**11.5**	**27.2**
1 mm	**222**	**393**
0.1 mm	**2100**	**3740**
α_R (default)	0.80	0.20

α_R ╲ Model	Option 1 (O1)	Option 4 (O4)
0.80	**≈ 1**	**2.44**
0.20	**2.61**	**7.66**
0.050	**7.12**	**36.5**
0.0050	**21.0**	**126**
0.0010	**41.7**	**224**
$\delta\ell_{\max}$ (default)	1 km	1 km

Table 3. Computation time needed by different Geant4 configurations for the simulation of the same physical problem, relatively to the Geant4 O1 $\delta\ell_{\max} = 10$ cm case. Two parameters are tested : the maximum allowed step ($\delta\ell_{\max}$) and the "dR over Range" (α_R).

References

Adachi, T., Takahashi, Y., Ohya, H., Tsuchiya, F., Yamashita, K., Yamamoto, M., and Hashiguchi, H.: Monitoring of Lightning Activity in Southeast Asia: Scientific Objectives and Strategies, Kyoto Working Papers on Area Studies: G-COE Series, 2008.

Agostinelli, S. et al.: GEANT4: A simulation toolkit, Nucl. Instrum. Meth., A506, 250–303, doi:10.1016/S0168-9002(03)01368-8, 2003.

Allison, J., Amako, K., Apostolakis, J., Araujo, H., Dubois, P. A., Asai, M., Barrand, G., Capra, R., Chauvie, S., Chytracek, R., Cirrone, G. A. P., Cooperman, G., Cosmo, G., Cuttone, G., Daquino, G. G., Donszelmann, M., Dressel, M., Folger, G., Foppiano, F., Generowicz, J., Grichine, V., Guatelli, S., Gumplinger, P., Heikkinen, A., Hrivnacova, I., Howard, A., Incerti, S., Ivanchenko, V., Johnson, T., Jones, F., Koi, T., Kokoulin, R., Kossov, M., Kurashige, H., Lara, V., Larsson, S., Lei, F., Link, O., Longo, F., Maire, M., Mantero, A., Mascialino, B., McLaren, I., Lorenzo, P. M., Minamimoto, K., Murakami, K., Nieminen, P., Pandola, L., Parlati, S., Peralta, L., Perl, J., Pfeiffer, A., Pia, M. G., Ribon, A., Rodrigues, P., Russo, G., Sadilov, S., Santin, G., Sasaki, T., Smith, D., Starkov, N., Tanaka, S., Tcherniaev, E., Tome, B., Trindade, A., Truscott, P., Urban, L., Verderi, M., Walkden, A., Wellisch, J. P., Williams, D. C., Wright, D., and Yoshida, H.: Geant4 developments and applications, IEEE Transactions on Nuclear Science, 53, 270–278, doi:10.1109/TNS.2006.869826, 2006.

Allison, J., Amako, K., Apostolakis, J., et al.: Recent developments in Geant4, Nuclear Instruments and Methods in Physics Research Section A: Accelerators, Spectrometers, Detectors and Associated Equipment, 835, 186 – 225, doi:https://doi.org/10.1016/j.nima.2016.06.125, http://www.sciencedirect.com/science/article/pii/S0168900216306957, 2016.

Apostolakis, J., Asai, M., Bogdanov, A., Burkhardt, H., Cosmo, G., Elles, S., Folger, G., Grichine, V., Gumplinger, P., Heikkinen, A., Hrivnacova, I., Ivanchenko, V., Jacquemier, J., Koi, T., Kokoulin, R., Kossov, M., Kurashige, H., McLaren, I., Link, O., Maire, M., Pokorski, W., Sasaki, T., Starkov, N., Urban, L., and Wright, D.: Geometry and physics of the Geant4 toolkit for high and medium energy applications, Radiation Physics and Chemistry, 78, 859 – 873, doi:https://doi.org/10.1016/j.radphyschem.2009.04.026, http://www.sciencedirect.com/science/article/pii/S0969806X09001650, workshop on Use of Monte Carlo Techniques for Design and Analysis of Radiation Detectors, 2009.

Babich, L., Donskoy, E., Kutsyk, I., and Roussel-Dupré, R.: The feedback mechanism of runaway air breakdown, Geophysical research letters, 32, L09809, doi:10.1029/2004GL021744, 2005.

Babich, L. P.: Generation of neutrons in giant upward atmospheric discharges, JETP letters, 84, 285–288, 2006.

Babich, L. P., Donskoy, E. N., Kutsyk, I. M., Kudryavtsev, A. Y., Roussel-Dupre, R. A., Shamraev, B. N., and Symbalisty, E. M.: Comparison of relativistic runaway electron avalanche rates obtained from Monte Carlo simulations and kinetic equation solution, IEEE transactions on plasma science, 29, 430–438, 2001.

Babich, L. P., Bakhov, K. I., Balakin, V. A., Donskoi, E. N., Zavada, N. I., Zelenskii, K. F., Il'kaev, R. I., Kutsyk, I. M., Loiko, T. V., Nedoikash, Y. M., Pavlovskaya, N. G., Roussel-Dupre, R. A., Symbalisty, E. M. D., and Shamraev, B. N.: An Experimental Investigation of an Avalanche of Relativistic Runaway Electrons under Normal Conditions, High Temperature, 42, 1–11, doi:10.1023/B:HITE.0000020085.61526.40, https://doi.org/10.1023/B:HITE.0000020085.61526.40, 2004a.

Babich, L. P., Donskoy, E. N., Il'kaev, R. I., Kutsyk, I. M., and Roussel-Dupre, R. A.: Fundamental parameters of a relativistic runaway electron avalanche in air, Plasma Physics Reports, 30, 616–624, doi:10.1134/1.1778437, https://doi.org/10.1134/1.1778437, 2004b.

Bethe, H. and Heitler, W.: On the stopping of fast particles and on the creation of positive electrons, Proceedings of the Royal Society of London A: Mathematical, Physical and Engineering Sciences, 146, 83–112, 1934.

Bowers, G. S., Smith, D. M., Martinez-McKinney, G., Kamogawa, M., Cummer, S., Dwyer, J., Wang, D., Stock, M., and Kawasaki, Z.: Gamma Ray Signatures of Neutrons From a Terrestrial Gamma Ray Flash, Geophysical Research Letters, 2017.

Briggs, M. S., Connaughton, V., Wilson-Hodge, C., Preece, R. D., Fishman, G. J., Kippen, R. M., Bhat, P., Paciesas, W. S., Chaplin, V. L., Meegan, C. A., et al.: Electron-positron beams from terrestrial lightning observed with Fermi GBM, Geophysical research letters, 38, L02808, doi:10.1029/2010GL046259, 2011.

Brown, J. M. C., Dimmock, M. R., Gillam, J. E., and Paganin, D. M.: A low energy bound atomic electron Compton scattering model for Geant4, Nuclear Instruments and Methods in Physics Research B, 338, 77–88, doi:10.1016/j.nimb.2014.07.042, 2014.

Carlson, B., Lehtinen, N. G., and Inan, U. S.: Neutron production in terrestrial gamma ray flashes, Journal of Geophysical Research: Space Physics, 115, A00E19, doi:10.1029/2009JA014696, 2010.

Celestin, S. and Pasko, V. P.: Soft collisions in relativistic runaway electron avalanches, Journal of Physics D: Applied Physics, 43, 315206, doi:10.1088/0022-3727/43/31/315206, 2010.

Celestin, S. and Pasko, V. P.: Energy and fluxes of thermal runaway electrons produced by exponential growth of streamers during the stepping of lightning leaders and in transient luminous events, Journal of Geophysical Research: Space Physics, 116, A03315, doi:10.1029/2010JA016260, 2011.

Celestin, S., Xu, W., and Pasko, V. P.: Terrestrial gamma ray flashes with energies up to 100 MeV produced by nonequilibrium acceleration of electrons in lightning, Journal of Geophysical Research (Space Physics), 117, A05315, doi:10.1029/2012JA017535, http://dx.doi.org/10.1029/2012JA017535, a05315, 2012.

Chanrion, O. and Neubert, T.: Production of runaway electrons by negative streamer discharges, J. Geophys. Res. (Space Phys), 115, A00E32, doi:10.1029/2009JA014774, 2010.

Chanrion, O., Bonaventura, Z., Çinar, D., Bourdon, A., and Neubert, T.: Runaway electrons from a "beam-bulk" model of streamer: application to TGFs, Environmental Research Letters, 9, 055003, doi:10.1088/1748-9326/9/5/055003, 2014.

5 Chanrion, O., Bonaventura, Z., Bourdon, A., and Neubert, T.: Influence of the angular scattering of electrons on the runaway threshold in air, Plasma Physics and Controlled Fusion, 58, 044001, doi:10.1088/0741-3335/58/4/044001, 2016.

Chilingarian, A., Daryan, A., Arakelyan, K., Hovhannisyan, A., Mailyan, B., Melkumyan, L., Hovsepyan, G., Chilingaryan, S., Reymers, A., and Vanyan, L.: Ground-based observations of thunderstorm-correlated fluxes of high-energy electrons, gamma rays, and neutrons, Physical Review D, 82, 043009, doi:10.1103/PhysRevD.82.043009, 2010.

10 Chilingarian, A., Hovsepyan, G., and Hovhannisyan, A.: Particle bursts from thunderclouds: Natural particle accelerators above our heads, Physical review D, 83, 062001, doi:10.1103/PhysRevD.83.062001, 2011.

Chilingarian, A., Mailyan, B., and Vanyan, L.: Recovering of the energy spectra of electrons and gamma rays coming from the thunderclouds, Atmospheric Research, 114, 1–16, doi:10.1016/j.atmosres.2012.05.008, 2012.

Chilingarian, A., Hovsepyan, G., Khanikyanc, G., Reymers, A., and Soghomonyan, S.: Lightning origination and thunderstorm ground
15 enhancements terminated by the lightning flash, EPL (Europhysics Letters), 110, 49 001, 2015.

Coleman, L. M. and Dwyer, J. R.: Propagation speed of runaway electron avalanches, Geophysical Research Letters, 33, L11810, doi:10.1029/2006GL025863, 2006.

Cooray, V., Arevalo, L., Rahman, M., Dwyer, J., and Rassoul, H.: On the possible origin of X-rays in long laboratory sparks, J. Atm. Sol.-Terr. Phys., 71, 1890, doi:10.1016/j.jastp.2009.07.010, 2009.

20 Cramer, E. S., Dwyer, J. R., Arabshahi, S., Vodopiyanov, I., Liu, N., and Rassoul, H.: An analytical approach for calculating energy spectra of relativistic runaway electron avalanches in air, Journal of Geophysical Research: Space Physics, 119, 7794–7823, 2014.

Cramer, E. S., Dwyer, J. R., and Rassoul, H. K.: Magnetic field modification to the relativistic runaway electron avalanche length, Journal of Geophysical Research (Space Physics), 121, 11, doi:10.1002/2016JA022891, 2016.

Dubinova, A., Rutjes, C., Ebert, U., Buitink, S., Scholten, O., and Trinh, G. T. N.: Prediction of Lightning Inception by Large Ice Particles
25 and Extensive Air Showers, Physical Review Letters, 115, 015 002, doi:10.1103/PhysRevLett.115.015002, https://link.aps.org/doi/10.1103/PhysRevLett.115.015002, 2015.

Dwyer, J., Saleh, Z., Rassoul, H., Concha, D., Rahman, M., Cooray, V., Jerauld, J., Uman, M., and Rakov, V.: A study of X-ray emission from laboratory sparks in air at atmospheric pressure, Journal of Geophysical Research: Atmospheres, 113, D23207, doi:10.1029/2008JD010315, 2008.

30 Dwyer, J. R.: A fundamental limit on electric fields in air, Geophysical Research Letters, 30, 2055, doi:10.1029/2003GL017781, http://www.agu.org/pubs/crossref/2003/2003GL017781.shtml, 2003.

Dwyer, J. R.: Relativistic breakdown in planetary atmospheres, Physics of Plasmas, 14, 042 901, doi:10.1063/1.2709652, 2007.

Dwyer, J. R.: Source mechanisms of terrestrial gamma-ray flashes, Journal of Geophysical Research: Atmospheres, 113, n/a–n/a, doi:10.1029/2007JD009248, http://dx.doi.org/10.1029/2007JD009248, d10103, 2008.

35 Dwyer, J. R.: The relativistic feedback discharge model of terrestrial gamma ray flashes, J. Geophys. Res. (Space Phys), 117, A02308, doi:10.1029/2011JA017160, 2012.

Dwyer, J. R., Grefenstette, B. W., and Smith, D. M.: High-energy electron beams launched into space by thunderstorms, Geophysical Research Letters, 35, L02815, doi:10.1029/2007GL032430, http://dx.doi.org/10.1029/2007GL032430, 2008.

Dwyer, J. R., Smith, D. M., and Cummer, S. A.: High-Energy Atmospheric Physics: Terrestrial Gamma-Ray Flashes and Related Phenomena, Space Science Review, 173, 133–196, doi:10.1007/s11214-012-9894-0, 2012.

Dwyer, J. R., Smith, D. M., Hazelton, B. J., Grefenstette, B. W., Kelley, N. A., Lowell, A. W., Schaal, M. M., and Rassoul, H. K.: Positron clouds within thunderstorms, Journal of Plasma Physics, 81, 475810405, doi:10.1017/S0022377815000549, 2015.

5   Eack, K. B., Beasley, W. H., Rust, W. D., Marshall, T. C., and Stolzenburg, M.: Initial results from simultaneous observation of X-rays and electric fields in a thunderstorm, Journal of Geophysical Research: Atmospheres, 101, 29 637–29 640, doi:10.1029/96JD01705, 1996.

Ferrari, A., Sala, P. R., Fasso, A., and Ranft, J.: FLUKA: A multi-particle transport code (Program version 2005), Tech. rep., 2005.

Fishman, G. J., Bhat, P. N., Mallozzi, R., Horack, J. M., Koshut, T., Kouveliotou, C., Pendleton, G. N., Meegan, C. A., Wilson, R. B., Paciesas, W. S., Goodman, S. J., and Christian, H. J.: Discovery of Intense Gamma-Ray Flashes of Atmospheric Origin, Science, 264,

10   1313–1316, doi:10.1126/science.264.5163.1313, 1994.

Grefenstette, B. W., Smith, D. M., Hazelton, B. J., and Lopez, L. I.: First RHESSI terrestrial gamma ray flash catalog, Journal of Geophysical Research (Space Physics), 114, A02314, doi:10.1029/2008JA013721, 2009.

Gurevich, A.: On the theory of runaway electrons, Sov. Phys. JETP, 12, 904–912, 1961.

Gurevich, A. and Zybin, K.: Kinetic equation for high energy electrons in gases, Physics Letters A, 237, 240–246, 1998.

15   Gurevich, A., Milikh, G., and Roussel-Dupre, R.: Runaway electron mechanism of air breakdown and preconditioning during a thunderstorm, Physics Letters A, 165, 463–468, doi:10.1016/0375-9601(92)90348-P, http://linkinghub.elsevier.com/retrieve/pii/037596019290348P, 1992.

Hirayama, H., Namito, Y., Nelson, W. R., Bielajew, A. F., Wilderman, S. J., and Michigan, U.: The EGS5 code system, Tech. rep., United States. Department of Energy, 2005.

20   Ihaddadene, M. A. and Celestin, S.: Increase of the electric field in head-on collisions between negative and positive streamers, grl, 42, 5644–5651, doi:10.1002/2015GL064623, 2015.

Ivanchenko, V. N., Bukin, A. D., Dubrovin, M. S., Eidelman, S. I., Grozina, N. A., and Tayursky, V. A.: UNIMOD2: Universal Monte Carlo code for simulation of e+ e- experiments, in: MC 91: Detector and event simulation in high-energy physics. Proceedings, Workshop, Amsterdam, Netherlands, April 8-12, 1991, pp. 79–85, 1991.

25   Kelley, N. A., Smith, D. M., Dwyer, J. R., Splitt, M., Lazarus, S., Martinez-McKinney, F., Hazelton, B., Grefenstette, B., Lowell, A., and Rassoul, H. K.: Relativistic electron avalanches as a thunderstorm discharge competing with lightning, Nature communications, 6, 2015.

Kochkin, P., Köhn, C., Ebert, U., and van Deursen, L.: Analyzing x-ray emissions from meter-scale negative discharges in ambient air, Plasma Sources Science and Technology, 25, 044 002, 2016.

Kochkin, P., van Deursen, A. P. J., Marisaldi, M., Ursi, A., de Boer, A. I., Bardet, M., Allasia, C., Boissin, J.-F., Flourens, F., and Østgaard,

30   N.: In-flight observation of gamma-ray glows by ILDAS, Journal of Geophysical Research: Atmospheres, doi:10.1002/2017JD027405, http://dx.doi.org/10.1002/2017JD027405, 2017.

Kochkin, P., Sarria, D., Skeie, C., Deursen, A. P. J., Boer, A. I., Bardet, M., Allasia, C., Flourens, F., and Østgaard, N.: In-Flight Observation of Positron Annihilation by ILDAS, Journal of Geophysical Research: Atmospheres, 0, doi:10.1029/2018JD028337, https://agupubs. onlinelibrary.wiley.com/doi/abs/10.1029/2018JD028337, 2018.

35   Köhn, C. and Ebert, U.: Calculation of beams of positrons, neutrons, and protons associated with terrestrial gamma ray flashes, Journal of Geophysical Research: Atmospheres, 120, 1620–1635, 2015.

Köhn, C., Ebert, U., and Mangiarotti, A.: The importance of electron–electron bremsstrahlung for terrestrial gamma-ray flashes, electron beams and electron–positron beams, Journal of Physics D: Applied Physics, 47, 252 001, http://stacks.iop.org/0022-3727/47/i=25/a= 252001, 2014.

Köhn, C., Diniz, G., and Harakeh, M. N.: Production mechanisms of leptons, photons, and hadrons and their possible feedback close to lightning leaders, Journal of Geophysical Research: Atmospheres, 122, 1365–1383, 2017.

Landau, L. D., Bell, J., Kearsley, M., Pitaevskii, L., Lifshitz, E., and Sykes, J.: Electrodynamics of continuous media, vol. 8, elsevier, 2013.

Lefeuvre, F., Blanc, E., and Pinçon, J. L.: TARANIS-a Satellite Project Dedicated to the Physics of TLEs and TGFs, in: American Institute of Physics Conference Series, vol. 1118 of *American Institute of Physics Conference Series*, pp. 3–7, doi:10.1063/1.3137711, 2009.

Lehtinen, N. G. and Østgaard, N.: X-ray Emissions in a Multiscale Fluid Model of a Streamer Discharge, Journal of Geophysical Research: Atmospheres, 123, 6935–6953, doi:10.1029/2018JD028646, https://agupubs.onlinelibrary.wiley.com/doi/abs/10.1029/2018JD028646, 2018.

Lehtinen, N. G., Bell, T. F., and Inan, U. S.: Monte Carlo simulation of runaway MeV electron breakdown with application to red sprites and terrestrial gamma ray flashes, jgr, 104, 24 699–24 712, doi:10.1029/1999JA900335, 1999.

Li, C., Ebert, U., and Hundsdorfer, W.: 3D hybrid computations for streamer discharges and production of runaway electrons, Journal of Physics D: Applied Physics, 42, 202003, doi:10.1088/0022-3727/42/20/202003, 2009.

Liu, C., Brennan, D. P., Bhattacharjee, A., and Boozer, A. H.: Adjoint Fokker-Planck equation and runaway electron dynamics, Physics of Plasmas, 23, 010 702, 2016.

Luque, A.: Relativistic Runaway Ionization Fronts, Physical Review Letters, 112, 045003, doi:10.1103/PhysRevLett.112.045003, 2014.

Luque, A.: Radio Frequency Electromagnetic Radiation From Streamer Collisions, Journal of Geophysical Research (Atmospheres), 122, 10, doi:10.1002/2017JD027157, 2017.

Mailyan, B. G., Briggs, M. S., Cramer, E. S., Fitzpatrick, G., Roberts, O. J., Stanbro, M., Connaughton, V., McBreen, S., Bhat, P. N., and Dwyer, J. R.: The spectroscopy of individual terrestrial gamma-ray flashes: Constraining the source properties, Journal of Geophysical Research (Space Physics), 121, 11, doi:10.1002/2016JA022702, 2016.

Marisaldi, M., Fuschino, F., Tavani, M., Dietrich, S., Price, C., Galli, M., et al.: Properties of terrestrial gamma ray flashes detected by AGILE MCAL below 30 MeV, Journal of Geophysical Research (Space Physics), 119, 1337–1355, doi:10.1002/2013JA019301, 2014.

McCarthy, M. and Parks, G.: Further observations of X-rays inside thunderstorms, Geophysical Research Letters, 12, 393–396, doi:10.1029/GL012i006p00393, 1985.

Moss, G. D., Pasko, V. P., Liu, N., and Veronis, G.: Monte Carlo model for analysis of thermal runaway electrons in streamer tips in transient luminous events and streamer zones of lightning leaders, Journal of Geophysical Research (Space Physics), 111, A02307, doi:10.1029/2005JA011350, 2006.

Neubert, T., Kuvvetli, I., Budtz-Jørgensen, C., Østgaard, N., Reglero, V., and Arnold, N.: The atmosphere-space interactions monitor (ASIM) for the international space station, in: Proceedings of the ILWS Workshop, edited by Gopalswamy, N. and Bhattacharyya, A., p. 448, 2006.

Østgaard, N., Gjesteland, T., Stadsnes, J., Connell, P., and Carlson, B.: Production altitude and time delays of the terrestrial gamma flashes: Revisiting the Burst and Transient Source Experiment spectra, Journal of Geophysical Research: Space Physics, 113, A02307, doi:10.1029/2007JA012618, 2008.

Parks, G. K., Mauk, B. H., Spiger, R., and Chin, J.: X-ray enhancements detected during thunderstorm and lightning activities, Geophysical Research Letters, 8, 1176–1179, doi:10.1029/GL008i011p01176, https://agupubs.onlinelibrary.wiley.com/doi/abs/10.1029/GL008i011p01176, 1981.

Perkins, S., Cullen, D., and Seltzer, S.: Tables and graphs of electron-interaction cross sections from 10 eV to 100 GeV derived from the LLNL Evaluated Electron Data Library (EEDL), Z = 1–100, Tech. rep., doi:10.2172/5691165, https://doi.org/10.2172/5691165, 1991.

Rahman, M., Cooray, V., Azlinda Ahmad, N., Nyberg, J., Rakov, V. A., and Sharma, S.: X rays from 80-cm long sparks in air, grl, 35, L06 805, doi:10.1029/2007GL032678, 2008.

5   Raizer, Y. P.: Gas discharge physics, vol. 2, Springer Berlin, 1997.

Roberts, O. J., Fitzpatrick, G., Stanbro, M., McBreen, S., Briggs, M. S., Holzworth, R. H., Grove, J. E., Chekhtman, A., Cramer, E. S., and Mailyan, B. G.: The First Fermi-GBM Terrestrial Gamma Ray Flash Catalog, Journal of Geophysical Research (Space Physics), 123, 4381–4401, doi:10.1029/2017JA024837, 2018.

Roussel-Dupre, R. A., Gurevich, A. V., Tunnell, T., and Milikh, G. M.: Kinetic theory of runaway air breakdown, Physical Review E, 49,

10   2257–2271, doi:10.1103/PhysRevE.49.2257, 1994.

Rutjes, C., Sarria, D., Skeltved, A. B., Luque, A., Diniz, G., Østgaard, N., and Ebert, U.: Evaluation of Monte Carlo tools for high energy atmospheric physics, Geoscientific Model Development, 9, 3961, doi:10.5194/gmd-9-3961-2016, http://www.geosci-model-dev.net/9/3961/2016/, 2016.

Rutjes, C., Diniz, G., Ferreira, I. S., and Ebert, U.: TGF afterglows: a new radiation mechanism from thunderstorms, Geophysical Research

15   Letters, doi:10.1002/2017GL075552, 2017.

Salvat, F., Fernández-Varea, J. M., and Sempau, J.: PENELOPE-2011: A Code System for Monte Carlo Simulation of Electron and Photon Transport, 2011.

Sarria, D., Blelly, P.-L., and Forme, F.: MC-PEPTITA: a Monte Carlo model for Photon, Electron and Positron Tracking In Terrestrial Atmosphere. Application for a Terrestrial Gamma-ray Flash, Journal of Geophysical Research: Space Physics, pp. n/a–n/a,

20   doi:10.1002/2014JA020695, http://dx.doi.org/10.1002/2014JA020695, 2014JA020695, 2015.

Sarria, D., Blelly, P.-L., Briggs, M. S., and Forme, F.: Studying the time histogram of a terrestrial electron beam detected from the opposite hemisphere of its associated TGF, Journal of Geophysical Research: Space Physics, pp. n/a–n/a, doi:10.1002/2015JA021881, http://dx.doi.org/10.1002/2015JA021881, 2016.

Sarria, D., Lebrun, F., Blelly, P.-L., Chipaux, R., Laurent, P., Sauvaud, J.-A., Prech, L., Devoto, P., Pailot, D., Baronick, J.-P., and Lindsey-

25   Clark, M.: TARANIS XGRE and IDEE detection capability of terrestrial gamma-ray flashes and associated electron beams, Geoscientific Instrumentation, Methods and Data Systems, 6, 239–256, doi:10.5194/gi-6-239-2017, https://www.geosci-instrum-method-data-syst.net/6/239/2017/, 2017.

Shao, T., Zhang, C., Niu, Z., Yan, P., Tarasenko, V. F., Baksht, E. K., Burahenko, A. G., and Shut'ko, Y. V.: Diffuse discharge, runaway electron, and x-ray in atmospheric pressure air in an inhomogeneous electrical field in repetitive pulsed modes, Applied Physics Letters,

30   98, 021503, doi:10.1063/1.3540504, 2011.

Skeltved, A. B., Østgaard, N., Carlson, B., Gjesteland, T., and Celestin, S.: Modeling the relativistic runaway electron avalanche and the feedback mechanism with GEANT4, Journal of Geophysical Research: Space Physics, 119, 9174–9191, doi:10.1002/2014ja020504, http://dx.doi.org/10.1002/2014JA020504, 2014.

Teruaki, E., Wada, Y., et al.: Photonuclear reactions triggered by lightning discharge, Nature, 551, doi:10.1038/nature24630, https://www.

35   nature.com/articles/nature24630, 2017.

Torii, T., Takeishi, M., and Hosono, T.: Observation of gamma-ray dose increase associated with winter thunderstorm and lightning activity, Journal of Geophysical Research: Atmospheres, 107, 4324, doi:10.1029/2001JD000938, 2002.

Tsuchiya, H., Enoto, T., Yamada, S., Yuasa, T., Kawaharada, M., Kitaguchi, T., Kokubun, M., Kato, H., Okano, M., Nakamura, S., et al.: Detection of high-energy gamma rays from winter thunderclouds, Physical review letters, 99, 165002, doi:10.1103/PhysRevLett.99.165002, 2007.

Williams, E. R.: Origin and context of C. T. R. Wilson's ideas on electron runaway in thunderclouds, Journal of Geophysical Research (Space Physics), 115, A00E50, doi:10.1029/2009JA014581, 2010.

Wilson, C. T. R.: The Acceleration of β-particles in Strong Electric Fields such as those of Thunderclouds, Proceedings of the Cambridge Philosophical Society, 22, 534, doi:10.1017/S0305004100003236, 1925.

5